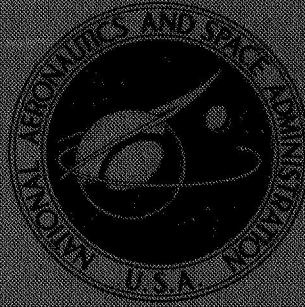


**NASA TECHNICAL
MEMORANDUM**



NASA TM X-2101

NASA TM X-2101

**CASE FILE
COPY**

**FLIGHT TEST RESULTS PERTAINING
TO THE SPACE SHUTTLECRAFT**

A symposium held at
Flight Research Center
Edwards, Calif.
June 30, 1970

NATIONAL AERONAUTICS AND SPACE ADMINISTRATION • WASHINGTON, D. C. • OCTOBER 1970

FLIGHT TEST RESULTS PERTAINING
TO THE SPACE SHUTTLECRAFT

A symposium held at
Flight Research Center
Edwards, Calif.
June 30, 1970

NATIONAL AERONAUTICS AND SPACE ADMINISTRATION

For sale by the Clearinghouse for Federal Scientific and Technical Information
Springfield, Virginia 22151 - CFSTI price \$3.00

PREFACE

This compilation consists of papers presented at the NASA Symposium on Flight Test Results Pertaining to the Space Shuttlecraft, held at the NASA Flight Research Center, Edwards, Calif., on June 30, 1970. The symposium was divided into the following sessions.

I. Lifting Body Flight Test Results

II. Additional Space Shuttle Oriented Studies

Papers were presented by representatives from the NASA Flight Research Center and the U. S. Air Force Flight Test Center.

A list of attendees is included.

CONTENTS

PREFACE	iii
-------------------	-----

I. LIFTING BODY FLIGHT TEST RESULTS

Session Chairman - Robert G. Hoey

1. BACKGROUND AND CURRENT STATUS OF THE LIFTING BODY PROGRAM	1
John G. McTigue	
2. STABILITY AND CONTROL DERIVATIVES OF THE LIFTING BODY VEHICLES	11
Robert W. Kempel, Larry W. Strutz, and Paul W. Kirsten	
3. ASSESSMENT OF LIFTING BODY VEHICLE HANDLING QUALITIES	29
John A. Manke, John P. Retelle, and Robert W. Kempel	
4. PERFORMANCE CHARACTERISTICS OF THE LIFTING BODY VEHICLES	43
Jon S. Pyle and Lawrence G. Ash	
5. CORRELATION OF FLIGHT-TEST LOADS WITH WIND-TUNNEL PREDICTED LOADS ON THREE LIFTING BODY VEHICLES	59
Ming H. Tang	
6. PILOT IMPRESSIONS OF LIFTING BODY VEHICLES	73
William H. Dana and J. R. Gentry	
7. SUMMARY OF PRIMARY RESULTS OF THE LIFTING BODY PROGRAM	89
Garrison P. Layton, Jr.	

II. ADDITIONAL SPACE SHUTTLE ORIENTED STUDIES

Session Chairman - Milton O. Thompson

8. APPROACH AND LANDING STUDIES	99
Berwin M. Kock and Fitzhugh L. Fulton, Jr.	
9. IFR EXPERIENCE WITH UNPOWERED, LOW-LIFT-DRAG-RATIO LANDING APPROACHES	109
Peter C. Hoag and B. Lyle Schofield	

10. RATIONALE FOR PROPOSED FLYING-QUALITIES SPECIFICATIONS	127
Euclid C. Holleman	
11. FINAL REMARKS AND FUTURE PLANS	147
Milton O. Thompson	

LIST OF ATTENDEES.	153
----------------------------	-----

1. BACKGROUND AND CURRENT STATUS OF THE LIFTING BODY PROGRAM

By John G. McTigue
NASA Flight Research Center

INTRODUCTION

The lifting body concept was originally conceived by the Ames Research Center, and the design was developed over a period of years, from 1957 to 1964. By using a cone as a basic entry shape and modifying it to obtain lift and control, the M-2 shape evolved. In a cooperative venture with the NASA Ames Research Center to determine if a pilot could maneuver, flare, and land this class of vehicle, the Flight Research Center constructed a lightweight version of the lifting body, the M2-F1 vehicle. This vehicle was constructed during the fall of 1962 and spring of 1963 and extensively flight tested during the summer of 1963.

Because of the success of the M2-F1 flight program, the research program was extended to include vehicles that would be representative of mission weight and wing loading. Figure 1 shows the three vehicles in the present lifting body program. On the left is the X-24A vehicle, which evolved from the U.S. Air Force's SV-5 PRIME vehicle; in the center is the M2-F3 vehicle, which is a modified version of the M2-F2 vehicle; and on the right is the HL-10 vehicle, which evolved from work at the NASA Langley Research Center.

OBJECTIVES OF TEST PROGRAM

The objectives of the flight test program were to: (1) investigate the approach and landing tasks, including landing techniques and pilot procedures; (2) evaluate handling characteristics of the lifting body class of vehicle for the terminal portion of flight below a Mach number of approximately 2.0; (3) determine general and specific flight control system requirements to allow the pilot to perform his assigned tasks; and (4) correlate wind-tunnel and flight characteristics, such as performance, control surface loads, and basic stability and control data, in order to assess wind-tunnel prediction techniques. For conventional aircraft a large amount of flight data and experience is available to help interpret wind-tunnel results, especially when there are discrepancies, and to help extrapolate wind-tunnel data and theory to other similar vehicles. For the lifting bodies, there is no such background information, because before this program there had been no actual flight experience with lifting bodies. Thus, a combined wind-tunnel/flight-test program was essential.

Another obvious objective of any flight program is to determine any unpredicted problems and assess their significance.

DESCRIPTION OF VEHICLES

Figure 2 shows some of the geometric characteristics of the three flight test vehicles which are representative of the many proposed moderate, hypersonic lift-to-drag-ratio (1.1 to 1.3) manned lifting entry vehicles capable of making unpowered horizontal landings. These vehicles are all generally similar in planform shape and have blunt noses, thick stabilizing control surfaces, and squared-off thick bases. However, some of the geometric and aerodynamic characteristics differ considerably. As indicated, a planform area of 160 ft² was used as a basis for construction on the M2-F2 and HL-10 vehicles; 191 ft² was used for the X-24A vehicle. Outstanding features of these vehicles are the half-cone shape of the M2-F2, the negative camber of the HL-10, and the positive camber of the X-24A.

Figure 3 shows the vertical tail and control surface configurations of the three lifting body vehicles to supplement the subsequent photographs and detailed discussion of each of the vehicles.

Figure 4, a rear view of the M2-F3 vehicle, shows that the vehicle has upper and lower control surfaces on the aft end of the body for longitudinal and lateral control. The lower flap is the primary pitch control. The upper flaps are used collectively for pitch trim, and lateral control is achieved by differential deflection of these flaps. Directional control is accomplished by deflection of the rudder surfaces on the out-board vertical fins. A rudder-to-aileron interconnect is also provided to optimize the lateral control response.

Figure 5 shows rear views of the HL-10 vehicle in the subsonic and transonic configurations. The elevons form the aft end of the body and are used for pitch and roll control. Directional control is accomplished by deflection of the rudder surfaces on the center fin. Additional symmetrical deflection of these surfaces also provides an adequate speed brake. During wind-tunnel testing of the original HL-10 configuration, instabilities were noted at high subsonic Mach numbers. To alleviate this problem, extra flap-like surfaces were fitted to the outer and center fins and the thick elevons to form the transonic configuration. To achieve stability in the transonic speed range, all the extra flap-like surfaces are flared. For landing, however, the increased drag associated with these extra surfaces in the flared configuration would be detrimental to the lift-to-drag ratio and, thus, the unpowered landing capability; therefore, the extra surfaces are faired into the main surfaces during approach and landing.

The X-24A vehicle, shown in figure 6 in the subsonic and transonic configurations, has eight movable control surfaces (two upper and two lower flaps, and split rudders on each of the outer vertical fins.) The rudders are used for directional control. There is also a rudder-to-aileron interconnect to optimize the lateral control response. The upper and lower flaps, which are used collectively for pitch control and differentially for roll control, are positioned or biased automatically as a function of Mach number along with the rudders to provide stability at transonic speeds and minimum drag at low speeds. There are provisions in the cockpit to manually override any of the automatic biasing features.

The internal subsystems of the vehicles are similar. They include a fully irreversible, dual hydraulic, stability-augmented control system, an XLR-11-13 rocket

propulsion system with 8000 pounds of thrust, and many other off-the-shelf items that are used identically in all three vehicles. The vehicles are made of aluminum and are designed for supersonic flight after being carried aloft and launched from a position under the wing of a B-52 airplane.

FLIGHT ENVELOPE EXPANSION

The flight envelope of the HL-10 vehicle, expressed in terms of altitude and Mach number, is shown in figure 7. The M-2 and X-24A vehicles have not achieved the peak Mach number and altitude of the HL-10 vehicle but are in a build-up program to attain essentially the same performance envelope. The first series of flight tests in each program were unpowered glide flights that were initiated by launch from a B-52 airplane at an altitude of 45,000 feet and a Mach number of 0.65 to 0.75, followed by a series of subsonic maneuvers, and ended by gliding to a landing. The second phase of the flight program consists of a series of flights using rocket power to attain the high speed, high altitude point for each flight, followed by a glide to landing after investigating the supersonic, transonic, and subsonic characteristics of the vehicle. The flight envelope is bounded by a lower dynamic pressure limit of 50 lb/ft² because of minimum control effectiveness and a structural limit at a dynamic pressure of 400 lb/ft². The HL-10 vehicle has exceeded the design envelope with a maximum Mach number of approximately 1.85 and a peak altitude of approximately 90,000 feet.

Before any of these vehicles are flown, a ground based simulation is generated using the best available wind-tunnel data. This simulation is then used to explore the flight characteristics throughout the nominal and off-nominal profiles. The vehicle characteristics are varied in accordance with the best estimate of the wind-tunnel accuracy. After the handling qualities of the vehicle are investigated on the simulator, the simulator is used for flight planning and pilot practice. The simulation is updated with flight data as the flight program progresses.

PROGRESS AND STATUS OF PROGRAM

Figure 8 is the schedule of events that led to this symposium. A contract was signed by NASA with the Northrop Corporation to design and build the M2-F2 and HL-10 vehicles in June 1964. The M2-F2 vehicle was delivered in July 1965 and the HL-10 vehicle in January 1966. At this time, the program became a joint NASA/U. S. Air Force program, and construction of the X-24A vehicle was started by The Martin Marietta Corporation approximately 2 months before a contract was signed with the Air Force in May 1966.

The M2-F2 vehicle was flown in July 1966, and 14 glide flights were made (represented by the ticks) in its original configuration. The rocket engine was installed and the second systems check glide flight was being performed in preparation for a powered flight when a gear-up landing was made at a speed in excess of 200 knots. The vehicle was repaired, and its first glide flight was made recently under the new designation of M2-F3. During the repair period, various modifications were incorporated; the most notable was the addition of the center vertical tail. Some of the effects of these changes will be discussed in other papers.

The first HL-10 flight was in December 1966; however, modifications necessitated by flow separation/stability and control problems resulted in a delay of more than a year from the first to the second glide flight. The effects of modifications which resulted from extensive wind-tunnel tests between the first and second flights will also be discussed later. The first HL-10 powered flight was made in October 1968, and the flight envelope expansion was completed in March 1970. Since then, one additional flight has been made to investigate powered approach.

The X-24A vehicle was delivered in September 1967, and the first glide flight was made in May 1969. The first powered flight was made in February 1970.

To date in the lifting body program, 67 flights have been made by 7 pilots. Fourteen HL-10 glide flights by 5 pilots and 22 powered flights by 4 pilots have expanded the flight envelope to an angle of attack of 30° , a Mach number of 1.85, and sensible dynamic pressure limits. The airplane is on flight status with the installation of a landing engine system for evaluation of powered approaches. This system has 1500 pounds of thrust for approximately 80 seconds and will be used in a program to determine if a requirement exists for onboard propulsion for vehicles with low lift-to-drag ratios.

Nine glide flights and 5 powered flights have been made in the X-24A vehicle by 2 pilots. The flight envelope has been expanded to a Mach number of 0.98, well within the transonic flight region, and will be expanded further.

Sixteen glide flights were made in the M2-F2 vehicle by 4 pilots, and one M2-F3 glide flight has been made.

Within these flight envelopes, sufficient data have been obtained to define the vehicle performance, stability, control, and damping derivatives, and handling qualities, and to determine how hinge moments and fin loads vary as a function of Mach number and angle of attack across the flight envelope. The M2-F2 flights also defined a major handling qualities problem, which has been solved.

DESCRIPTION OF A TYPICAL FLIGHT

Figure 9 is a pictorial representation of an actual lifting body flight trajectory. The flight controller on the ground monitors radar plotting displays that show the flight paths of the B-52 airplane and the lifting body vehicle in plan and elevations. From this information, he guides the B-52 airplane to a predetermined launch point. Ten seconds before launch, timing is taken over by the lifting body pilot. He executes the release of the lifting body vehicle from the B-52 airplane and starts the rocket engine to obtain the high speed, high altitude point of the flight plan. Then, during the glide-descent, he performs a program of maneuvers to explore the vehicle's characteristics. To allow the lifting body pilot time to adequately perform these research maneuvers, the ground controllers assess the ground track and profile and update the flight plan with calls to the pilot. However, flights have been performed with no ground guidance to demonstrate the capability of the lifting body pilot to make his own judgment of the energy situation and maneuver to the desired landing point.

During the final approach to the landing, the pilot receives cross checks on air-speed and height above the ground from the escort pilot who is flying formation with him.

CONCLUDING REMARKS

Although the overall flight test program has not been without problems, it has progressed much like the early flight programs with any other new aircraft. Problems have been overcome in various ways, and, in so doing, confidence in the advantages of using lifting bodies as manned spacecraft has been gained.

The purpose of this symposium is to present the results from the flight-test program and the correlations of these data with predictions. Evaluations and impressions of the lifting body vehicles' overall handling qualities will also be presented by several of the pilots in the program. Finally, future plans for the lifting body flight program will be discussed.

THREE LIFTING BODY VEHICLES

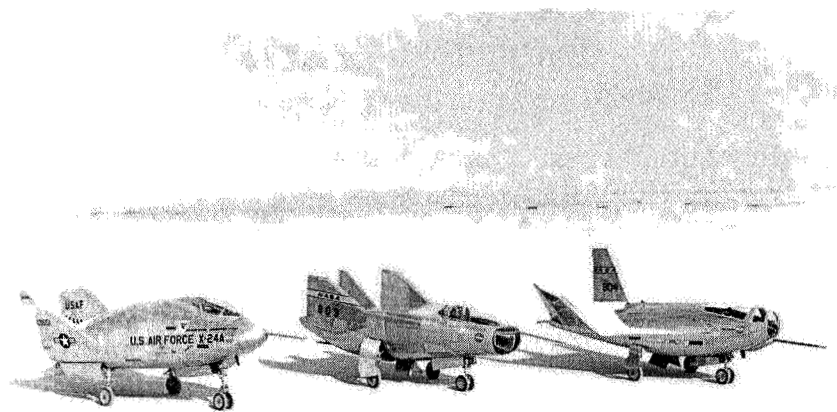


Figure 1

LIFTING BODY FLIGHT TEST VEHICLES

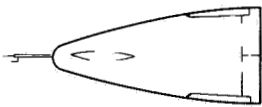
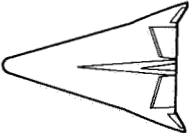
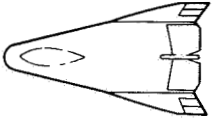


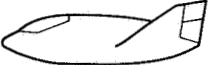
	M2-F2	HL-10	X-24A
			
			
BODY PLANFORM AREA, FT ²	160	160	191
BODY SPAN, FT	9.5	14.5	13.5
BODY LENGTH, FT	22	22	24.5
LANDING WT, LB	6150	6400	6000
LANDING WING LOADING, LB/ FT ²	38	40	31

Figure 2

CONTROL SURFACES ON THREE LIFTING BODY VEHICLES

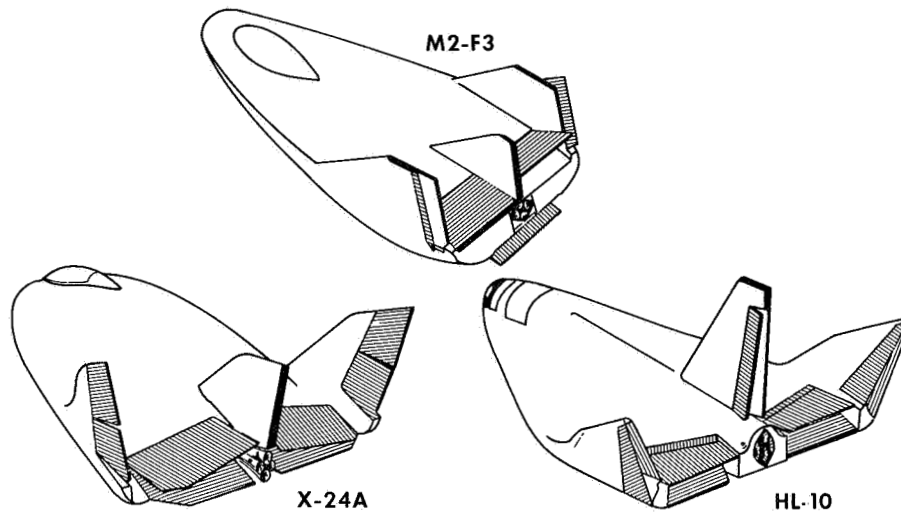


Figure 3

M2-F3 CONFIGURATION

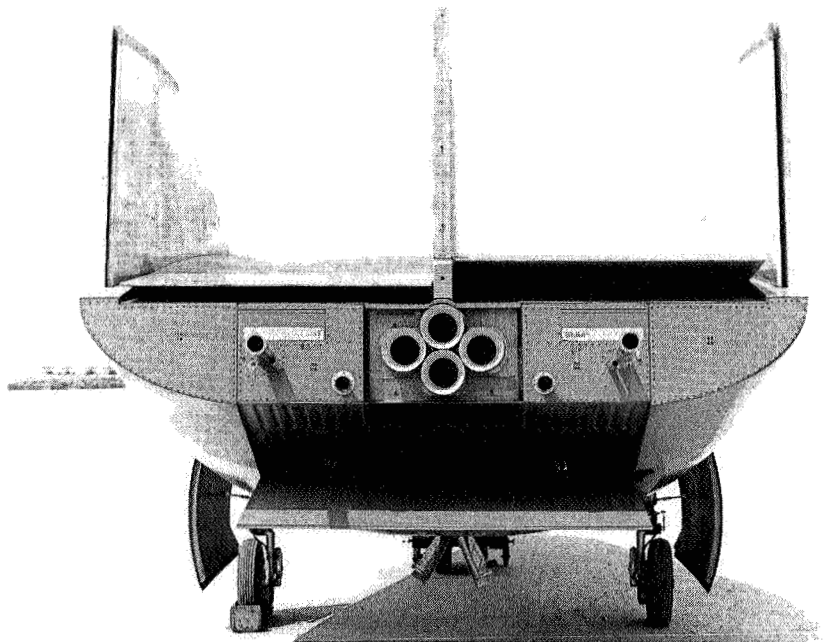


Figure 4

REAR VIEW OF THE HL-10

SUBSONIC

TRANSONIC

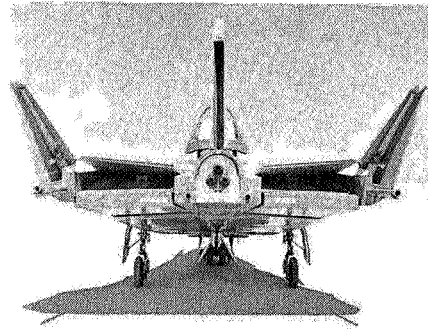
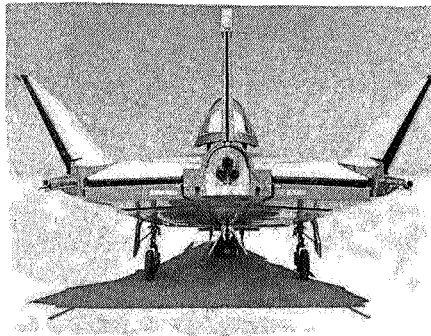


Figure 5

X-24A

SUBSONIC CONFIGURATION

TRANSONIC CONFIGURATION

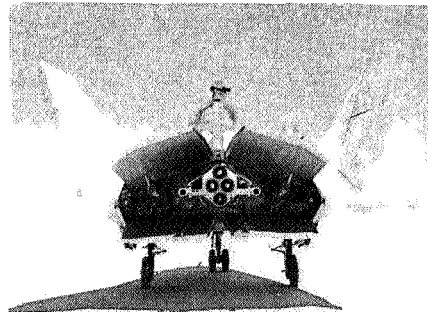
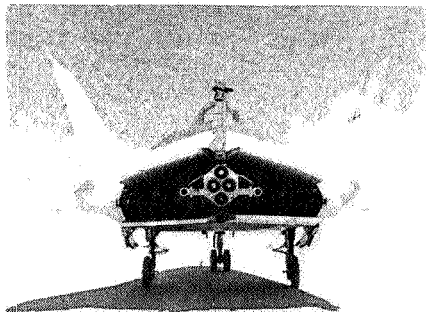


Figure 6

HL-10 FLIGHT ENVELOPE

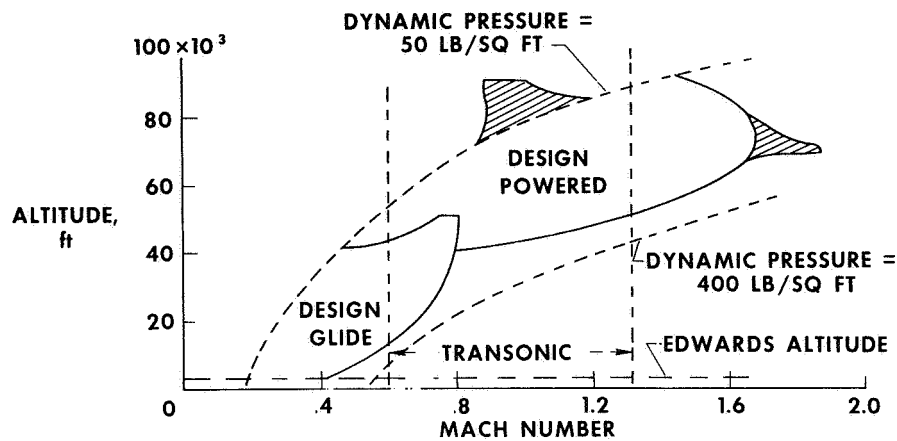


Figure 7

M2-F2/F3, HL-10, AND X-24A SCHEDULE OF EVENTS

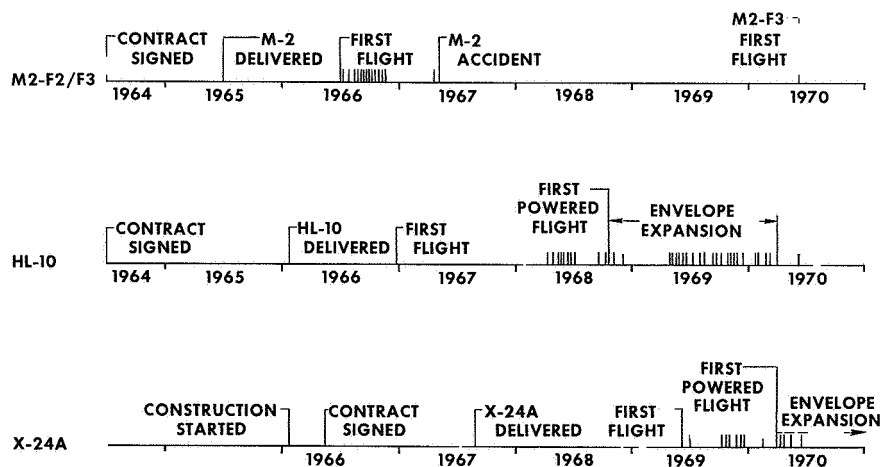


Figure 8

POWERED FLIGHT TRAJECTORY

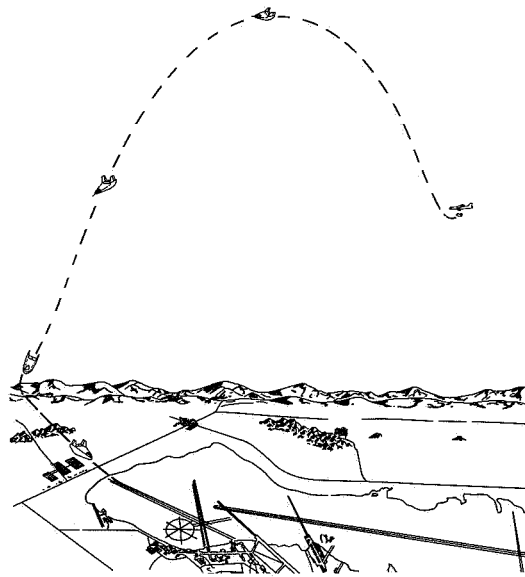


Figure 9

2. STABILITY AND CONTROL DERIVATIVES OF THE LIFTING BODY VEHICLES

By Robert W. Kempel, Larry W. Strutz,
NASA Flight Research Center

and Paul W. Kirsten
Air Force Flight Test Center

INTRODUCTION

Predictions of the flight characteristics of lifting bodies have been based almost exclusively on wind-tunnel data for small-scale models. A need thus exists to compare the results from small-scale and full-scale wind-tunnel tests with results from flight tests to establish some measure of the accuracy of the predictions and to assess the sensitivity of the vehicle's handling qualities to typical discrepancies between flight and wind-tunnel results. Comparisons of these types have been one of the primary objectives of the M2-F2, HL-10, and X-24A flight programs. In this paper the more important longitudinal and lateral-directional aerodynamic stability and control derivatives obtained from flight are compared with small- and full-scale wind-tunnel results where applicable. Significant trends and important differences are pointed out, and the implications discussed.

SYMBOLS

All derivatives, angles, and angular rates are referenced to vehicle body axes.

C_l	rolling-moment coefficient
C_{l_β}	effective dihedral derivative, $\frac{\partial C_l}{\partial \beta}$, per deg
$C_{l_{\delta_a}}$	aileron effectiveness derivative, $\frac{\partial C_l}{\partial \delta_a}$, per deg
$C_{l_{\delta_r}}$	rudder rolling-moment derivative, $\frac{\partial C_l}{\partial \delta_r}$, per deg
C_m	pitching-moment coefficient

$C_{m_q} + C_{m\dot{\alpha}}$	pitch-damping derivative, $\frac{\partial C_m}{\partial \left(\frac{q\bar{c}}{2V}\right)} + \frac{\partial C_m}{\partial \left(\frac{\dot{\alpha}\bar{c}}{2V}\right)}$, per rad
C_{m_α}	longitudinal static-stability derivative, $\frac{\partial C_m}{\partial \alpha}$, per deg
$C_{m\delta_e}$	pitch control effectiveness derivative, $\frac{\partial C_m}{\partial \delta_e}$, per deg
C_n	yawing-moment coefficient
$C_{n\beta}$	directional-stability derivative, $\frac{\partial C_n}{\partial \beta}$, per deg
$C_{n\delta_a}$	aileron yawing-moment derivative, $\frac{\partial C_n}{\partial \delta_a}$, per deg
$C_{n\delta_r}$	rudder effectiveness derivative, $\frac{\partial C_n}{\partial \delta_r}$, per deg
\bar{c}	mean aerodynamic chord, ft
M	Mach number
p	angular roll rate, deg/sec
q	angular pitch rate, deg/sec
r	angular yaw rate, deg/sec
V	velocity, ft/sec
α	angle of attack, deg
$\dot{\alpha}$	rate of change of angle of attack, deg/sec
β	angle of sideslip, deg
δ_a	aileron deflection, deg

δ_e	elevator deflection, deg
δ_r	rudder deflection, deg
δ_{rb}	rudder bias angle, deg

DISCUSSION

Determination of Flight Derivatives

Before each lifting body flight, a limited number of specific maneuvers are planned which excite the vehicle's natural modes of motion. The flight records obtained are displayed on a cathode ray tube by using a digital function generator. By manually adjusting the aerodynamic coefficients of the differential equations of motion (refs. 1 to 4) on a hybrid computer, a match of the flight records on the cathode ray tube is obtained. An error-minimizing match, weighted by the operator's judgment, provides the flight-determined derivatives.

Figure 1 shows a typical computer match of the flight time histories of an HL-10 lateral-directional maneuver at a Mach number of 1.2 and an angle of attack of 21.6° . The initial excitation was provided by a rudder doublet and terminated by an aileron doublet. This combination of control manipulation gave the fullest practical excitation of the lateral modes. The derivatives of the mathematical model of the computer were varied until the best possible simultaneous match was obtained for the complete response, as shown for the roll rate, yaw rate, and sideslip angle. This method of vehicle excitation and derivative analysis generally resulted in consistent and repeatable determinations of the derivatives.

Longitudinal Characteristics

The least troublesome mode in terms of derivative extraction and handling qualities was the longitudinal short-period mode. Results for this mode from each of the three test vehicles will be reviewed in this section.

M2-F2 vehicle.— Shown in figure 2 are the M2-F2 longitudinal pitch control effectiveness derivative $C_{m\delta_e}$ and static-stability derivative $C_{m\alpha}$ as a function of angle of attack for Mach numbers of 0.4 to 0.6. The involved control surface is shaded in the sketch. The flight-determined control effectiveness was generally higher than the predicted values over the entire angle-of-attack range. The static stability was found to be higher at the lower angles of attack but was in generally good agreement at the higher angles. Conversely, good agreement exists between full- and small-scale wind-tunnel results for the control effectiveness and the static-stability derivatives. The differences between flight and wind-tunnel data, however, had little effect on the dynamics of the vehicle and were not apparent to the pilot except for a noticeable difference in elevator setting required for trim. These differences were attributed to combined discrepancies in zero-lift pitching moment, static stability, and control effectiveness.

HL-10 vehicle.— Figure 3 shows $C_{m\delta_e}$ and $C_{m\alpha}$ values for the HL-10 vehicle in the subsonic configuration over the Mach number range of 0.4 to 0.7. The sketch shows the controlling surfaces. Here, as in figure 2, the flight results are generally higher than the wind-tunnel data. Also, there is a substantial difference between the small-scale and full-scale wind-tunnel results for control effectiveness; the small-scale data are in better agreement with flight results. Both the control effectiveness and static stability of the HL-10 vehicle are considerably higher than for the M2-F2 vehicle. These higher levels, in combination with a relatively low stick gearing required for overall maneuverability and trimmability, have caused pilot-induced-oscillation tendencies with the HL-10 vehicle during the landing approach and flare maneuver, particularly at reduced pitch stability-augmentation-system gains.

Although no data are presented, it should be mentioned that the general level of X-24A subsonic longitudinal static stability and control effectiveness is similar to that of the M2-F2 vehicle.

Damping.— Figure 4 presents the pitch-damping derivative $C_{m_q} + C_{m\dot{\alpha}}$ for all three vehicles at subsonic speeds as a function of angle of attack. The predicted range of the pitch-damping derivative for the three vehicles, which is based on limited wind-tunnel data and theoretical considerations, is between -0.3 and -0.4 per rad. The flight results for each of the three vehicles are generally higher than predicted. The pilots have consistently commented that the natural damping of the three vehicles was better than indicated on the flight simulators, which confirms the trend shown in this figure. This trend has, of course, been most apparent at the lower subsonic and transonic speeds.

HL-10 transonic configuration.— The HL-10 vehicle is the only lifting body that has been flown supersonically. Presented in figure 5 are the HL-10 pitch-damping, control effectiveness, and static-stability derivatives as a function of Mach number at an angle of attack of approximately 14° . The sketch shows the vehicle in the transonic configuration with the pertinent control surfaces shaded. The pitch damping determined from flight data is higher than predicted subsonically and lower than predicted supersonically. The flight control effectiveness is generally in good agreement with wind-tunnel data, but the stability levels are generally higher. The static stability decreases sharply between Mach numbers of 1.0 and 0.9. This decrease in stability was accompanied by a nose-up trim shift which caused some pilot concern because of the rapid rate at which it occurred as the vehicle decelerated from supersonic to subsonic speeds.

Lateral-Directional Characteristics

As pointed out previously, the longitudinal modes are generally the least troublesome in terms of derivative extraction and handling-qualities problems. Traditionally, the lateral-directional modes have been more difficult to analyze and have provided more than their share of handling-qualities problems. The M2-F2, HL-10, and X-24A vehicles have remained true to this tradition.

The M2-F2 vehicle may be regarded as an early attempt to achieve acceptable lateral characteristics with minimum compromise of an idealized reentry shape. The HL-10 vehicle, on the other hand, was subsequently tailored toward more favorable

lateral response characteristics while retaining the desired reentry performance. The X-24A vehicle may be described as a still later attempt to optimize the lateral stability and control design so that the effects on overall performance would be minimal. All three configurations, however, are characterized by low aspect ratio, low roll inertia, and relatively large vertical surfaces. Although a generally acceptable level of directional stability is obtained in each instance, the dihedral effect is very high and the roll control power relatively low by conventional standards. Consequently, each configuration has exhibited anomalous lateral behavior in some portions of its flight envelope.

HL-10 vehicle.— Figures 6 to 8 present the lateral-directional static-stability, aileron control, and rudder control derivatives, respectively, for the HL-10 subsonic configuration as a function of angle of attack at Mach numbers from 0.4 to 0.7. The applicable control surfaces are shaded in the sketches.

The flight results for the effective dihedral (fig. 6) are generally higher than the wind-tunnel data. The directional-stability derivative is in reasonable agreement with the small-scale data but is higher than the trend of the full-scale data.

The aileron control derivatives (fig. 7) determined from flight indicate that the control effectiveness derivative $C_{l_{\delta_a}}$ tends to be higher than the wind-tunnel predictions, whereas the flight values for the yawing-moment derivative $C_{n_{\delta_a}}$ generally scatter around the tunnel data. It should be noted that the aileron-induced yaw is positive, that is, favorable, for normally negative values of the effective dihedral derivative $C_{l_{\beta}}$.

In general, the HL-10 lateral handling characteristics were good, primarily because of the relatively low level of effective dihedral (in comparison with that of the M2-F2 or X-24A vehicles) and adequate aileron control characteristics. These results are particularly significant in that the HL-10 vehicle is less sensitive than the other lifting bodies to lateral disturbances such as turbulence because of its relatively low dihedral effect. Also, the ailerons are effective enough to provide adequate maneuverability and damping augmentation throughout the flight envelope. Because of the favorable yawing-moment characteristics, the HL-10 vehicle did not require a rudder-to-aileron interconnect for turn coordination.

The rudder control derivatives (fig. 8) are in good agreement with both full-scale and small-scale wind-tunnel results. The rolling-moment derivative $C_{l_{\delta_r}}$ is slightly higher than the small-scale predictions and agrees slightly better with full-scale results. The rudder effectiveness derivative $C_{n_{\delta_r}}$ is in very good agreement with the full-scale and small-scale data.

M2-F2 vehicle.— The M2-F2 lateral-directional characteristics were noticeably different from those of the HL-10 vehicle. Figures 9 to 11 show the results for the M2-F2 vehicle in essentially the same format as the three previous figures. The aileron yawing-moment characteristics determined from the first flight of the M2-F3 vehicle (center-fin version of the M2-F2 vehicle) are included to illustrate the primary effect of this modification.

The most apparent M2-F2 characteristic is the much higher effective dihedral derivative $C_{l_{\beta}}$ (fig. 9) than for the HL-10 vehicle. The dihedral effect and the

directional-stability derivatives both increase with angle of attack, whereas the HL-10 values were relatively invariant. For these two derivatives the flight results appear to correlate somewhat better with the full-scale wind-tunnel data than the small-scale data, even though there is considerable data scatter.

The aileron effectiveness derivative $C_{l\delta_a}$ (fig. 10) is lower than that for the HL-10 vehicle and is in generally good agreement with full-scale and small-scale wind-tunnel results. The aileron yawing moment for the M2-F2 vehicle is adverse, and the flight and wind-tunnel results are in good agreement. The large adverse aileron yaw of the M2-F2 vehicle, coupled with its high dihedral effect, resulted in roll reversal throughout the entire flight envelope. A rudder-to-aileron interconnect was essential to provide acceptable roll control. The lateral-directional dynamics were greatly influenced by the interaction of the adverse aileron yaw, aileron effectiveness, natural damping characteristics, and very high dihedral effect. These characteristics combined in such a way to produce coupling of the roll subsidence and spiral modes to form a lightly damped oscillatory mode, that is, the coupled roll-spiral mode which existed at low angles of attack and which tended to cause the vehicle to be sensitive to pilot-induced oscillations in the preflare approach flight conditions.

With the addition of a fixed center fin (M2-F3), the aileron yawing-moment derivatives became favorable, or proverse, as shown in figure 10, and limited flight evaluation indicated that the lateral handling qualities were satisfactory without the aid of an interconnect. In addition, there was no tendency toward lateral pilot-induced oscillations.

The rudder control derivatives (fig. 11) were generally in good agreement with wind-tunnel results. The flight-determined rudder rolling-moment derivative $C_{l\delta_r}$ was in slightly better agreement with full-scale wind-tunnel data than with small-scale data, whereas the rudder effectiveness derivative $C_{n\delta_r}$ scatters about both full-scale and small-scale wind-tunnel data.

X-24A vehicle.—As mentioned earlier, the X-24A vehicle was designed to optimize lateral stability and control so that the effects on overall performance would be minimal. Thus, stability and control characteristics of this vehicle have been sensitive to variations of the aerodynamic characteristics. Figures 12 to 14 present X-24A lateral-directional stability and control data in a format similar to that used for the HL-10 and M2-F2 vehicles.

Although the X-24A effective dihedral derivative (fig. 12) is approximately at the same high level as that for the M2-F2 vehicle, the directional-stability derivative diminishes noticeably with increasing angle of attack. Mach number effects have been apparent on the X-24A vehicle at Mach 0.6 and greater, particularly in the directional-stability derivative. At transonic Mach numbers this derivative becomes negative at higher angles of attack. More important, the X-24A aileron effectiveness (fig. 13) is substantially lower than that for the M2-F2 vehicle, which is lower than that for the HL-10 vehicle. As shown in the sketch, the controlling surfaces are on the lower surface of the vehicle. The general level of the aileron yawing-moment derivative also differs from that of the HL-10 and M2-F2 vehicles. Although wind-tunnel predictions are near zero, the flight results show slightly favorable values. These results have necessitated substantial modifications to the aileron-to-rudder interconnect, stability augmentation system, and aileron surface rates to obtain acceptable vehicle handling

characteristics. The lateral control and response characteristics of the X-24A vehicle have been particularly sensitive to very small variations of $C_{n\delta_a}$ because of the relatively low level of aileron effectiveness and very high effective dihedral.

The rudder rolling-moment derivative $C_{l\delta_r}$ (fig. 14) is considerably larger than that for the HL-10 or M2-F2 vehicles because of the use of the upper portion of the rudders for yaw control, as shown in the sketch. Flight data were in good agreement with full-scale wind-tunnel data, which were significantly lower than small-scale data. The rudder effectiveness derivative $C_{n\delta_r}$ is presented only for the small-scale wind-tunnel data at a rudder bias of 0° and -10° . Full-scale wind-tunnel data for 0° rudder bias were generally 10 percent lower than small-scale data and at -10° rudder bias were 10 percent to 15 percent lower below 6° angle of attack. The wind-tunnel data were in relatively good agreement above 8° angle of attack. Flight data at 0° rudder bias were in good agreement with wind-tunnel data, with a slightly lower trend at a rudder bias of -10° .

Transonic characteristics of the HL-10 and X-24A vehicles.—Although much transonic flight testing still lies ahead for the X-24A vehicle, some trends for the HL-10 and X-24A vehicles have become apparent. The HL-10 vehicle, for example, experienced a divergent Dutch roll mode oscillation on three separate occasions. These divergencies occurred near Mach 1.2 and above 20° angle of attack. Figures 15 and 16 present the effective dihedral, directional stability, and aileron control characteristics of the HL-10 vehicle as a function of angle of attack at a Mach number of 1.2. Above an angle of attack of 20° , the flight-determined values for the directional-stability derivative $C_{n\beta}$ and aileron control effectiveness derivative $C_{l\delta_a}$ show continuing downward trends. The aileron yawing-moment derivative $C_{n\delta_a}$ from flight continues upward well above the wind-tunnel trend. This combination of derivatives was shown to produce a divergent Dutch roll tendency induced by the roll stability augmentation system. These divergent oscillations, however, did not present particularly difficult problems. Recovery in each situation was accomplished by decreasing the angle of attack.

Limited transonic data have also been obtained for the X-24A vehicle. Figure 17 shows the variations of the effective dihedral and directional-stability derivatives with Mach number for an angle of attack of approximately 14° . Above a Mach number of about 0.5, the directional-stability derivative drops sharply and becomes negative in the Mach range from 0.8 to 1.2. This reduction in $C_{n\beta}$ with Mach number has been associated with flow separation over the tip fins as determined by visual studies and by hinge-moment analysis. Static lateral-directional stability is retained, however, because of the high level of effective dihedral. No handling-qualities problems have been encountered.

CONCLUDING REMARKS

For the M2-F2, HL-10, and X-24A vehicles the flight-determined values of longitudinal stability and control derivatives, particularly in pitch damping, were higher

than wind-tunnel values. The effects of these differences on the overall handling qualities, however, were of little consequence.

The flight-determined lateral-directional stability and control derivatives were found, for the most part, to be in fair agreement with wind-tunnel predictions. Each of the three vehicles exhibited very high dihedral effect, which tended to greatly influence lateral dynamic characteristics. The HL-10 vehicle had lower dihedral effect, higher aileron control effectiveness, and more favorable yaw due to aileron deflection than the M2-F2 and X-24A vehicles. The M2-F2 vehicle had high adverse aileron yaw, which necessitated a high authority rudder-to-aileron interconnect. Incorporation of a center fin eliminated the adverse aileron yaw and the need for an interconnect. The X-24A lateral stability and handling characteristics were very sensitive to differences in aileron yawing-moment characteristics because of the vehicle's low directional stability, low aileron effectiveness, and very high dihedral effect.

REFERENCES

1. Rampy, John M. ; and Berry, Donald T. : Determination of Stability Derivatives From Flight Test Data by Means of High Speed Repetitive Operation Analog Matching. Tech. Doc. No. 64-8, Air Force Flight Test Center, U. S. Air Force, May 1964.
2. Taylor, Lawrence W. , Jr. ; Iliff, Kenneth W. ; and Powers, Bruce G. : A Comparison of Newton-Raphson and Other Methods for Determining Stability Derivatives From Flight Data. Paper 69-315, AIAA, Mar. 1969.
3. Yancey, Roxanah B. ; Rediess, Herman A. ; and Robinson, Glenn H. : Aerodynamic-Derivative Characteristics of the X-15 Research Airplane as Determined From Flight Tests for Mach Numbers From 0.6 to 3.4. NASA TN D-1060, 1962.
4. Wolowicz, Chester H. : Considerations in the Determination of Stability and Control Derivatives and Dynamic Characteristics From Flight Data. AGARD Rep. 549-Part 1, 1966.

TYPICAL COMPUTER MATCH **TRANSONIC CONFIGURATION; HL-10; $M = 1.2$; $\alpha = 21.6^\circ$**

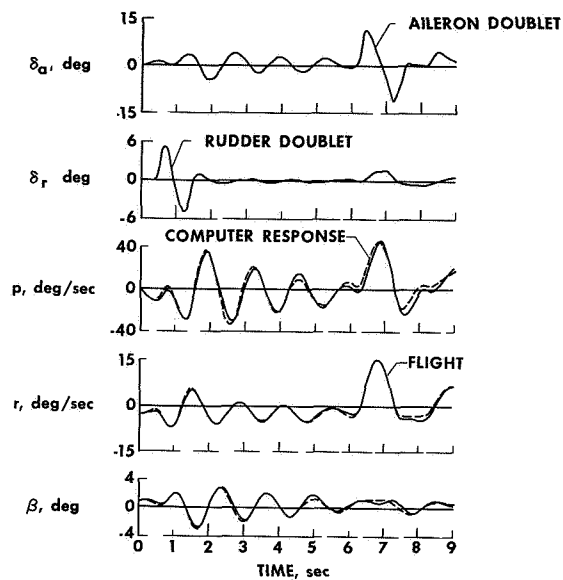


Figure 1

M2-F2 LONGITUDINAL STABILITY AND CONTROL EFFECTIVENESS

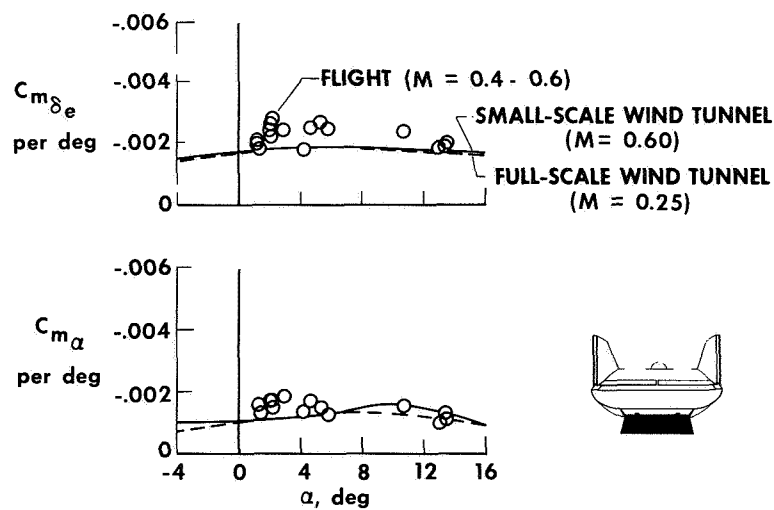


Figure 2

HL-10 LONGITUDINAL STABILITY AND CONTROL EFFECTIVENESS

SUBSONIC CONFIGURATION

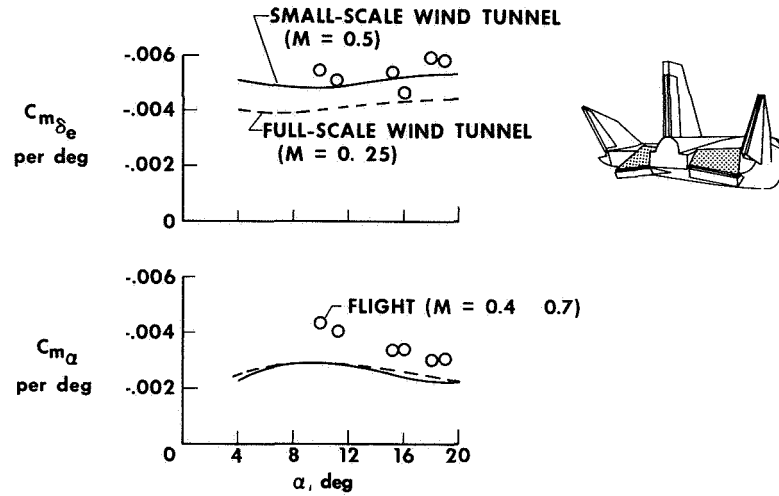


Figure 3

LONGITUDINAL DAMPING CHARACTERISTICS

$M \approx 0.5$

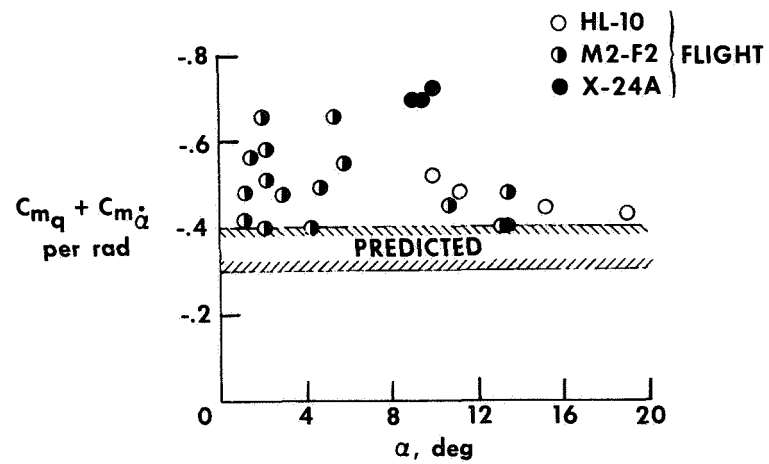


Figure 4

HL-10

LONGITUDINAL AERODYNAMIC CHARACTERISTICS

TRANSONIC CONFIGURATION; $\alpha \approx 14^\circ$

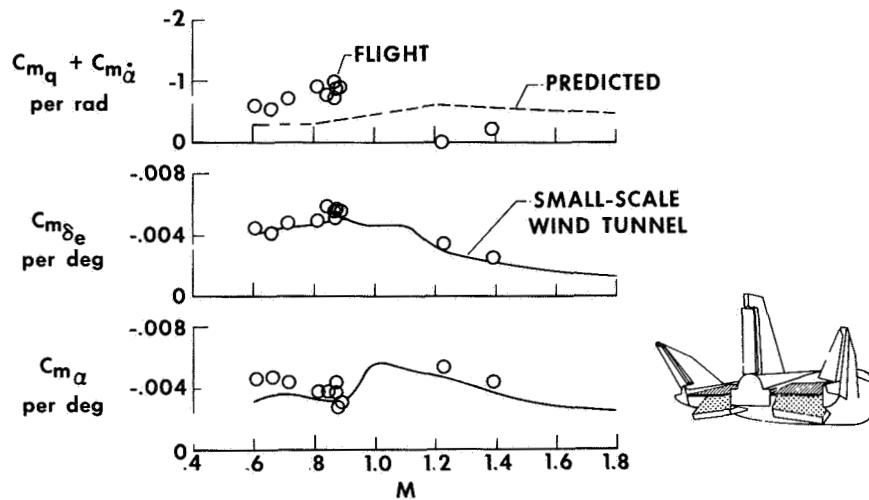


Figure 5

HL-10 LATERAL-DIRECTIONAL STATIC STABILITY

SUBSONIC CONFIGURATION

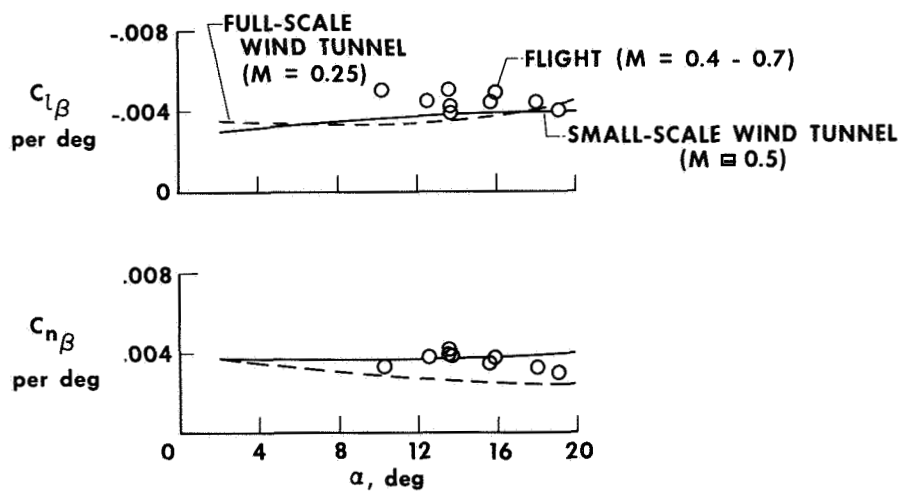


Figure 6

HL-10 AILERON CONTROL CHARACTERISTICS

SUBSONIC CONFIGURATION

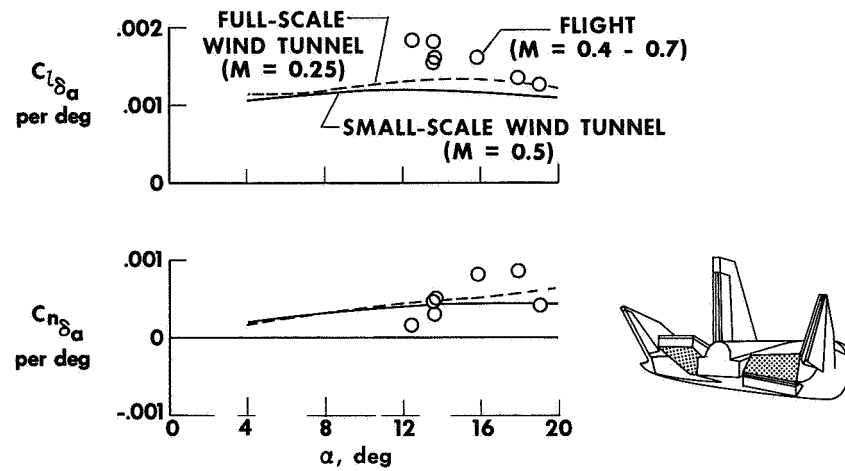


Figure 7

HL-10 RUDDER CONTROL CHARACTERISTICS

SUBSONIC CONFIGURATION

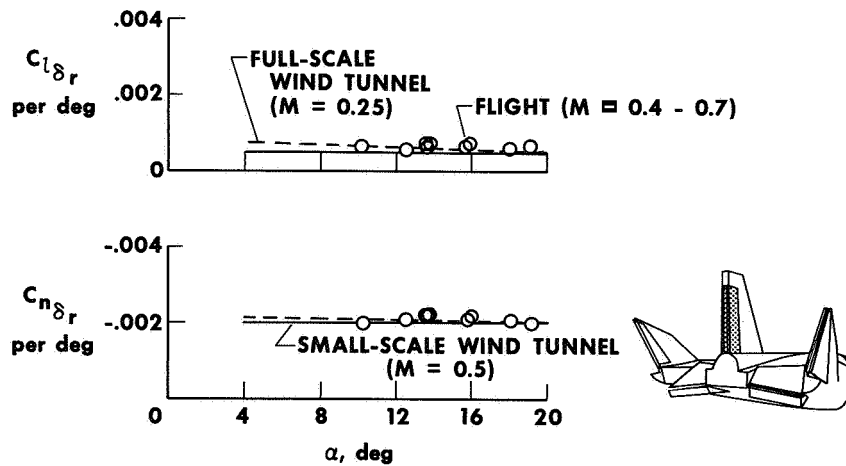


Figure 8

M2-F2 LATERAL-DIRECTIONAL STATIC STABILITY

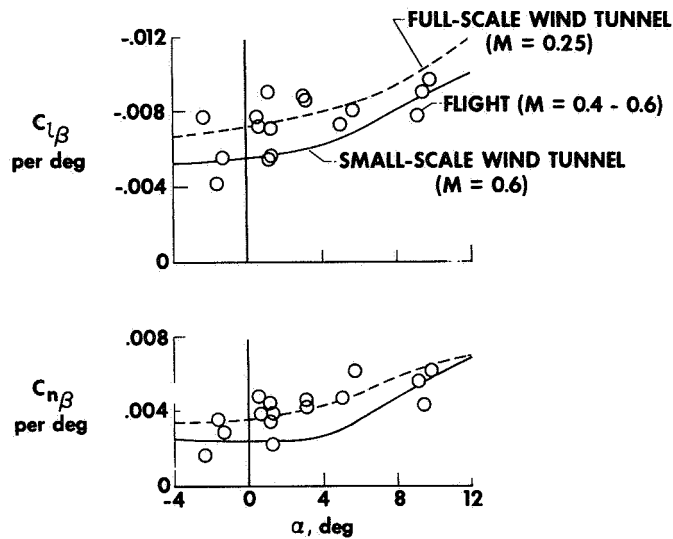


Figure 9

M2-F2 AILERON CONTROL CHARACTERISTICS

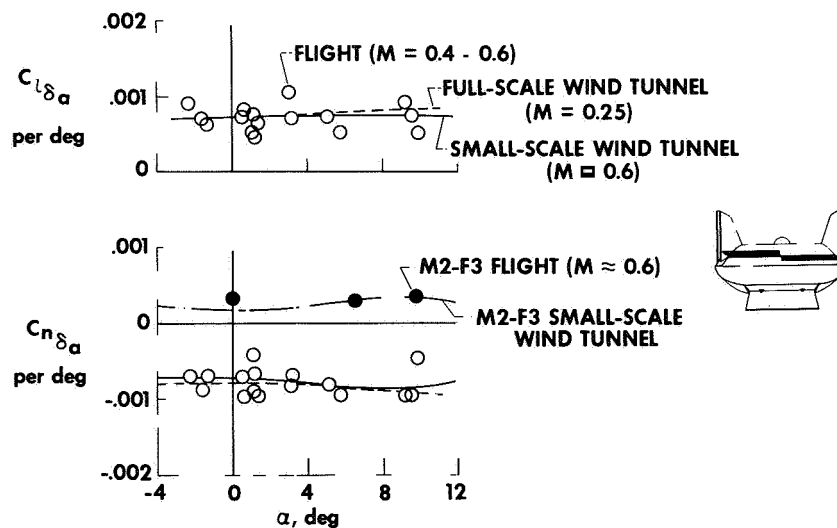


Figure 10

M2-F2 RUDDER CONTROL CHARACTERISTICS

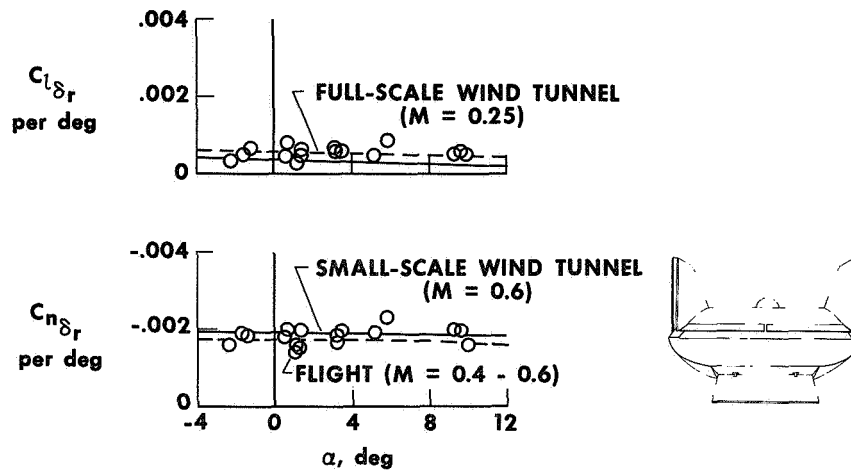


Figure 11

X-24A LATERAL-DIRECTIONAL STATIC STABILITY SUBSONIC CONFIGURATION

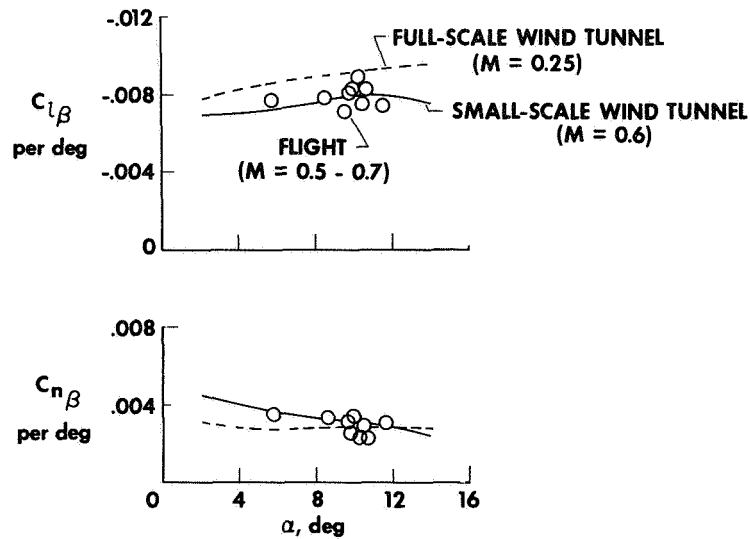


Figure 12

X-24A AILERON CONTROL CHARACTERISTICS SUBSONIC CONFIGURATION

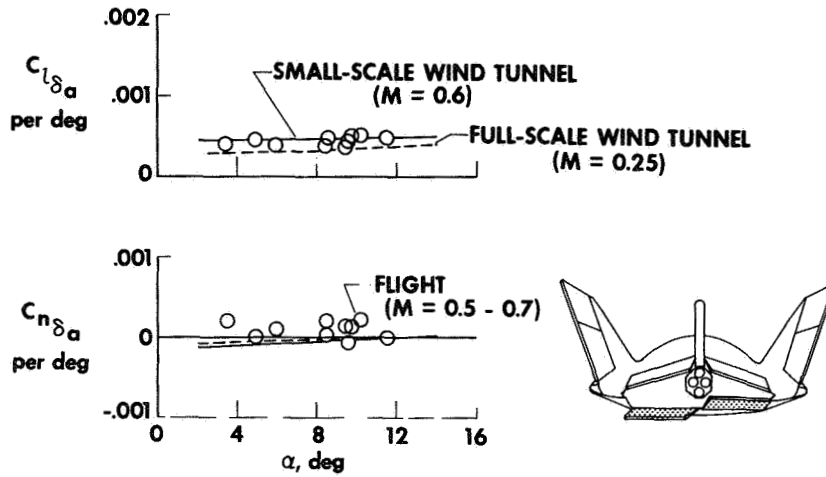


Figure 13

X-24A RUDDER CONTROL CHARACTERISTICS SUBSONIC CONFIGURATION

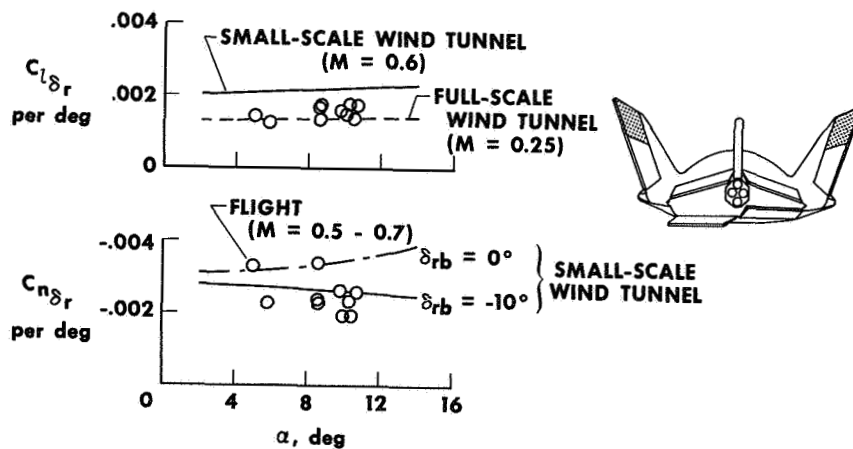


Figure 14

HL-10 LATERAL-DIRECTIONAL STATIC STABILITY

TRANSONIC CONFIGURATION; $M = 1.2$

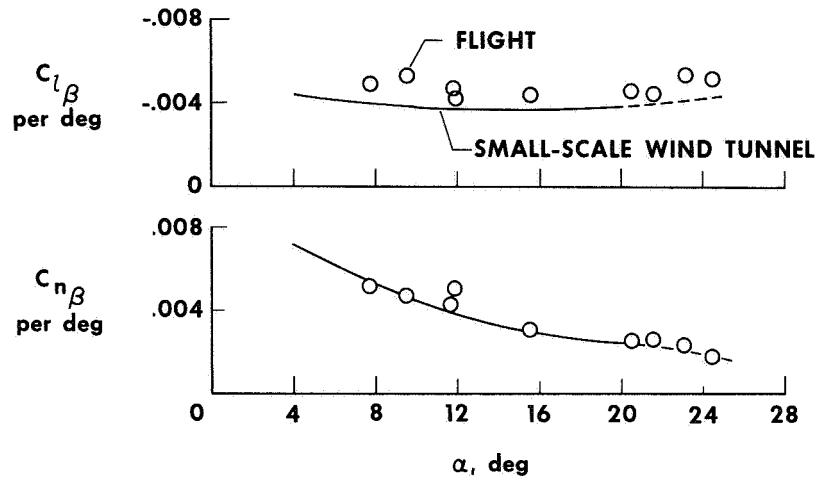


Figure 15

HL-10 AILERON CONTROL CHARACTERISTICS

TRANSONIC CONFIGURATION; $M = 1.2$

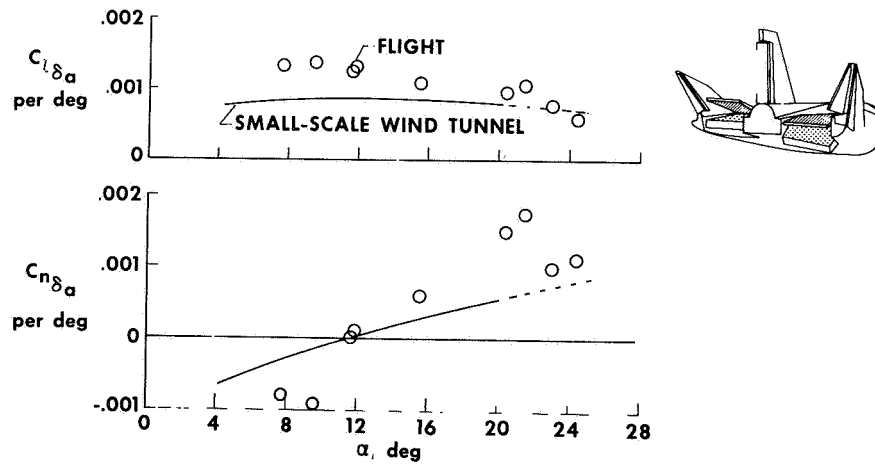


Figure 16

X-24A LATERAL-DIRECTIONAL STATIC STABILITY **TRANSONIC CONFIGURATION; $\alpha \approx 14^\circ$**

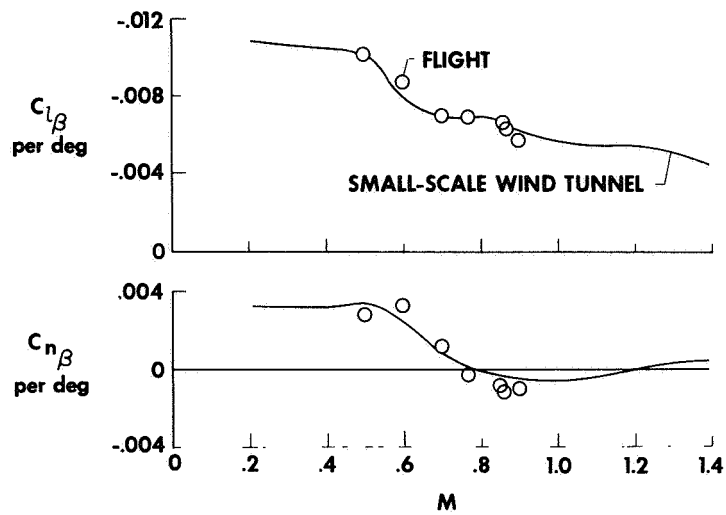


Figure 17

3. ASSESSMENT OF LIFTING BODY VEHICLE HANDLING QUALITIES

By John A. Manke,
NASA Flight Research Center

John P. Retelle,
Air Force Flight Test Center

and Robert W. Kempel
NASA Flight Research Center

3

INTRODUCTION

Handling qualities have always been vitally important to the pilot. Before the current series of lifting body flight tests, there was speculation and concern about how this class of wingless vehicle would handle. The general behavior of the three lifting bodies in flight is described in broad terms in this paper, and some specific examples of behavior that may be of special interest from the pilot's viewpoint are presented. In addition, comments are offered concerning simulation requirements.

SYMBOLS

C_L	lift coefficient, $\frac{\text{Lift}}{qS}$
$C_{n\delta_a}$	aileron yawing-moment derivative, per deg
I_{XZ}	product of inertia, slug-ft ²
I_Z	moment of inertia about Z-body axis, slug-ft ²
L_β	dihedral effect or rolling moment due to sideslip, $\frac{1}{\text{sec}^2}$
M	Mach number

N_β	directional stability or yawing moment due to sideslip, $\frac{1}{\text{sec}^2}$
N_β^*	dynamic directional stability, $\frac{1}{\text{sec}^2}$
p	rolling angular velocity, deg/sec
q	dynamic pressure, lb/ft ²
S	reference planform area, ft ²
α	angle of attack, deg
β	angle of sideslip, deg
$\delta_{a_{\text{stick}}}$	lateral stick deflection, in.
δ_e	pilot's input to elevator, deg
δ_{ef}	elevator flap position, deg
φ	angle of bank, deg

DISCUSSION

General Flight Behavior

In general, lifting body vehicles fly like conventional aircraft, although they do not behave like their winged counterparts in every detail. Figure 1 shows the envelope achieved by the HL-10 vehicle in terms of angle of attack and Mach number. The transonic configuration was used for flight above Mach 0.7. In this configuration, the handling qualities do not appear to change significantly with Mach number, except that damping seems to decrease somewhat with increasing Mach number, particularly in the pitch axis. With the dampers on, pilot ratings were generally in the 2 to 3 range of the Cooper-Harper rating scale, indicating that minimal pilot compensation was required for desired performance. With the dampers off, the HL-10 handling qualities are surprisingly good. Considerable maneuvering was performed, and numerous configuration changes were made with all dampers off. Pilot ratings were in the 4 to 5 range,

indicating that considerable pilot compensation was required for desired performance but was primarily a nuisance factor. All the pilots believe that the vehicle is completely flyable with the dampers off in this configuration and that a mission could be completed successfully. Typical pilot comments indicate that with the dampers off the vehicle has high control sensitivity in the roll axis and particularly good damping in the pitch axis. The crosshatched area in the upper right corner of the envelope defines an area of lateral instability which is apparent as a dampers-induced, neutrally damped Dutch roll of relatively low frequency. It was of no particular concern to the pilot. The $N_{\beta} = 0$ area was not investigated in flight.

The transition between configurations is normally made between Mach 0.6 and 0.7, as indicated by the shaded area. At Mach numbers below this region, the HL-10 vehicle is flown in the reduced drag, subsonic configuration. In this configuration, dampers-on pilot ratings averaged between 2 and 2.5 in all axes. Pilot comments indicate that the handling qualities were as good as or better than most current fighter aircraft. Dampers-off handling qualities in this configuration are even better than in the transonic configuration. Frequently comments were made that the HL-10 vehicle with its dampers off handles better than an F-104 airplane with its dampers off. The area of high pitch sensitivity in the approach will be discussed in detail later. As a point of interest, zero lift on the HL-10 vehicle occurs at 4° to 6° angle of attack.

Figure 2 is the flight envelope for the X-24A vehicle. In the transonic configuration, the primary difference between the X-24A and the HL-10 vehicles is that the X-24A vehicle has considerably lower roll response than the HL-10 vehicle, as shown by the region at high angle of attack, but the response is still considered adequate for the mission. Because of the high dihedral effect and high value of ϕ/β , small angle-of-sideslip excursions produce an occasional nuisance type of roll input.

In the transonic region, the X-24A vehicle has been flown many times beyond the $N_{\beta} = 0$ boundary indicated on the envelope. This will also be discussed in more detail later. The vehicle has not been flown enough with the dampers off in the transonic configuration to warrant comment at this time.

In the subsonic configuration, some lateral-directional problems manifested themselves during the first few flights. However, control system modification and changes in roll and yaw damper gains have improved the handling qualities so that they are now as good as those of the HL-10 vehicle. In fact, the longitudinal handling qualities of the X-24A vehicle are superior to those of the HL-10 vehicle during approach and landing.

Although flight results have been gratifying, it is important to note that only one of the lifting bodies has flown beyond Mach 1, and to imply that there will not be problems with the other two vehicles would be presumptuous. On the last flight of the X-24A vehicle, controllability problems appeared at about Mach 0.96 and low angles of attack. These problems were not predicted by the wind-tunnel data, which points out the absolute necessity for a comprehensive flight-test program paced by a cautious exploration of potential problem areas.

Longitudinal Handling Characteristics

In general, the longitudinal handling qualities of the three vehicles have been conventional except for a few trim change problems that may be inherent in this class of vehicle. One of the major concerns before the HL-10 vehicle was flown in the transonic configuration was the large longitudinal trim change resulting from transitioning between the subsonic and transonic configurations. The simulation studies indicated that relatively large excursions in angle of attack and normal acceleration would occur during the transition because of the large change required in longitudinal stick position. They also indicated that the best technique would be to change configuration in several steps. However, figure 3 shows pleasant results of the flight program: maintaining a constant angle of attack during the configuration change was absolutely no problem. The pilot was able to maintain nearly constant angle of attack despite the large change in longitudinal stick position in the 5 seconds it took to reconfigure the vehicle. Additionally, it was found that the best technique was to change the configuration in one continuous motion. Apparently, the motion and visual cues in actual flight significantly reduced the piloting task.

For the X-24A vehicle, the rudder position was biased automatically as a function of deflection of the upper flaps to significantly reduce the trim change resulting from configuration changes. The rudder bias provides a pitching moment that counteracts the pitching moment of the flaps. It would be ideal to have an automatic mode that would change total flap wedge angle continuously as a function of Mach number. The X-24A vehicle has this automatic capability, but it has not yet been utilized. First, the flap wedge angle versus Mach number curve must be determined exactly. A failure or miscalculation in the automatic mode could produce a completely unflyable vehicle in a few seconds.

Simulation studies indicated a sizable trim change in the Mach range of 0.95 to 1.0, but they also indicated that this region would be traversed at a rate that would present no great piloting problem. In flight, however, most of the trim change occurred in a much smaller Mach number range, between 0.97 and 0.96. During the deceleration phase of the flight, this Mach range was crossed so rapidly that the trim change appeared to the pilot initially as a constant speed pitchup. With more experience, it was found that there was an optimum angle of attack that could be used to minimize the pitchup problem. In addition, the time of onset could be predicted accurately; therefore, on later flights the pitchup never came as a surprise. This area was eventually traversed with the pitch damper off with no significant problems. The important point is that wind-tunnel data should be obtained at very close intervals near Mach 1 in order to have the best information possible with which to analyze the transonic trim change.

During the powered flight program of the HL-10 vehicle, no significant trim change due to rocket engine thrust was detected. The X-24A vehicle, on the other hand, exhibits a marked trim change with thrust. Computations indicate that a misalignment of approximately 7 inches between the rocket engine centerline and the vehicle center of gravity would be required to account for the flight-measured trim change. However, precise measurements indicate a misalignment of less than 2 inches. At this time there is no satisfactory explanation for the effect, although it is suspected that aerodynamic effects resulting from the engine exhaust plume contribute significantly to the problem. In powered flight, the X-24A exhaust plume is deflected upward in rooster

tail fashion. Because it is a nose-up trim change, the upward deflected plume is probably significant. As a result of the trim change with thrust, the low angles of attack originally predicted during powered flight cannot be attained. An effect such as this could produce undesirable aerodynamic forces during the boost phase of a shuttle operation. It might also be a problem during approach and landing if landing engines are used. We intend to investigate the problem further.

A very undesirable characteristic of the M2-F2, M2-F3, and X-24A vehicles that is in the category of a trim change is a substantial nose-down pitching moment at landing gear extension. In the lifting body flights the landing gear is extended just before touchdown. Because of this gear transient, touchdown on one of the early M2-F2 flights occurred less than 1 second after gear extension. This particular characteristic causes the pilot a great deal of concern, particularly on his first few flights. He eventually learns to partially compensate for the effect by leading with aft stick motion, but even then it is considered to be unsatisfactory. For a practical operational shuttle the gear and gear doors should be designed so that the landing gear can be extended early enough in the pattern to alleviate pitch transient problems without incurring a large decrease in lift-to-drag ratio. From our lifting body experience, we do not like extending the gear 20 feet above the ground, and we do not like large gear transients.

Flight Research Center experience with rate command control systems in the X-15 and F-111 aircraft indicates that this type of control system can probably alleviate most longitudinal trim changes. We believe that a rate command control system, particularly in the pitch axis, should be given considerable attention in shuttle design.

The longitudinal handling qualities on the early flights of the HL-10 vehicle indicated a pilot-induced-oscillation tendency. Figure 4 shows that about 60° of elevator authority for 9 inches of longitudinal stick travel was afforded to adequately provide trim over the operational Mach/angle-of-attack range. This high gearing ratio was a result of the requirement for two configurations. The subsonic configuration operates in the negative elevon range and the transonic configuration in the positive elevon range. After the first flight, it was apparent that the gearing ratio had to be decreased. Flight data indicated that only 38° of total elevator travel would be necessary to cover the required Mach/angle-of-attack envelope. Several ranges of gearing ratios were tried. The figure shows the maximum and minimum gearing ratios that were used and the ratio that was ultimately arrived at. The final configuration is nonlinear to provide the lower gearing ratio required for landing and at the same time provide for the elevator range required for supersonic trim. Also, the elevator range used for approach and landing required less than 1 inch of stick deflection on the first flight. The present gearing ratio requires almost 2 inches of longitudinal stick deflection. Even with the present gearing, the pilots indicate that the vehicle is somewhat sensitive during the landing phase, but it is still acceptable. It should be pointed out that these changes to the control system were possible only because the original design provided the mechanism with which the control system could be modified quickly. This built-in flexibility is a feature of all three lifting bodies.

Lateral-Directional Handling Characteristics

The lifting body configurations have many similar lateral-directional

characteristics. They have relatively high dihedral effect and low roll moments of inertia, and they may have relatively low directional stability. Natural roll damping, normally provided by wings, is conspicuously absent. The lateral control surfaces are necessarily quite close to the rolling axis and are relatively ineffective. The flow field produced over the upper rear surfaces of these vehicles results in very large interaction effects between the horizontal and vertical control surfaces. For example, the rolling moment produced by rudder deflection can be easily as large as the rolling moment produced by the ailerons. The combination of these effects, occurring simultaneously, has produced unusual dynamic lateral responses to control inputs and turbulence.

It was apparent with the X-24A vehicle that very low values of directional stability might be expected in the flight region traversed during the transition to climbout on high performance flights. Figure 5 shows the zero directional-stability boundary ($N_\beta = 0$) for the X-24A vehicle. A more realistic boundary for defining directional-stability limits is shown as $N_\beta^* = 0$. This parameter relies on the high dihedral of the vehicle to increase the effective directional stability. Simulator studies show that aircraft stability remains acceptable until the N_β^* boundary is approached, at which time the vehicle becomes statically unstable. The shaded area in the figure represents the approximate angle-of-attack and Mach number conditions during rotation for the maximum performance flight. The symbols represent actual flight-test maneuvers flown with a negative N_β . Pilot comments indicate that there was no perceptible change in flight characteristics as the $N_\beta = 0$ boundary was crossed. Additional data will be obtained on future flights to extend the flight envelope to the desired maximum performance operating point. The results obtained confirm that lifting body configurations are flyable with negative body axis N_β .

Another area of concern, particularly with the X-24A and M2-F2 vehicles, is low roll control power and apparent roll reversal. Aileron deflections can produce large yawing moments in addition to the desired rolling moments. These large yawing moments couple with the large dihedral to either augment or inhibit the commanded roll. For adverse yaw due to aileron, this reduces the effective aileron roll power and sometimes causes an aileron reversal. To reduce the effects of adverse yaw, a rudder-to-aileron interconnect is used on the X-24A and M2-F2 vehicles. The HL-10 and X-24A vehicles were also designed with canted hinge lines for the flaps in an attempt to minimize the yaw due to aileron. Figure 6 shows how the X-24A roll power, in terms of steady-state roll rate per stick deflection, varies with angle of attack at Mach 0.9. Flight experience has verified the effectiveness of the interconnect indicated by the simulator data. The line at $p/\delta_{a\text{stick}} = 0$ represents the roll reversal boundary. The higher percentages of interconnect gain permit the vehicle to fly at higher angles of attack before roll reversal is encountered. The dashed line represents the automatic programming of interconnect with angle of attack. The HL-10 vehicle does not have this roll control problem and consequently does not require an interconnect. Also, wind-tunnel data and results from the first M2-F3 flight indicate that the center fin modification minimized the yaw due to aileron (which was characteristic of the M2-F2 vehicle) so that an interconnect is not required, although the vehicle does have the capability built in.

At certain flight conditions and damper gains, the X-24A and M2-F2 vehicles

exhibit an unorthodox lateral-directional mode of motion, the coupled roll-spiral mode, often referred to as a "lateral phugoid." The significance of this mode can be illustrated by examining the solution to the lateral-directional characteristic equation of motion for the basic vehicle and the pilot's control actions as he attempts to maneuver or maintain wings-level flight. Figures 7 and 8 show the lateral-directional modes of motion and a time history of aircraft motion in roll for a conventional aircraft. In figure 7, which is a classical mathematical solution to the aircraft modes of motion in root-locus format, damping increases along the X-axis to the left, and frequency increases along the Y-axis. The pole locations from the solution of the characteristic equation are shown: an oscillatory Dutch roll mode, a heavily damped roll mode, and a neutrally stable spiral mode. As the flight conditions change, the Dutch roll pole moves about, and the roll and spiral modes move back and forth along the X-axis. The arrows indicate what happens if the control feedback loop is closed by a pilot who is trying only to maintain a specific bank angle. The Dutch roll pole will close on the Dutch roll zero and vary the damping for both the roll and spiral modes, as shown by the arrows.

Figure 8 is a time history of bank angle and pilot lateral control stick inputs during a control task of rolling to and stabilizing at a given bank angle and then rolling back to wings level. The data show the pilot's ability to be precise with very little aileron motion. The aircraft settles on the desired attitude after the transient motion, which was caused by the Dutch roll mode and pilot feedback.

Figures 9 and 10 are root-locus and time history plots, similar to the preceding two figures, of the lateral-directional modes of motion that may occur for lifting bodies. Normally, the modes of motion of a lifting body are similar to those of conventional aircraft; however, certain combinations of damper gains and flight conditions may cause the roll and spiral mode poles to meet on the X-axis and form the coupled roll-spiral mode. This mode is oscillatory, of rather low frequency, and lightly damped, if at all. Figure 9 shows the unstable pole position. The pilot's efforts to command a bank angle produce the closure, as shown by the arrows. The roll-spiral pole closes on the Dutch roll zero and in so doing becomes more unstable. Figure 10 shows the high frequency Dutch roll motion and the lower frequency and longer period motion that result when the coupled roll-spiral becomes divergent. As shown, the pilot was unable to regain control of the aircraft.

Theoretical predictions and simulator studies have been used to identify flight regions and stability-augmentation-system gain combinations at which the coupled roll-spiral mode may be encountered. On the simulator, the problem appears to be dangerous, since the motion frequency is low and oscillations of fairly large amplitude can develop before the pilot realizes the seriousness of the situation. We have attempted to avoid these areas on M2-F2 and X-24A flights; however, we do plan to cautiously explore the coupled roll-spiral mode on future flights of the X-24A vehicle.

The coupled roll-spiral mode is sensitive to so many parameters that it is impossible to present a simple solution to the problem. Because the space shuttle configuration may be susceptible to the coupled roll-spiral mode, however, we would recommend early analysis to determine if such a mode exists. Its presence may dictate some modification in basic aerodynamic design, or it could constitute a challenge to the control systems specialist.

Simulation

All our lifting body flight programs were prefaced by an extensive simulator study. Generally, the simulation has been accurate, although each of the lifting bodies exhibited early handling-qualities problems that were not predicted by the simulation studies. Because control system requirements are based on simulation studies, it is important that good wind-tunnel data be available early in the program to facilitate an early simulation. A large wind-tunnel error could have serious effects on a program, as with the X-24A vehicle for which the flight-derived value of $C_{n\delta_a}$ was opposite in sign to wind-tunnel data in some flight regions. This type of error is significant in a vehicle that uses a rudder-to-aileron interconnect to compensate for adverse or proverse yaw.

Some difficulty has been experienced in predicting problems associated with the pilot in the loop, particularly in the approach and landing. In these phases of the mission, pilot gain is much higher in flight than in simulation, and motion and visual cues are used extensively by the pilot. In addition, the simulation has not accurately predicted the effects of turbulence, particularly the pilot's reactions to turbulence upsets.

For the shuttle vehicle, the complete integration of the pilot in the program at the earliest possible time is essential. Handling-qualities specifications relate and integrate a variety of experience and background and, therefore, form a useful guide to a designer. However, if the proper simulation techniques are used, a team of experienced test pilots, working with engineers, can establish the best compromise of basic stability, control, and augmentation for the specific shuttle mission. In all such studies a careful estimate of possible uncertainties in critical stability and control parameters should be made, and the design decisions should be based on the most pessimistic derivatives.

The requirement for an in-flight performance simulator for technique determination and pilot training in the approach and landing phases of the mission should be emphasized. Fixed-base simulators have been inadequate for these flight phases. In the lifting body program, F-104 aircraft, configured to represent lifting body lift-to-drag ratios, are used successfully for this purpose. More than 6000 approaches have been flown in F-104 aircraft in support of the lifting body program.

CONCLUDING REMARKS

Although the lifting body vehicles have been susceptible to a number of problems, some unique, it has been demonstrated that, with proper attention to preflight development and an aggressive flight development program, these vehicles can be made to handle as well as more conventional aircraft. A small team of dedicated engineers and pilots, working together, can provide shuttle vehicles that will handle as well as or better than current transport airplanes.

HL-10 FLIGHT ENVELOPE

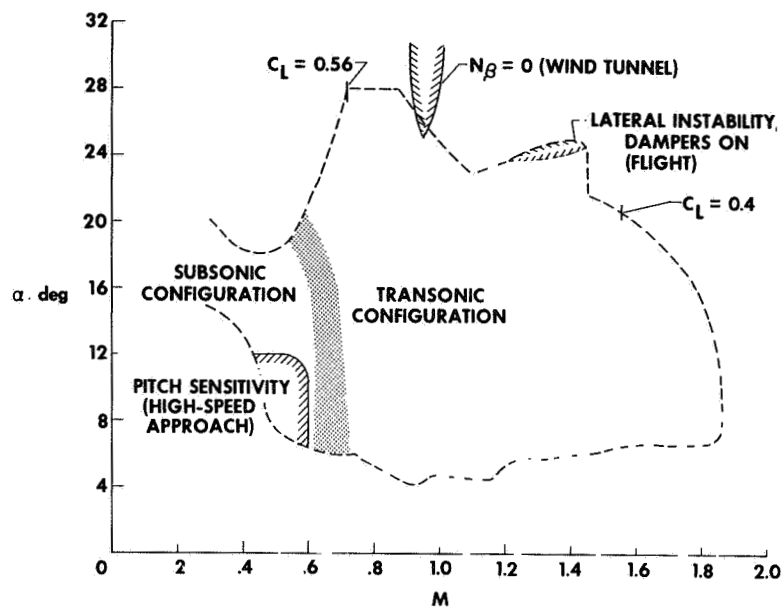


Figure 1

X-24A FLIGHT ENVELOPE

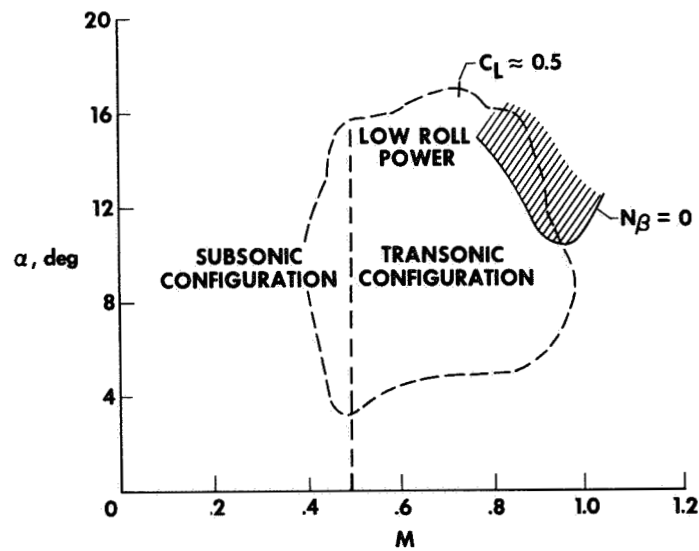


Figure 2

TRIM EFFECTS ON HL-10 DUE TO CONFIGURATION CHANGE

$M = 0.65$

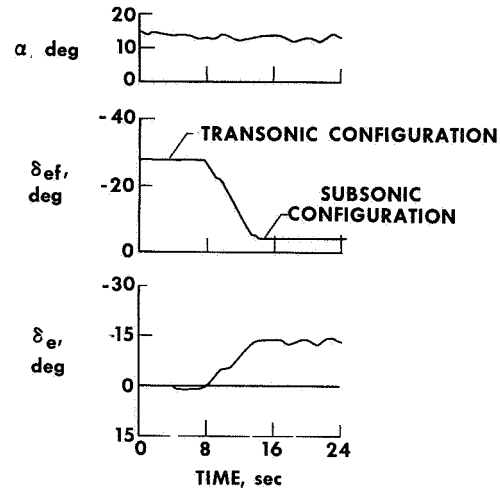


Figure 3

HL-10 LONGITUDINAL STICK GEARING

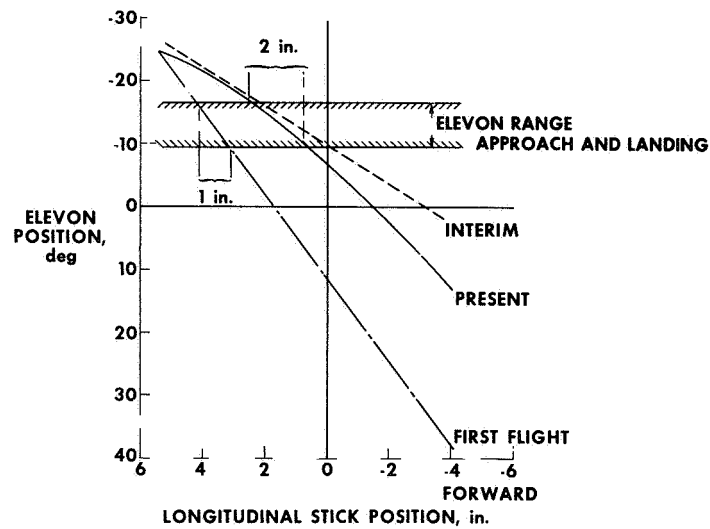


Figure 4

X-24A DIRECTIONAL-STABILITY BOUNDARIES

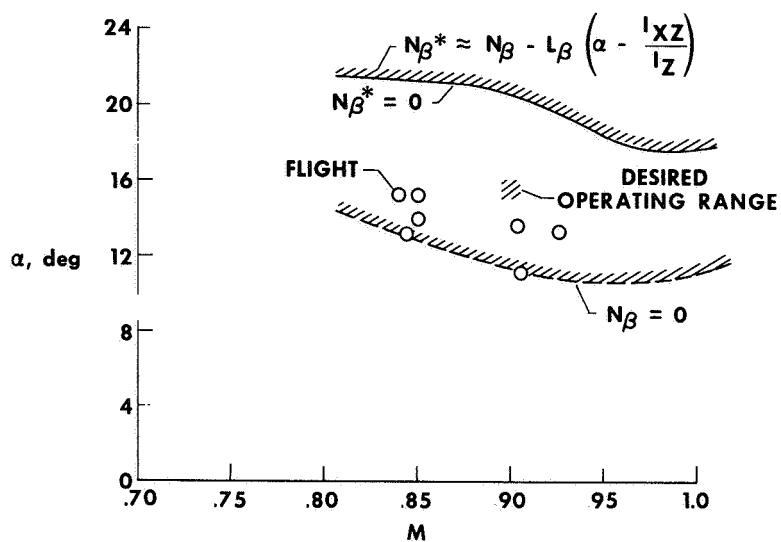


Figure 5

EFFECT OF INTERCONNECT ON X-24A ROLL POWER

SIMULATOR DATA; $M = 0.9$

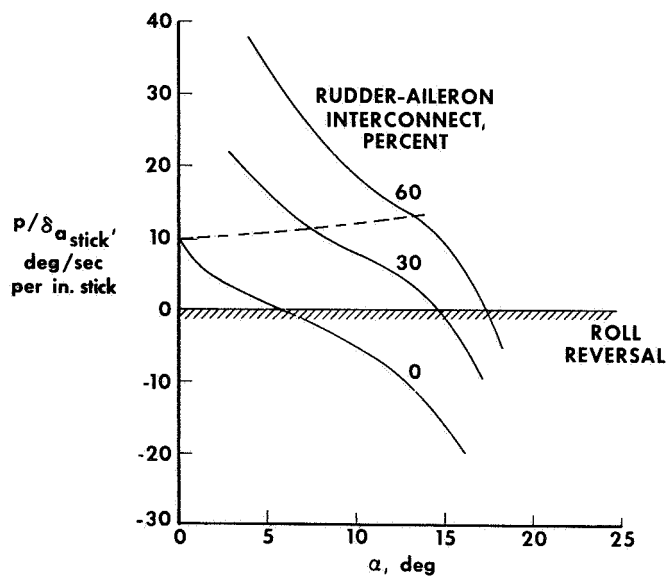


Figure 6

POLE POSITION AND ROOT-LOCUS CLOSURE CONVENTIONAL AIRCRAFT

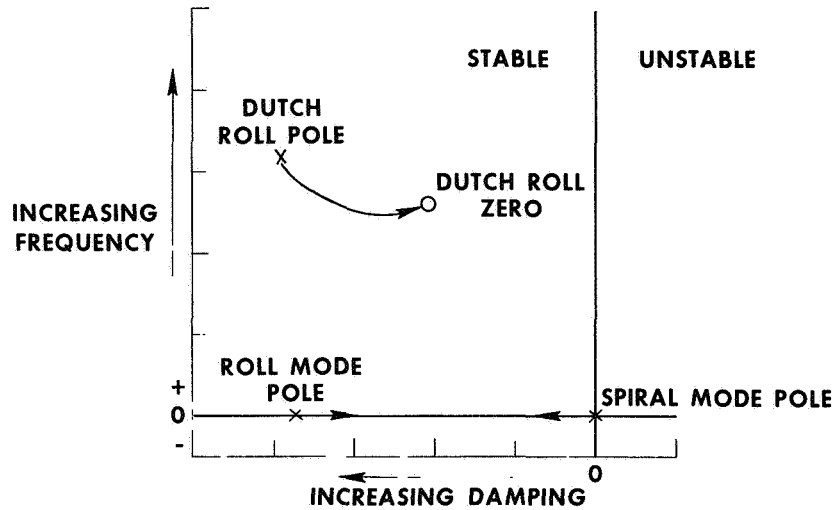


Figure 7

AIRCRAFT MOTION CONVENTIONAL AIRCRAFT

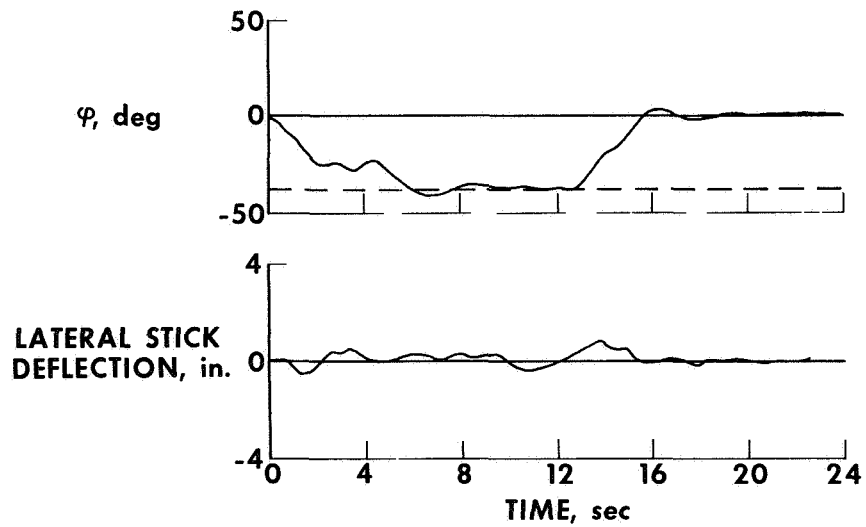


Figure 8

VEHICLE MOTION

LIFTING BODY

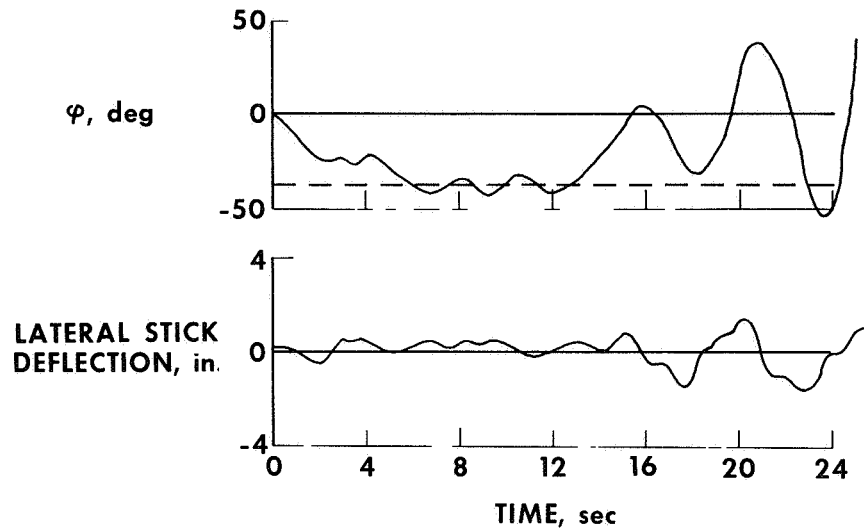


Figure 9

POLE POSITION AND ROOT-LOCUS CLOSURE

LIFTING BODY

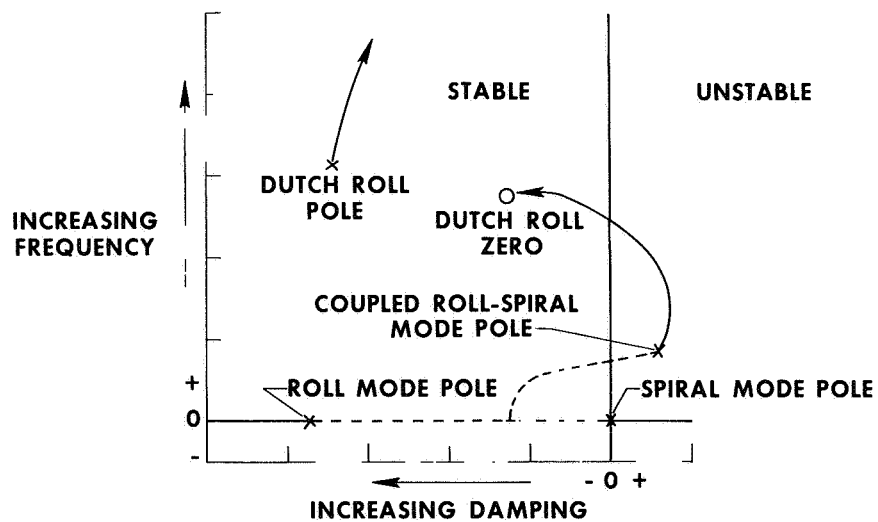


Figure 10

4. PERFORMANCE CHARACTERISTICS OF THE LIFTING BODY VEHICLE

By Jon S. Pyle
NASA Flight Research Center
and Lawrence G. Ash
Air Force Flight Test Center

INTRODUCTION

Designers have relied heavily upon aerodynamic theory and wind-tunnel testing of large and small models to obtain accurate estimates of the performance characteristics for a new configuration and to provide a realistic simulation of the vehicle's flying characteristics before its first flight. However, the highly unusual shapes of the lifting body vehicles have raised some questions of how accurately their lift and drag characteristics could be defined with these prediction techniques. Thus it is pertinent to compare the lift and drag data obtained in flight for three lifting body vehicles (ref. 1 and unpublished results) with wind-tunnel measurements obtained on the actual flight vehicles (refs. 2 and 3 and unpublished results) and on small-scale models of the flight vehicles (ref. 4 and unpublished results). These comparisons, together with discussions of separated flow problems and the effects of ablated surfaces, should be useful to the designers of space shuttlecraft.

SYMBOLS

C_D	drag coefficient, $\frac{\text{Drag}}{qS}$
$C_{D_{\text{base}}}$	drag coefficient due to adverse pressure on base of vehicle
C_{D_0}	drag coefficient at zero-lift coefficient
$\frac{\Delta C_D}{\Delta C_L^2}$	drag-due-to-lift factor
ΔC_{DA}	increase in drag coefficient due to presence of a roughened surface, based on wetted area

C_L	lift coefficient, $\frac{\text{Lift}}{qS}$
C_m	pitching-moment coefficient about vehicle center of gravity
k	height of ablated roughness, in.
L/D	lift-drag ratio
L/D_{\max}	maximum lift-drag ratio
$\Delta L/D$	change in lift-drag ratio due to presence of a roughened surface
M	Mach number
N_{Re}	Reynolds number based on vehicle length
q	dynamic pressure, lb/ft^2
S	reference planform area, ft^2
α	angle of attack, deg
δ_{rb}	rudder bias deflection, deg
δ_{u}	upper flap deflection, deg

DISCUSSION

General

The variation of lift coefficient with angle of attack for the M2-F2 vehicle obtained from flight data and from small- and full-scale wind-tunnel results is presented in figure 1. The flight data were obtained for Mach numbers of 0.47 and 0.62, which are near the approach speeds of the lifting body class of vehicle. The flight lift-curve slope is slightly lower than the small-scale model data for $M = 0.6$ and the full-scale wind-tunnel results for $M = 0.2$. The slopes from flight and wind-tunnel tests for the other lifting bodies are in fairly close agreement, although in some instances there is a displacement of the curves.

Because the most meaningful comparisons would probably involve the drag, drag-due-to-lift, and lift-drag ratio, subsequent comparisons will be made in terms of the various drag parameters. All the drag data presented represent longitudinally trimmed conditions, about a common center of gravity location, for any specific configuration. The small-scale wind-tunnel drag results have been adjusted to the flight Reynolds numbers by using the Kármán-Schoenherr relationship of skin friction and Reynolds number (ref. 5) and for the effects of compressibility by using the reference-temperature method of Sommer and Short (ref. 6).

Subsonic Drag Characteristics

M2-F2 configuration.— The M2-F2 flight drag and L/D characteristics are compared in figures 2 and 3 with full-scale and small-scale wind-tunnel results. Flight data are presented for Mach numbers of 0.47 and 0.62 to indicate that this Mach number variation has an insignificant effect on the drag results of the M2-F2 configuration. The comparison of flight and small-scale wind-tunnel data shows fairly close agreement of drag at low lift coefficients; however, the agreement of flight and full-scale wind-tunnel drag at low lift coefficients is poor, with flight providing much lower values. These differences and similar differences that will be shown for the other lifting body vehicles cannot be readily explained. Although there is an appreciable difference in Mach number between full-scale wind-tunnel results and the flight and small-scale data, this cannot conclusively explain the increase in drag coefficient. However, there is strong evidence that the technique for supporting the vehicle in the full-scale wind tunnel may have affected the agreement of the drag results at the low lift coefficients.

At lift coefficients above 0.3 where differences in drag-due-to-lift begin to have a significant effect, the slopes of the flight data in figures 2 and 3 begin to deviate from the slopes of the wind-tunnel data, indicating that the flight drag-due-to-lift is higher than the wind-tunnel results had predicted. This deviation becomes significant at lift coefficients above those for L/D_{\max} . As shown, the values of L/D_{\max} agree fairly well, although they do occur at different lift coefficients.

HL-10 configuration.— Figures 4 and 5 show the variation of drag coefficient and lift-drag ratio with lift coefficient for the HL-10 vehicle in the original subsonic configuration. Although this is not the present HL-10 flight configuration, it is the only configuration for which both full-scale and small-scale wind-tunnel results are available for comparison with flight results. The flight drag data at the lower lift coefficients are again lower than the full-scale wind-tunnel results but higher than the small-scale results. The merging of the drag polars at a lift coefficient of 0.25 indicates that the drag-due-to-lift factors for each of the data sources are also different. In terms of L/D , the merging of the drag polars occurs near L/D_{\max} so that the difference between flight and wind-tunnel results is not significant.

Figure 6 illustrates the effect of Mach number on the values of L/D_{\max} obtained with the original HL-10 configuration during subsonic flight testing and full-scale and small-scale wind-tunnel tests. The sketch is a cross-section of the tip fin as viewed from above showing the original contour of the fin with the inboard and outboard flaps in the subsonic configuration. A gradual loss in performance with Mach number is shown in the small-scale wind-tunnel results. This subtle change in performance was

not a sufficient indication of the severe flow problems that were to occur on the first flight of the HL-10 lifting body, and, thus, the abrupt decrease in flight lift-drag ratio above 0.5 Mach number was not anticipated. It was later determined that this loss in performance was caused by a severe flow separation over the inboard surface of the tip fins. This separation affected the flow over much of the aft-boattailed portion of the vehicle and caused a significant change in vehicle stability, control effectiveness, and drag

As a result of additional wind-tunnel tests, the HL-10 vehicle was modified to alleviate the separation problem. As shown in the sketch in figure 7, the leading edges of the tip fins were drooped, which seemed to force additional flow over the inboard surfaces and keep the flow attached over a greater area to a higher Mach number. The small-scale wind-tunnel lift-drag ratios again indicate a gradual loss with Mach number as do the flight data for the Mach numbers covered. Additional flight results (not shown in the figure) at a slightly different flap setting have indicated that the decrease in performance is gradual from Mach numbers of 0.35 to approximately 0.7. As would be expected of a modification which reduced the extent of separated flow, a significant increase in the L/D_{\max} of the HL-10 vehicle was achieved. This increase can be seen by comparing the flight results in figures 6 and 7. If the maximum values of L/D are compared at a Mach number of 0.55 (which is above the Mach number at which separation occurred on the original HL-10 configuration), the L/D_{\max} of the modified HL-10 is approximately 35 percent higher than that of the original configuration. Had it been possible to detect the significance of the separation problem in the early wind-tunnel tests the modification to the tip fins could have been made when the vehicle was being constructed which would have saved almost 15 months between the first and second HL-10 flights

X-24A configuration - The drag and lift-drag-ratio characteristics obtained with the X-24A vehicle in the subsonic configuration are presented in figures 8 and 9. It is interesting to note the agreement of the results at low lift coefficients for this particular configuration. Again, the slope of the drag polar obtained in flight is larger than the slopes of the wind-tunnel data, but, with this configuration, the full-scale wind-tunnel results overpredicted the flight L/D_{\max} . As shown in figures 2 and 4, full-scale wind-tunnel drag values at low-lift coefficients for the M2-F2 and HL-10 lifting bodies were much higher than flight values, which is inconsistent with the close agreement shown for the X-24A vehicle.

Figure 10 shows the variation of L/D_{\max} with Mach number as determined during X-24A flight and full-scale and small-scale wind-tunnel tests. The small-scale wind-tunnel and flight results suggest similar growth patterns of separated flow as L/D_{\max} decreases with increasing Mach number. This reduction although definite was gradual indicating that severe flow separation on the X-24A vehicle was never a significant problem, probably because of the drooped leading edges of the tip fins. The drooped leading edges were somewhat similar to those on the HL-10 tip fins that alleviated the flow separation problem and improved the L/D level, although on the X-24A vehicle they were incorporated into the vehicle design during the wind-tunnel studies before the aircraft was fabricated.

Summary of subsonic lift-drag characteristics. - The zero-lift drag coefficient and drag-due-to-lift measured in flight are compared in the following table with the small-scale and full-scale wind-tunnel results for each configuration tested:

Configuration	Full-scale wind tunnel				Small-scale wind tunnel			
	M2-F2	HL-10 original	X-24A		M2-F2	HL-10		X-24A
			$\delta_u = -13^\circ$	$\delta_u = -21^\circ$		Original	Modified	
C_{D0}	Flight 28% lower	Flight 23% lower	Same	Flight 16% lower	Flight 3% lower	Flight 23% higher	Flight 5% lower	Same
$\frac{\Delta C_D}{\Delta C_L^2}$	Flight higher	Flight higher	Flight higher		Flight higher	Flight higher		Flight higher

It should be noted that the flight drag at low-lift coefficients agreed fairly closely with the small-scale results. An exception was the original HL-10 small-scale results which also did not predict the severe separation problem encountered during the first HL-10 flight. The full-scale wind-tunnel tests seemed to produce significantly higher drag values at low lift coefficients than were measured in flight. However, a different technique applied by the wind-tunnel personnel in obtaining tare corrections appeared to alleviate this problem on the X-24A vehicle in the -13° upper flap configuration. Data for the X-24A vehicle at an interim upper flap setting of -21° indicate that some interaction between the higher flap setting and the mounting technique might have occurred. Thus, the alternate method of obtaining tare corrections is questionable.

Data presented in reference 7 for an earlier version of the M-2 vehicle, the M2-F1, indicated that the discrepancy between flight and full-scale wind-tunnel low-lift drag coefficients was not necessarily caused by the difference between the flight and wind-tunnel Mach numbers. With this vehicle the flight tests were conducted at the same Mach number and Reynolds number as the full-scale wind-tunnel tests. The results of the M2-F1 flight tests indicated the same lower C_{D0} results and a higher drag-due-to-lift factor than the full-scale wind-tunnel results as are shown in the table for the other lifting body vehicles. Therefore, the differences noted between flight and full-scale wind-tunnel results cannot be definitely attributed to the differences in Mach numbers.

The comparisons of the flight and wind-tunnel drag-due-to-lift factors indicate higher values for the flight results. These differences exist for the most part at lift coefficients above 0.3; at lower lift coefficients the wind-tunnel and flight data are in close agreement. It is fortunate that the maximum lift-drag ratios occur with most of the lifting body configurations before the drag-due-to-lift difference becomes significant; therefore, the maximum lift-drag ratios measured during flight agree fairly well with both sources of wind-tunnel results.

The causes of the discrepancies between the flight and wind-tunnel results are not obvious; however, some conjecture can be made concerning areas pertaining to the wind-tunnel results that may need additional study. There are unresolved questions about the effects of buoyancy of these large bulbous shapes, particularly those mounted in the full-scale wind tunnel. Some interference effects of the mounting struts and stings are expected, and in the full-scale wind-tunnel results an interference was noted during a tuft study on the outboard surfaces of the X-24A tip fins.

An additional conclusion reached during the analysis of the lifting body results might be helpful during the design of the space shuttle. In comparing flight and wind-tunnel results, it became obvious that the lift and drag characteristics are generally extremely sensitive to small changes in body contour and control surface settings, perhaps even more so than conventional configurations. Therefore, if good correlation and realistic predictions are desired, it is important that wind-tunnel tests be made with models which accurately represent the flight vehicle.

Transonic Drag Characteristics

The comparisons of flight and wind-tunnel results presented thus far have been limited to the speeds used during the final approach of this class of vehicle. It may be of interest to discuss some of the transonic HL-10 lift and drag characteristics presented in figure 11 that were measured in flight and in the small-scale wind-tunnel tests (ref. 4). The data at Mach numbers of 0.95 and 1.1 in the top plot indicate differences between the flight and wind-tunnel results at the lower lift coefficients. Although these differences do not present any problem to the flight planner in terms of managing the energy of the vehicle during a reentry, they do represent definite deficiencies in the small-scale wind-tunnel simulation of the actual flight characteristics. The flight and model drag polars generally merge at lift coefficients of 0.3 to 0.4. This becomes obvious in the lower figure in which the flight and wind-tunnel L/D_{\max} results agree closely throughout the Mach number range from 0.6 to 1.2.

Base Drag Characteristics

A substantial part of the drag for the lifting body class of aircraft is caused by the blunt base. The sketch in figure 12 indicates the placement of base pressure orifices (shown as solid circles) which were used to define the base drag on the HL-10 lifting body configuration. The heavy lines indicate the various control surfaces, and the shaded area represents the elevons. The figure presents the ratio of the flight-measured base drag to the zero-lift drag through the Mach number range of the HL-10 vehicle. The sharp discontinuity in the curve at Mach 0.6 indicates the change in vehicle configuration where the elevon flaps, speed brakes, and tip fin flaps are all extended to increase the stability of the vehicle. Because the base drag represents a significant portion of the vehicle drag, any effort to reduce the base drag might increase the performance of a lifting body vehicle that has a blunt base. In addition, the mounting technique used for the small-scale wind-tunnel tests might have a distinct effect upon the drag measured on the model (ref. 8). Therefore, it would seem extremely important to obtain base pressure measurements during future tests for both wind-tunnel models and the full-scale vehicles. The resulting comparisons could be used to define the effects that mounting technique might have on later model studies.

Although comparisons of flight and model base pressures for each of the lifting bodies are not yet available, preliminary flight results obtained from the HL-10 vehicle have indicated that the model sting may increase the base pressure at Mach numbers near 0.6. The model sting does not appear to have any significant effects at the transonic speeds and, at present, adequate results are not available to make it possible to apply

a correction for the sting at other speeds where it may affect the data.

Effects of Ablated Surfaces

Preliminary aerodynamic data obtained during wind-tunnel tests of two lifting body vehicles coated with ablated (or simulated ablated) surfaces are presented in figure 13. The longitudinal stability in terms of pitching-moment coefficient and the percentage loss in lift-drag ratio are shown as a function of angle of attack. The data are from two separate studies in which the X-24A vehicle and a closely related subscale configuration were used. For the full-scale X-24A wind-tunnel tests (ref. 9), the wetted surfaces were coated with sand and glue to simulate an ablated surface. Wind-tunnel tests (unpublished) on the subscale lifting body configuration were conducted with an ablative coating before and after the coating experienced ablation action, which caused a significant increase in the surface roughness. It should be noted, however, that this roughness texture was not scaled to the model configuration but was typical of a full-scale ablated surface.

The top plot of figure 13 shows a loss in longitudinal stability for each vehicle coated with an ablated or simulated ablated surface. Along with the loss in stability, the lower plot indicates that the presence of an ablated surface caused from 20 to 30 percent loss in the values of L/D_{\max} for these configurations. Although some deterioration of the aerodynamic characteristics was expected because of the roughness that protrudes through the laminar sublayer, the losses discovered during these tests were too severe to be caused only by the increase in friction drag. It is believed that these severe losses of stability and L/D_{\max} were caused by rather extensive growth of separated areas of flow. However, in this instance the separation was aggravated by the addition of a roughened surface

The effect of roughness is shown in another way in figure 14. This presentation is believed to contain evidence of flow separation in addition to the usual effects of roughness as shown by the greater slope of the wind-tunnel data points relative to the prediction curves. Most wind-tunnel and flight-test data for smooth surfaces have shown more tendency toward early separation at low Reynolds numbers, where the ratio of boundary-layer thickness to chord length is highest (ref. 10). The wind-tunnel results of this figure show this same tendency, and it appears that the steeper slope of the data represents a tendency toward separation which is sensitive to Reynolds number for the smooth configuration only. However, flight experience with the unmodified HL-10 lifting body and the X-15 airplane (ref. 11) and the full-scale wind-tunnel data of reference 9 suggest that roughness--varying from fabrication roughness on sheet metal to simulated and genuine ablative coatings--could aggravate an incipient flow separation problem and cause a loss in the vehicle's stability or lift-drag ratio or both.

CONCLUDING REMARKS

Flight and wind-tunnel lift and drag data obtained on three lifting body vehicles have been compared. With the exception of the drag-due-to-lift factor, the flight and small-scale wind-tunnel results generally agree, however, it is extremely important that the

model contours match the flight vehicle and the flow on the model be carefully observed, because minor separation problems on the model may become severe on the full-scale vehicle in flight.

The full-scale wind-tunnel results obtained with the flight vehicle generally predicted higher zero-lift drag coefficients and lower drag-due-to-lift factors than were observed during the flight tests.

The lifting body configurations with severe boattailed afterbodies indicate significant effects of Mach number, with a definite tendency toward separated flow on the upper boattailed surfaces.

The major portion of the HL-10 transonic zero-lift drag is due to the base drag of the vehicle; therefore, any effort to reduce the base drag might increase the performance capabilities of lifting body vehicles. The presence of the sting in the base region on the model suggests the need to obtain adequate base pressure measurements in wind-tunnel and flight tests if realistic base drag comparisons are desired.

The presence of an ablated surface on a lifting body vehicle caused a decrease in the vehicle's longitudinal stability and as much as a 30 percent loss in the maximum lift-drag ratio.

REFERENCES

1. Pyle, Jon S. ; and Swanson, Robert H. : Lift and Drag Characteristics of the M2-F2 Lifting Body During Subsonic Gliding Flight. NASA TM X-1431, 1967.
2. Mort, Kenneth W. ; and Gamse, Berl : Full-Scale Wind-Tunnel Investigation of the Aerodynamic Characteristics of the M2-F2 Lifting Body Flight Vehicle. NASA TM X-1588, 1968.
3. Gamse, Berl ; and Mort, Kenneth W. : Full-Scale Wind-Tunnel Investigation of the HL-10 Manned Lifting Body Flight Vehicle. NASA TM X-1476, 1967.
4. Harris, Charles D. : Transonic Aerodynamic Characteristics of a Manned Lifting Entry Vehicle With Modified Tip Fins. NASA TM X-1918, 1970.
5. Peterson, John B. , Jr. : A Comparison of Experimental and Theoretical Results for the Compressible Turbulent-Boundary-Layer Skin Friction With Zero Pressure Gradient. NASA TN D-1795, 1963.
6. Sommer, Simon C. ; and Short, Barbara J. : Free-Flight Measurements of Turbulent-Boundary-Layer Skin Friction in the Presence of Severe Aerodynamic Heating at Mach Numbers From 2.8 to 7.0. NACA TN 3391, 1955.
7. Horton, Victor W. ; Eldredge, Richard C. ; and Klein, Richard E. : Flight-Determined Low-Speed Lift and Drag Characteristics of the Lightweight M2-F1 Lifting Body. NASA TN D-3021, 1965.
8. Saltzman, Edwin J. ; and Garringer, Darwin J. : Summary of Full-Scale Lift and Drag Characteristics of the X-15 Airplane. NASA TN D-3343, 1966.
9. Pyle, Jon S. , and Montoya, Lawrence C. : Effect of Roughness of Simulated Ablated Material on Low Speed Performance Characteristics of a Lifting-Body Vehicle. NASA TM X-1810, 1969.
10. Blackwell, James A. , Jr. : Preliminary Study of Effects of Reynolds Number and Boundary-Layer Transition Location on Shock-Induced Separation. NASA TN D-5003, 1969.
11. Montoya, Lawrence C. : Drag Characteristics Obtained From Several Configurations of the Modified X-15-2 Airplane up to Mach 6.7. NASA TM X-2056, 1970.

M2-F2 LIFT CHARACTERISTICS

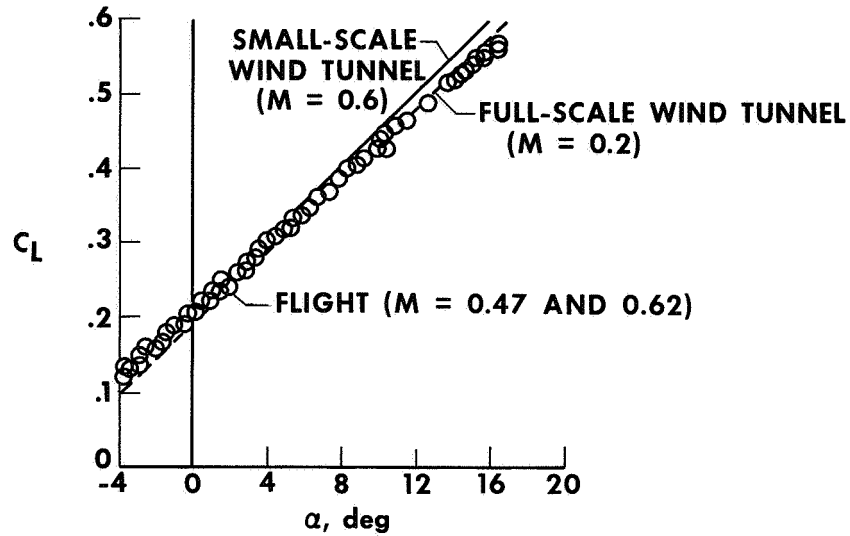


Figure 1

M2-F2 DRAG CHARACTERISTICS

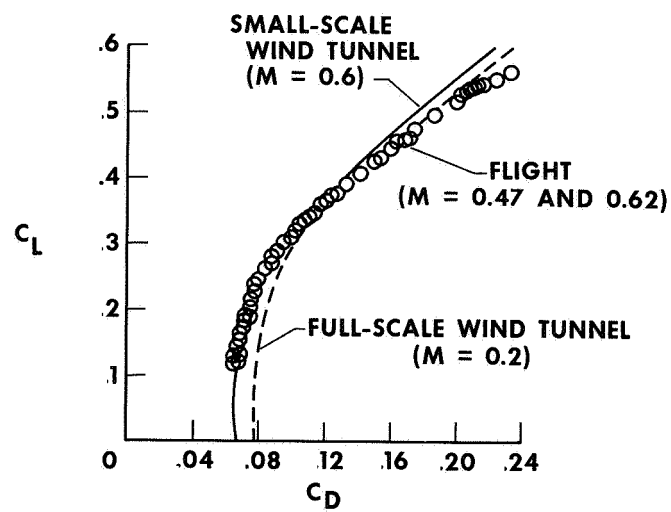


Figure 2

M2-F2 L/D CHARACTERISTICS

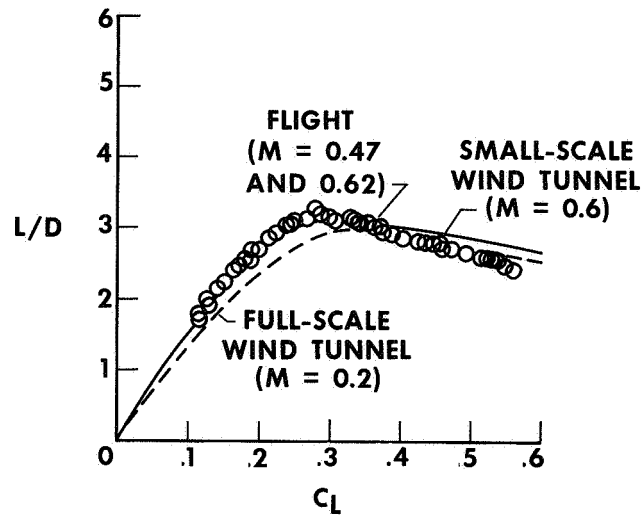


Figure 3

HL-10 DRAG CHARACTERISTICS ORIGINAL TIP FINS, SUBSONIC CONFIGURATION

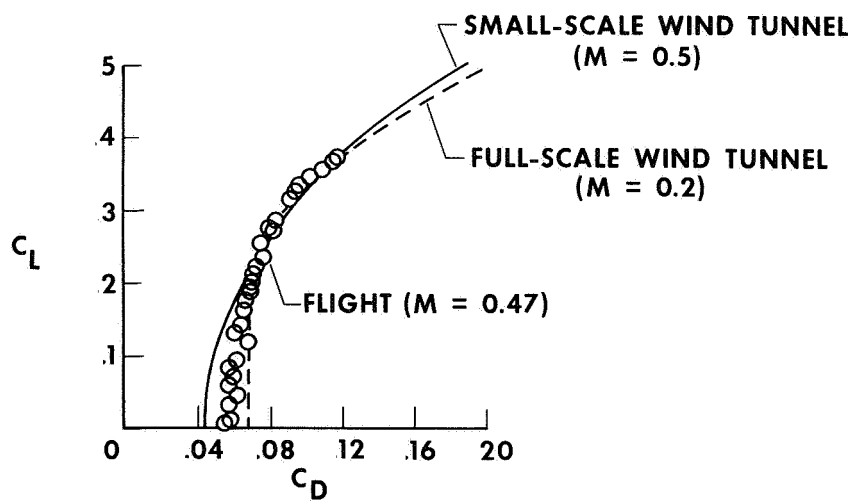


Figure 4

HL-10 L/D CHARACTERISTICS

ORIGINAL TIP FINS, SUBSONIC CONFIGURATION

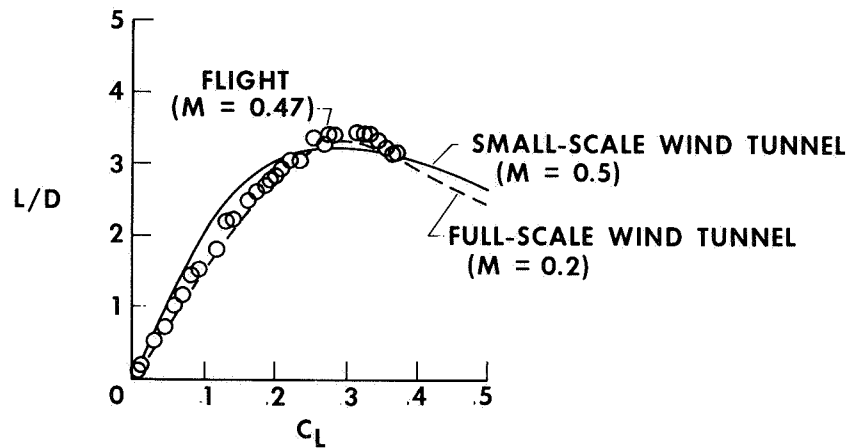


Figure 5

HL-10 L/D_{MAX} CHARACTERISTICS

ORIGINAL TIP FINS, SUBSONIC CONFIGURATION

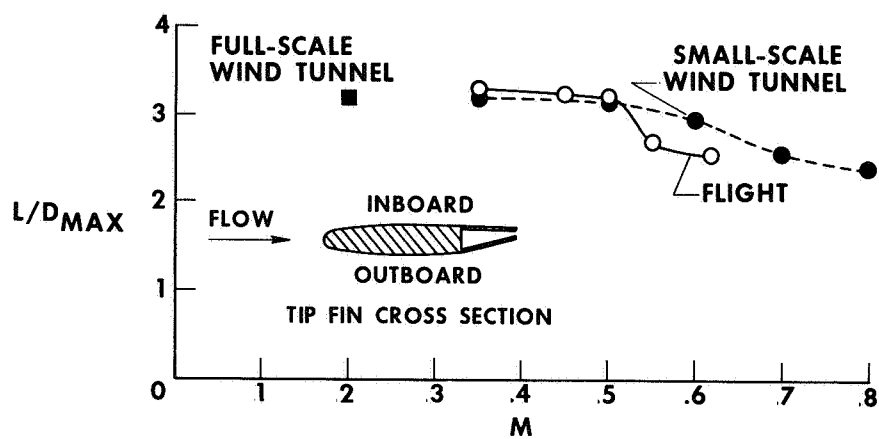


Figure 6

HL-10 L/D_{MAX} CHARACTERISTICS

MODIFIED TIP FINS, SUBSONIC CONFIGURATION

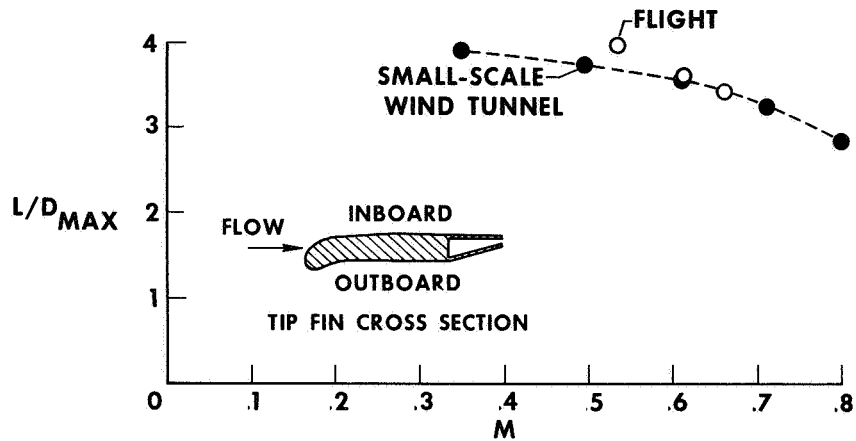


Figure 7

X-24A DRAG CHARACTERISTICS

SUBSONIC CONFIGURATION ($\delta_U = -13^\circ$, $\delta_{rb} = -10^\circ$)

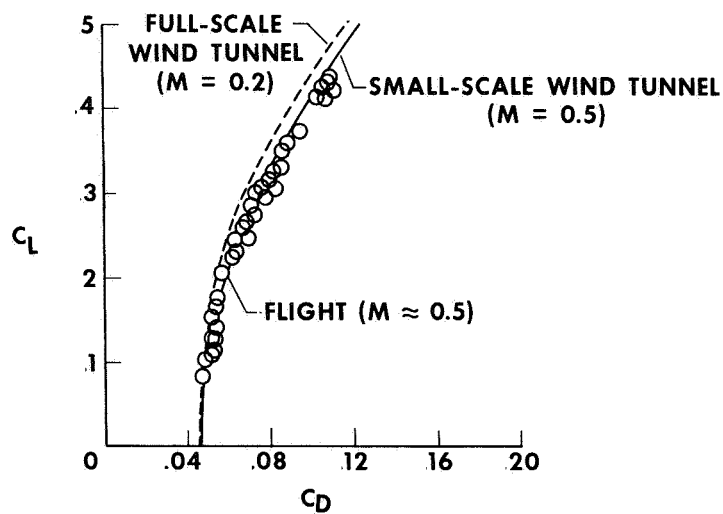


Figure 8

X-24A L/D CHARACTERISTICS

SUBSONIC CONFIGURATION ($\delta_u = -13^\circ$, $\delta_{rb} = -10^\circ$)

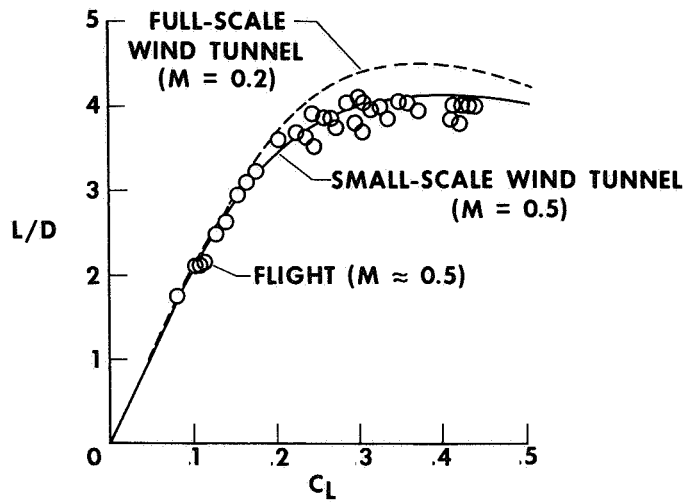


Figure 9

X-24A L/D_{MAX} CHARACTERISTICS

$\delta_u = -21^\circ$; $\delta_{rb} = -10^\circ$

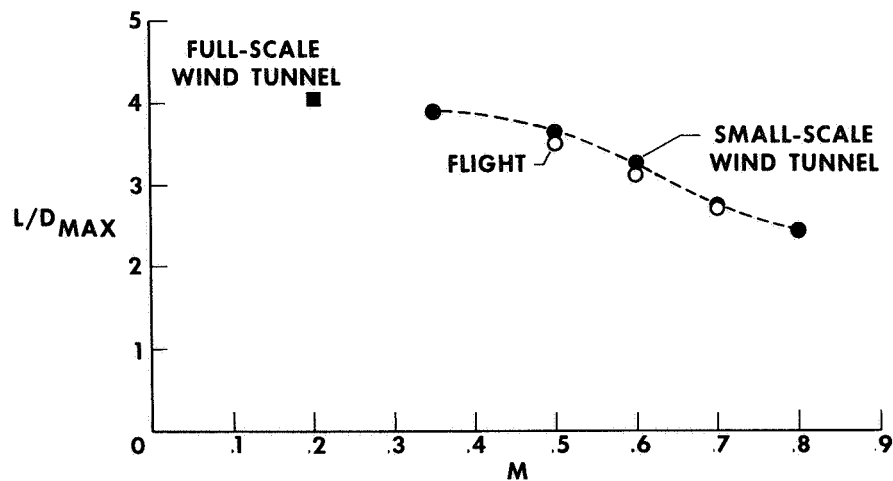


Figure 10

EFFECT OF MACH NUMBER ON DRAG

HL-10; MODIFIED TIP FINS; TRANSONIC CONFIGURATION

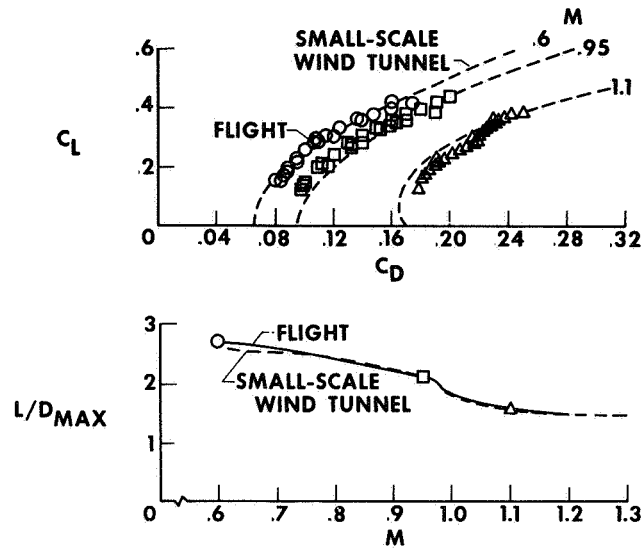


Figure 11

HL-10 BASE DRAG CHARACTERISTICS

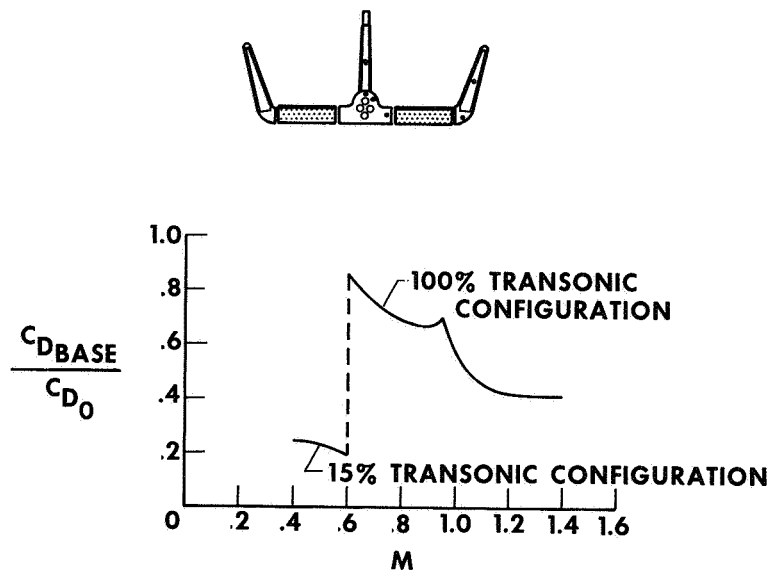


Figure 12

EFFECT OF AN ABLATED SURFACE ON AERODYNAMIC CHARACTERISTICS

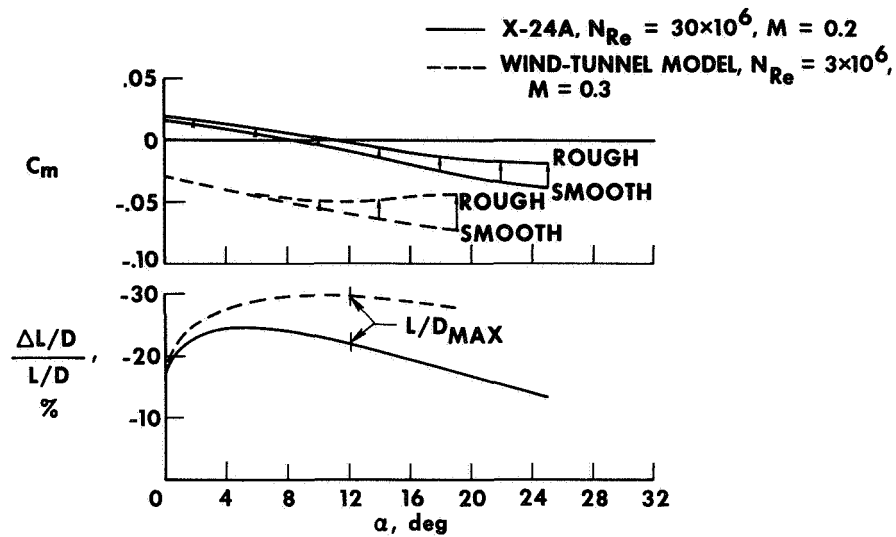


Figure 13

DRAG DUE TO ROUGHNESS OF AN ABLATED SURFACE

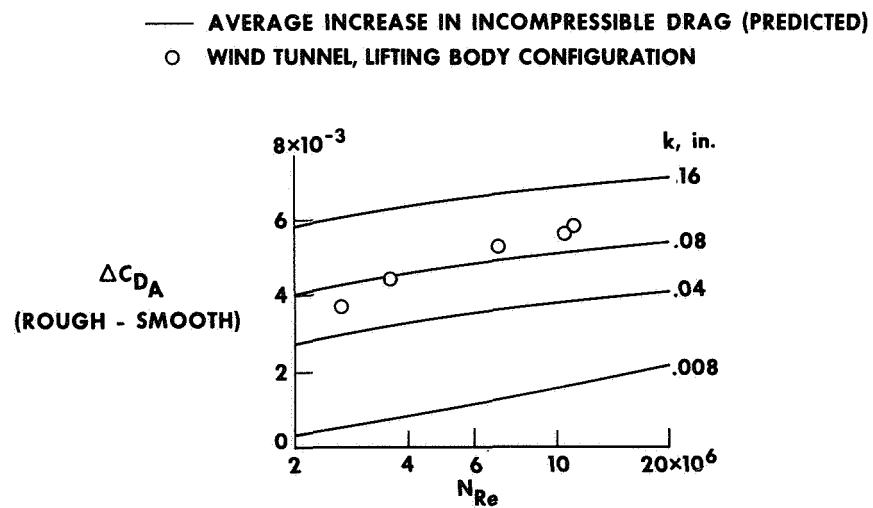


Figure 14

5. CORRELATION OF FLIGHT-TEST LOADS WITH WIND-TUNNEL PREDICTED LOADS ON THREE LIFTING BODY VEHICLES

By Ming H. Tang
NASA Flight Research Center

INTRODUCTION

An essential area of research with the unique M2-F2, HL-10, and X-24A lifting body configurations is the assessment of the ability to predict flight loads from wind-tunnel tests. Flight measurements and correlation with predictions are necessary in verifying the structural integrity of existing vehicles and establishing the groundwork for weight savings on future vehicles of similar shapes.

As part of the overall lifting body flight investigation at the Flight Research Center, detailed aerodynamic-load studies are being made on each of the three vehicles. This paper presents the preliminary results from these studies.

SYMBOLS

C_h	control-surface hinge-moment coefficient, $\frac{HM}{qS\bar{c}}$
C_Y	outboard-fin load coefficient, $\frac{Shear}{qS}$
C_{Y_β}	component of outboard-fin load due to angle of sideslip
$C_{Y_{\delta_l}}$	component of outboard-fin load due to lower-flap deflection
$C_{Y_{\delta_r}}$	component of outboard-fin load due to rudder deflection
$C_{Y_{\delta_{rb}}}$	component of outboard-fin load due to rudder bias
$C_{Y_{\delta_u}}$	component of outboard-fin load due to upper-flap deflection

C_{Y_0} outboard-fin load coefficient at $\alpha = \beta = \delta = 0^\circ$

\bar{c} average control-surface chord, in.

HM hinge moment, in-lb

M free-stream Mach number

q free-stream dynamic pressure, lb/ft²

S surface area, ft²

α vehicle angle of attack, deg

β vehicle angle of sideslip, deg

δ control-surface deflection, deg

Subscripts:

e elevon

ef elevon flap

fi inboard tip-fin flap

fo outboard tip-fin flap

l lower flap

r rudder

rb rudder bias

rl lower rudder

ru upper rudder

u upper flap

DISCUSSION

Figure 1 shows the fins and control surfaces (shaded areas) on the three vehicles that are instrumented with strain gages for loads measurements. Outboard-fin loads were measured on the M2-F2 and the X-24A vehicles, and center fin loads were measured on the HL-10 and the X-24A vehicles. Hinge moments were measured on all the control surfaces of the three vehicles. In general, the fins and rudders can be considered to be in a vertical plane and the flaps and elevons in a horizontal plane.

Outboard-Fin Loads

In the vertical plane, the fin loads can be separated into their various components, as shown in figure 2. The largest component of the fin-load coefficient is the C_{Y_0} term, defined at zero angle of attack, zero sideslip, and zero control-surface deflection. This component of the total fin load is the result solely of the flow around the basic vehicle shape. The variation of C_Y with angle of attack, similar to a lift curve, increases with increasing angle of attack until flow separation occurs. The sideslip and rudder components of C_Y either add to or subtract from the total load, depending on their respective signs. The upper-flap component always subtracts from the fin load as the upper flaps are opened from the zero position. The lower-flap component always adds to the fin load as the lower flaps are opened from the zero position.

Figure 3 is a plot of M2-F2 outboard-fin load coefficient versus angle of attack at Mach 0.70 and 0.60, zero sideslip, zero rudder deflection, and corrected to zero flap deflections (ref. 1). For both the flight and wind-tunnel data, C_{Y_0} is about 0.6. The flight and wind-tunnel variation of fin load with angle of attack agrees well until the flow separates. The flight data then decrease at a lower angle of attack than the wind-tunnel data. In general, the components of the fin load due to sideslip, rudder, and upper- and lower-flap deflections indicated fair agreement between the flight and wind-tunnel results, as shown in the following table:

Component	Flight	Small-scale wind tunnel
C_{Y_β}	0.029	0.037
$C_{Y_{\delta_r}}$.013	.013
$C_{Y_{\delta_u}}$.005	-----
$C_{Y_{\delta_l}}$.003	.002

Figure 4 is a plot of C_Y versus angle of attack for the X-24A outboard fin at Mach 0.25 (ref. 2) and 0.60. The extrapolated C_{Y_0} component for the flight data is about 0.1 higher than that presented by the wind-tunnel results; however, the variation of outboard-fin load coefficient with angle of attack showed fair agreement between the flight and wind-tunnel data. The variation of the components of the outboard-fin loads with angle of sideslip and control-surface deflection showed similar fair agreement between flight and wind-tunnel data, as shown in the following table:

Component	Flight	Full-scale wind tunnel	Small-scale wind tunnel
C_{Y_β}	0.032	0.029	0.035
$C_{Y_{\delta_{rb}}}$.018	.028	.027
$C_{Y_{\delta_u}}$.010	.011	.010
$C_{Y_{\delta_l}}$.003	.005	-----

In summary, the outboard-fin loads for both the M2-F2 and the X-24A vehicles experience a large C_{Y_0} component at zero vehicle attitude and control-surface deflections. In addition, the outboard-fin loads show a large increase with increasing angle of attack, because of the flow around the forebody.

Control-Surface Hinge Moments

Because of the unusual configurations and the many varied control surfaces on the aft region of each lifting body vehicle, all the control surfaces are instrumented to measure hinge moments.

During the first HL-10 flight, severe flow separation was experienced over the fins and control surfaces at subsonic speeds. Figure 5 shows the flow separation as illustrated by a time history of inboard-fin and elevon-flap hinge moments. The various surface locations are shown by the darkened areas of the sketches at the extreme right in the figure. The left side of the figure presents data obtained during flight with separated flow with the HL-10 vehicle in its original configuration; the right side shows similar data after the tip fins were modified by extending and drooping the leading edges. (See top view cross section of tip fins and aft fuselage at the bottom of the figure.)

As shown, the unsteady responses were large for the original configuration involving separated flow. The peak-to-peak amplitudes of the oscillation of the inboard-fin flap hinge moment represent 10 percent of the design-limit load. After the modification, the flow over the same surfaces was steady for the subsonic configuration. With some combinations of angle of attack and Mach number, the HL-10 still experiences flow separation over these surfaces, but the intensity is much lower than during the first flight.

Figure 6 shows the flight variation of the HL-10 outboard-fin flap and rudder hinge moments with changes in angle of attack for the transonic configuration at Mach 0.9,

zero sideslip, and zero rudder deflection. Figure 7 shows the flight and wind-tunnel (ref. 3) variation of elevon and elevon-flap hinge moments with angle of attack at the same conditions. The rudder and the outboard-fin flap hinge moments show essentially no change with changes in angle of attack. The elevon and elevon-flap hinge moments decrease with increasing angle of attack (downward directed load on the surface is defined as positive). The flight elevon hinge-moment coefficients are lower than the wind-tunnel coefficients, and the flight elevon-flap hinge-moment coefficients are somewhat higher than the predictions from the wind-tunnel tests. The trends shown by both figures at Mach 0.9 apply to subsonic as well as supersonic flight.

Figure 8 shows the effect of Mach number on the HL-10 outboard- and inboard-fin flap and rudder hinge moments for the transonic configuration at 14° angle of attack, zero sideslip, zero elevon deflection, and zero rudder deflection. For all three surfaces the full-scale wind-tunnel hinge moments agree with the magnitude of the subsonic flight data. However, the slope of the small-scale wind-tunnel inboard-fin flap hinge moments with Mach number is shallower than that of the flight data. Both the outboard-fin flap and the rudder show the expected increase in hinge-moment coefficients from a Mach number of 0.8 to 1.

Figure 9 shows the Mach number effect on the HL-10 elevon and elevon-flap hinge moments at the same conditions as in figure 8. Similar to the outboard-fin flap and rudder hinge moments, the elevon-flap data also indicate an increase in transonic hinge-moment coefficients. Again, the full-scale wind-tunnel data show reasonable agreement with the subsonic flight data. The flight elevon hinge-moment coefficients are lower than those predicted by the small-scale wind-tunnel results; however, the elevon-flap hinge-moment coefficients show good agreement with the wind-tunnel data.

Because the control surfaces on the HL-10 vehicle are near the rocket engine and because the HL-10 base area is large in the transonic configuration, a change in hinge moments might be expected during rocket engine operation. This change is shown in figures 10 and 11. Figure 10 is a plot of the outboard- and inboard-fin flap hinge-moment coefficients versus angle of attack at Mach 1.2, and figure 11 is a plot of the rudder and elevon-flap hinge-moment coefficients versus angle of attack, also at Mach 1.2. The data in these figures show a definite decrease in hinge moments for all four control surfaces during rocket engine operation that is pronounced at lower angles of attack for the outboard- and the inboard-fin flaps and remains somewhat constant for the rudder and elevon-flap hinge moments. The decrease is caused by the increase in base pressure during rocket engine operation which increases the pressure on the inner sides of the control surfaces and reduces the magnitudes of the hinge moments

Although figures 10 and 11 show the power effect at Mach 1.2, the same decrease in hinge moments first becomes apparent on the HL-10 at Mach 1. The same effect becomes apparent at Mach 0.9 for the X-24A control-surface hinge moments

In view of the appreciable change in hinge moments between power-on and power-off conditions, further analytical and wind-tunnel investigations of this effect should be considered in shuttlecraft research and development.

Similar to the HL-10, the X-24A control-surface hinge moments are sensitive primarily to changes in surface deflection and large variations in vehicle attitude. Figure 12 shows the variation of the X-24A upper-rudder hinge moments with angle of

attack at a rudder bias of -10° and 0° . The upper-rudder hinge moments increase with increasing angle of attack, similar to the outboard-fin load described previously. Movement of the surface outboard from -10° to 0° rudder bias increased the upper-rudder hinge-moment coefficients by almost 0.2. The flight data and the full-scale and small-scale wind-tunnel tests all showed the same large increase in hinge-moment coefficients due to rudder bias.

Figure 13 is a similar comparison of wind-tunnel hinge moments with flight results for the X-24A lower rudder. Again, the trend is the same as for the upper rudder, but the slope of hinge-moment coefficient with angle of attack for the lower rudder is smaller than that for the upper rudder.

The correlation of the X-24A flight hinge moments with the wind-tunnel predictions (ref. 2) on all the control surfaces is considered good for this type of measurement. The especially close agreement between the small-scale-model data and the flight data can be attributed to accurate scaling between the model and the flight vehicle and to the large number of pressure orifices used on the small-scale model in obtaining the wind-tunnel hinge moments.

CONCLUDING REMARKS

Flight loads were measured on the fins and control surfaces of the M2-F2, HL-10, and X-24A lifting body vehicles. Because of the flow around the forebodies of the vehicles, the outboard-fin load coefficient at zero angle of attack, sideslip, and control-surface deflection and the outboard-fin load coefficient due to angle of attack were found to be the largest contributors to the overall fin load. These components were adequately predicted by the wind-tunnel tests.

Control-surface hinge moments were sensitive to surface deflection and variation in vehicle attitude and Mach number and, because of the proximity of the surfaces to the rocket engine, also indicated a power effect. Correlation between the flight and the wind-tunnel hinge moments was generally good.

Because of the unconventional shapes and the presence of complex flow patterns around the fins and control surfaces of the vehicles, theoretical calculations of the aerodynamic loads would be extremely difficult. Thus, it is essential that adequate wind-tunnel tests be used to obtain structural-design data for a vehicle of this type.

REFERENCES

1. Jenkins, Jerald M.; Tang, Ming H.; and Pearson, George P. E.: Vertical-Tail Loads and Control-Surface Hinge-Moment Measurements on the M2-F2 Lifting Body During Initial Subsonic Flight Tests. NASA TM X-1712, 1968.
2. Tang, Ming H.; and DeAngelis, V. Michael: Fin Loads and Control-Surface Hinge Moments Measured in Full-Scale Wind-Tunnel Tests on the X-24A Flight Vehicle. NASA TM X-1922, 1969.
3. Harris, Charles D.: Control-Surface Hinge-Moment and Elevon Normal-Force Characteristics at Transonic Speeds on a Manned Lifting Entry Vehicle. NASA TM X-1241, 1966.

INSTRUMENTED SURFACES ON THREE LIFTING BODY VEHICLES

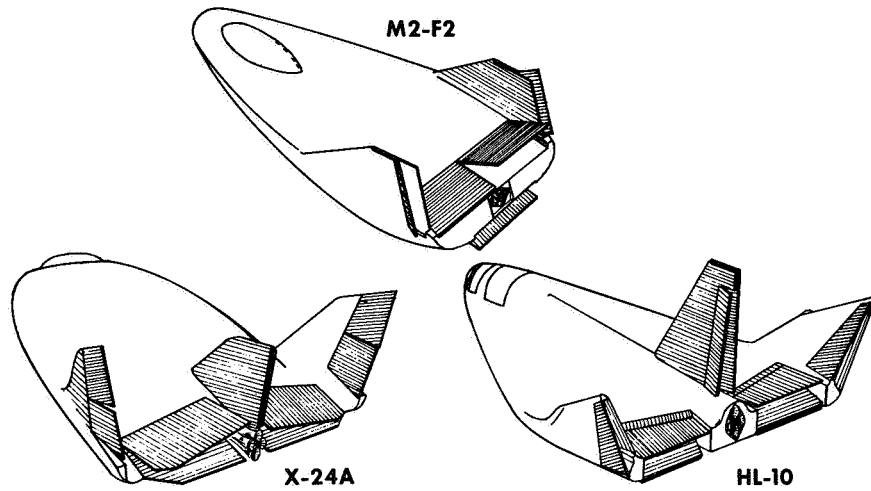


Figure 1

COMPONENTS OF OUTBOARD-FIN LOAD COEFFICIENT

$$C_Y = \frac{\text{SHEAR}}{qS}$$

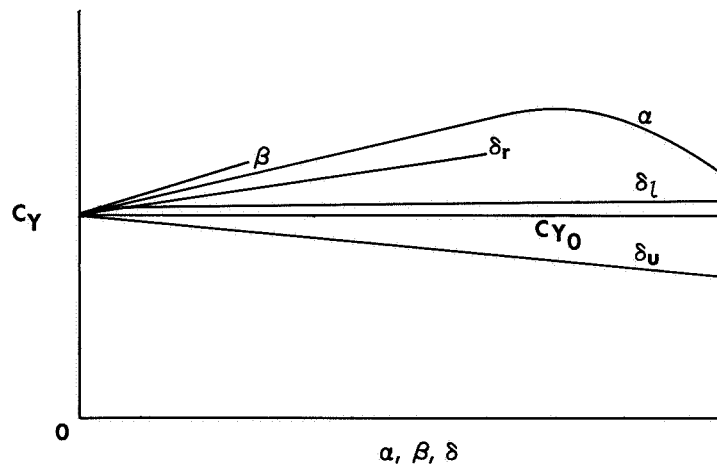


Figure 2

M2-F2 OUTBOARD-FIN LOAD

$\beta = \delta_r = 0^\circ$; CORRECTED TO $\delta_u = \delta_l = 0^\circ$

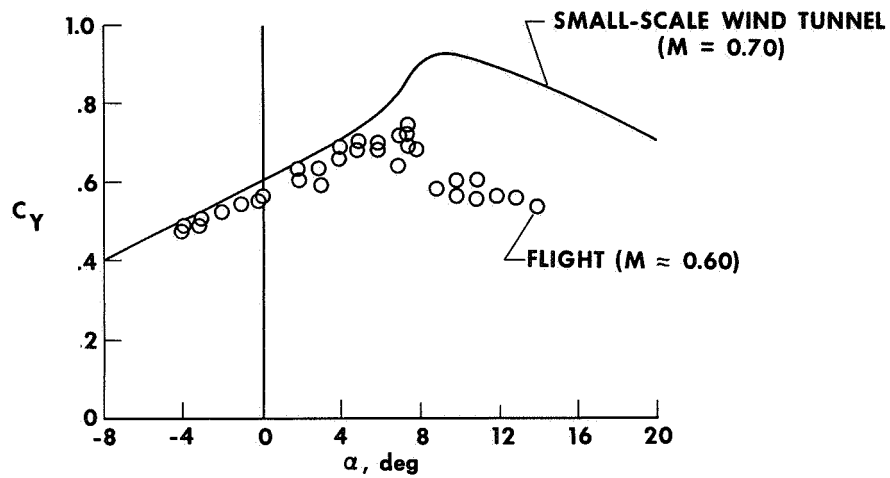


Figure 3

X-24A OUTBOARD-FIN LOAD

$\beta = \delta_r = \delta_{rb} = 0^\circ$; CORRECTED TO $\delta_u = \delta_l = 0^\circ$

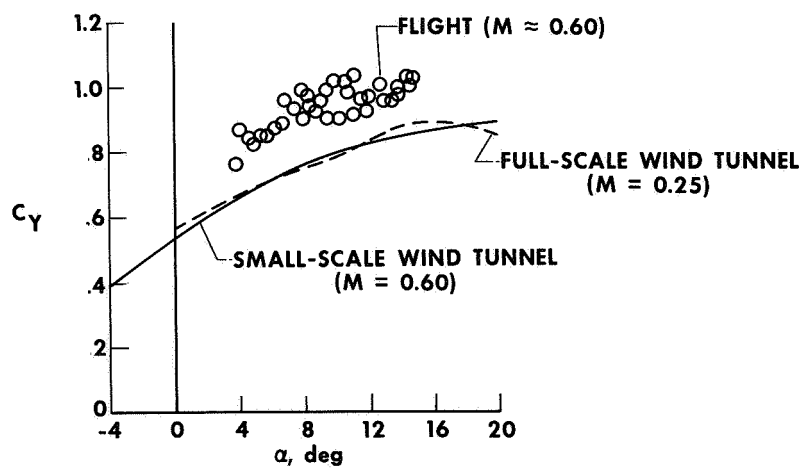


Figure 4

TIME HISTORY OF HL-10 HINGE MOMENTS

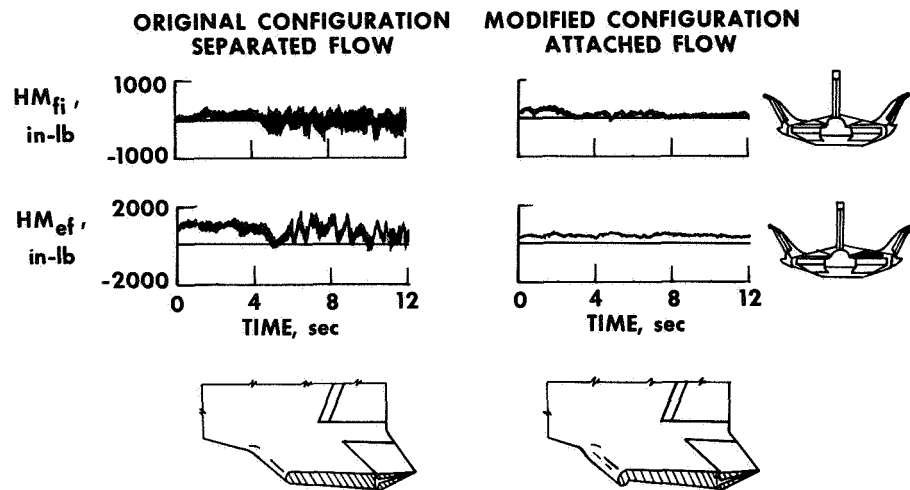


Figure 5

ANGLE-OF-ATTACK EFFECT ON HL-10 HINGE-MOMENT COEFFICIENTS

$$M = 0.9; \beta = \delta_r = 0^\circ$$

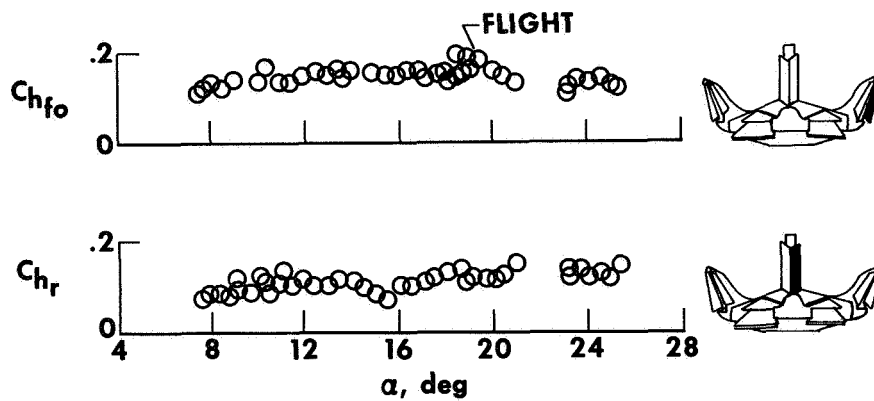


Figure 6

ANGLE-OF-ATTACK EFFECT ON HL-10 HINGE-MOMENT COEFFICIENTS

$M = 0.9$; $\beta = \delta_r = 0^\circ$; CORRECTED TO $\delta_e = 0^\circ$

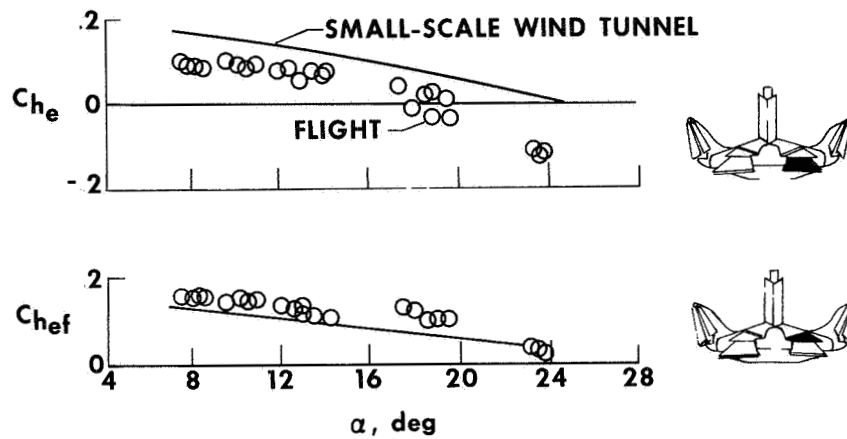


Figure 7

MACH NUMBER EFFECT ON HL-10 HINGE-MOMENT COEFFICIENTS

$\alpha = 14^\circ$; $\beta = \delta_r = \delta_e = 0^\circ$

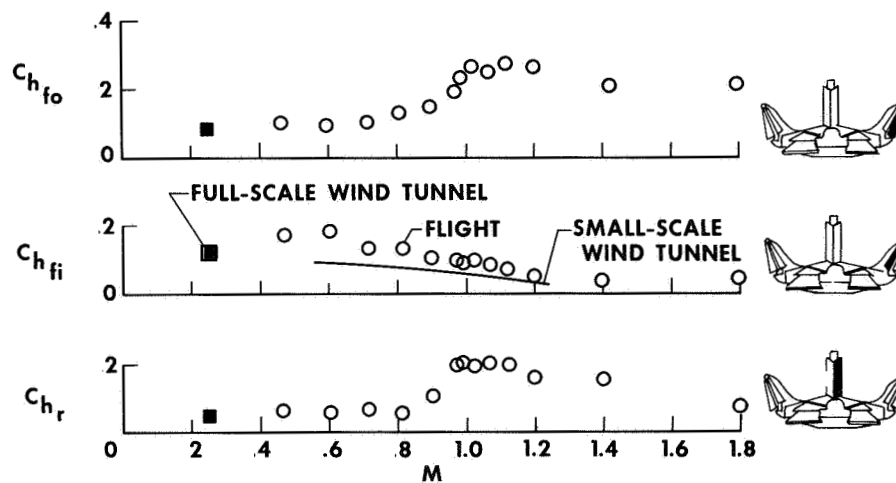


Figure 8

MACH NUMBER EFFECT ON HL-10 HINGE-MOMENT COEFFICIENTS

$$\alpha = 14^\circ; \beta = \delta_r = \delta_e = 0^\circ$$

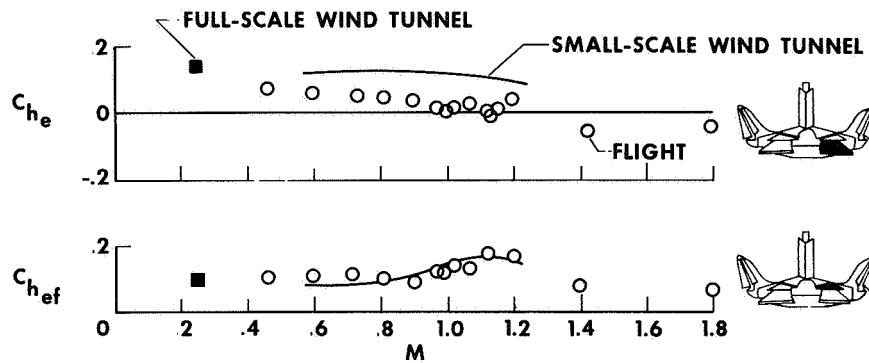


Figure 9

POWER EFFECT ON HL-10 HINGE-MOMENT COEFFICIENTS

$$M = 1.2$$

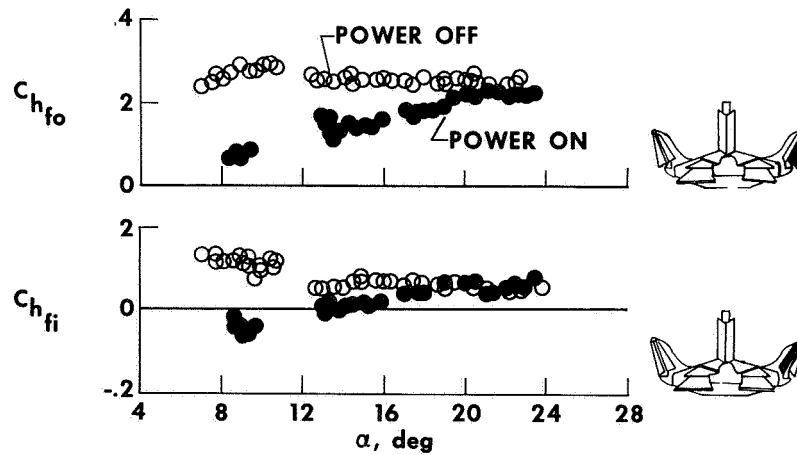


Figure 10

POWER EFFECT ON HL-10 HINGE-MOMENT COEFFICIENTS

$M = 1.2$

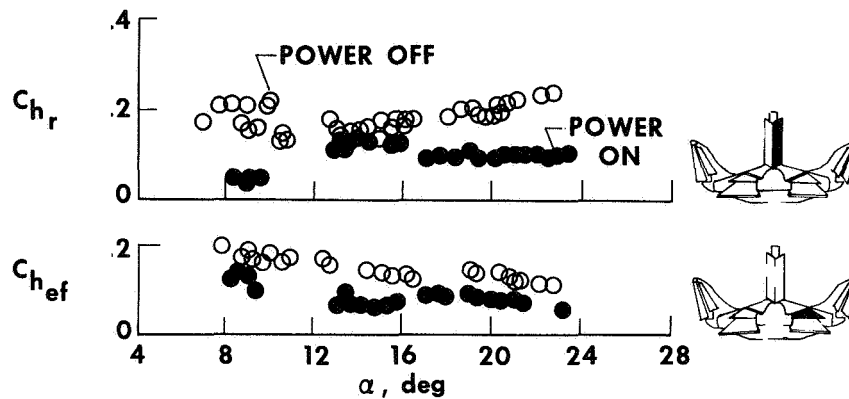


Figure 11

X-24A UPPER RUDDER HINGE-MOMENT COEFFICIENTS

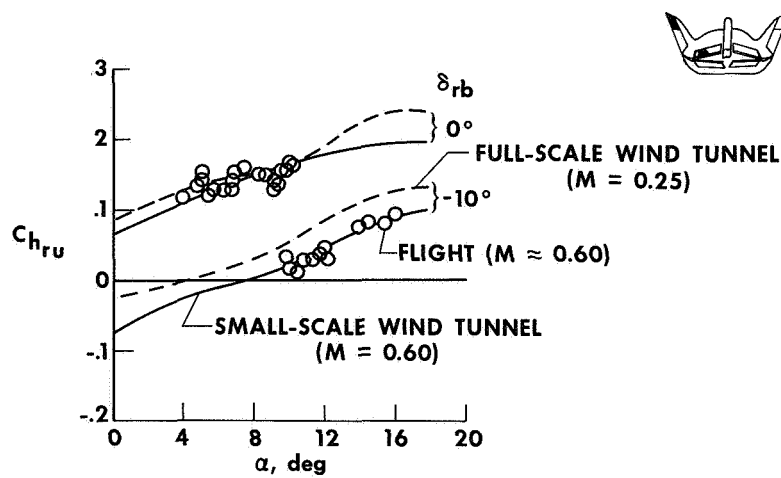


Figure 12

X-24A LOWER RUDDER HINGE-MOMENT COEFFICIENTS

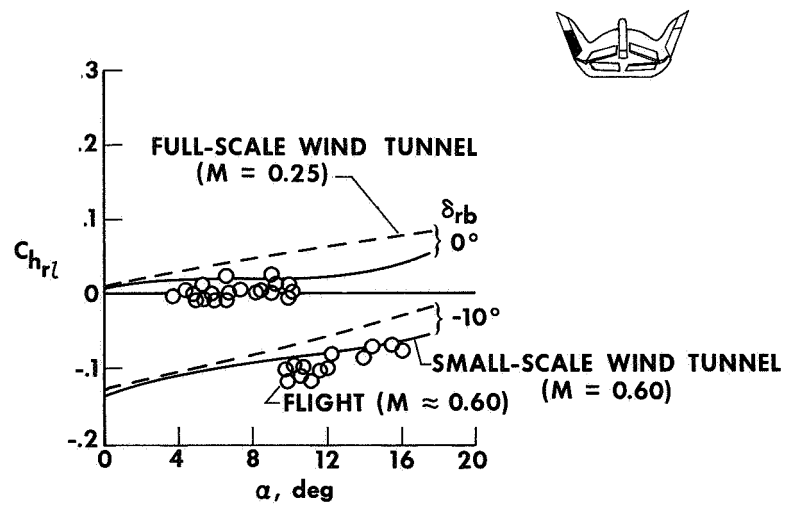


Figure 13

6. PILOT IMPRESSIONS OF LIFTING BODY VEHICLES

By William H. Dana
NASA Flight Research Center
and J. R. Gentry
Air Force Flight Test Center

INTRODUCTION

Piloting aspects of the lifting body vehicles are discussed in this paper by two of the pilots assigned to the flight program. Subjects discussed include: approach, landing, and energy management considerations; field of view requirements, stability considerations, and vehicle riding qualities, including the effects of turbulence. Remarks pertinent to the various subject areas are made by each pilot.

SYMBOLS

$a_{y_{cg}}$	lateral acceleration at the vehicle center of gravity, g units
$a_{y_{pilot}}$	lateral acceleration at the pilot's station, g units
C_L	lift coefficient, $\frac{\text{Lift}}{qS}$
q	acceleration due to gravity, ft/sec^2
L/D	lift-to-drag ratio
M	Mach number
p	rolling angular velocity, deg/sec
q	dynamic pressure, lb/ft^2
S	reference planform area, ft^2

δ_{stick} control-stick deflection, in.

φ angle of bank, deg

APPROACH AND LANDING

DANA: Approach maneuvering for the M2-F3, HL-10, and X-24A lifting bodies is synonymous with terminal energy management. The controllability of all these vehicles is of high enough quality that any maneuvering performed after arriving over the landing site and prior to making the landing flare is done specifically to arrive at the prescribed touchdown point at the desired landing velocity.

The basic approach pattern used for the lifting bodies was inherited from the X-15 program (fig. 1). For the X-15 airplane, the pattern began at the high key point (high key), a position at which the vehicle is on the heading of the landing runway approximately over the desired touchdown point. A 180° turn was then made to the low key point (low key). This circling approach was selected by the pilots for three reasons:

(1) Variation of airspeed, speed brake deflection, and turn rate from the high key to the low key permits very precise positioning at low key.

(2) Pilot judgment of proper space positioning at low key is more acute in a turning approach than in a straight-in approach.

(3) An undershoot or overshoot is much more likely in a straight-in approach than in a circling approach, because one of the variables, turn rate, is not available as an energy management device.

It was natural to transfer these techniques to the lifting bodies. However, because a comfortable 360° approach requires a high key altitude of about 35,000 feet and because the first several flights for each lifting body were glide flights from launch altitudes of only 40,000 or 45,000 feet, a 360° approach required an inordinately large portion of the flight, and the pilot would have been forced to compromise the quality of either the approach pattern or the research data, or both. To avoid this dilemma, it has been the general procedure in the lifting body program to fly a 180° circling approach beginning at 20,000 feet altitude, or low key, with attention focused on data acquisition down to that point. The accuracy of the low key position has been maintained by providing heading and altitude advisories transmitted from mission control. This has proved to be a happy compromise, resulting in excellent touchdown accuracy. For some of the powered flights, energy dispersion has forced the pilot to abandon data acquisition somewhat before 20,000 feet altitude, but low key energy has been notably constant. The methods used by the pilots for energy management have been flight path maneuvering, judicious selection of the time for close up of flared surfaces from the transonic configuration, modulation of airspeed, and speed brake deflection.

Figure 2 illustrates the use of flight track variation for energy management on a representative HL-10 powered flight. This happens to be a 240° overhead approach, because landing to the south on the north-south lakebed runway provides the easiest

return of the lifting body to our facility and because the launch occurs to the southwest to place the vehicle within glide range of a launch lake 20 miles to the southwest if no engine light is obtained after launch. We have also recovered from powered flights by using 180° and 420° approaches dictated by launch or landing constraints. The solid circles in the figure represent the preplanned points of close up of flared surfaces from the transonic configuration. Stability considerations dictate that this close up not be made at Mach numbers greater than 0.7; if the powered flight trajectory or winds cause the HL-10 vehicle to be low or slow, or both, approaching the close up point, a lower indicated airspeed is flown (preferably the airspeed for maximum L/D) and the close up is made as soon as the Mach number decays to 0.7. If the HL-10 vehicle is high or fast at the end of the powered flight, a longer flight path to low key is devised and close up of the flared surfaces is postponed.

Figure 3 illustrates the variation in L/D available to the pilot with transition from the transonic to the subsonic configuration. After close up to the subsonic configuration, energy is controlled on the straightaway by airspeed variation and by modulation of speed brakes. It is interesting to note that all the lifting body pilots use the high airspeed side of the L/D curve when using airspeed variation for energy management. This is instinctive because energy can be dived off if a desired ground reference is being overshot. If the reference is being undershot, the vehicle can be "pulled up" to the reference point. Were the pilot flying on the back side of the L/D curve, appropriate energy management maneuvers would be contrary to pilot instinct.

After reaching the low key position, the pilot devotes his attention primarily to making the landing approach (fig. 4). A final approach indicated airspeed of 270 knots to 300 knots is acquired and maintained until the flare altitude of 1000 feet above ground level is reached. At this altitude, approximately a 1.5 g flareout is initiated to bring the lifting body to level flight at 100 feet. At this altitude, at an indicated airspeed of about 220 knots to 240 knots, the landing gear are extended and a gradual descent to touchdown is made. Indicated touchdown velocities have varied from 155 to 223 knots.

GENTRY: I would like to discuss the rationale of our landing pattern a bit more. One facet of our lifting body operation that always seems to arouse interest, and in some instances, causes alarm, is our relatively steep, unpowered landing approach. As mentioned previously, our approach and landing procedures and philosophies are to a certain extent carryovers from the X-15 program. Before we first flew the M2-F2 aircraft, the trade-offs which must be made in selecting the preflare approach speeds were examined in detail. Many advocated a low speed, shallow approach, and, based on experience, this probably would have been more natural to a pilot. In addition, the flare initiation altitude would have been easier to judge. With low L/D vehicles, though, the postflare float time used to adjust the rate of descent for touchdown would have been very short and, consequently, there would have been little margin for error. We even considered using the landing rockets to increase the float time; however, a failure of this system following a low energy approach would have been catastrophic. Also, our original goal or program objective was to demonstrate an unpowered horizontal landing.

We reasoned that although a steep, high energy approach might be more critical in the flare and be somewhat more demanding upon the pilot, there would be more float time available after flare completion and hence more margin for error. The high speeds associated with steep approaches would also provide ample g capability for the flare and roundout. The lack of g available with the shallow approach had caused

concern. To make the situation even more favorable, the landing gear, which were originally designed for extension by a combination of airloads and gravity in approximately 5 seconds, were modified for pneumatic extension in slightly more than 1 second. This kept our configuration L/D at a maximum until just before touchdown. It also minimized the possibility of asymmetric gear extension and the resulting roll and yaw transients.

Often, designers and engineers fail to appreciate the advantages of the steep, unpowered approach until they have been fully appraised of its benefits. I believe that the high energy approach is more accurate, safer, and actually less critical than the low energy approach. Because I am basically a tactical fighter pilot by trade, I can talk about accuracy more knowledgeably when considering the problem of ordnance delivery on a target. In the absence of a sophisticated bombsight or bombing system, we know that dive bombing is the most accurate means of delivery. In general, we also know that the steeper the dive angle, the greater the accuracy. Our approach task poses basically the same problem. We want to position the vehicle on a flight path or dive angle to intercept a preflare aim point on the ground. This task is minimized by using a relatively steep approach (10° to 25°).

Our whole pattern, then, is just a means of establishing ourselves on this flight path. Because we generally fly well on the front side of the L/D curve, we never plan to be, and seldom are, short of energy. We modulate this energy to arrive on our desired flight path either by slowing or accelerating, or we can remain at approximately the same speed and use the speed brakes to alter our flight path as required. I cannot emphasize too much the need for speed brakes or some similar energy management device. Speed brakes can be used like engines to vary the landing pattern parameters. In addition, their weight is minimal, and they require no fuel. Figure 5 indicates the L/D variation available in the X-24A vehicle with the use of various deflections of the upper flaps. The upper flaps can be extended to perform the speed brake function.

During the past year, we have been attempting to land at a preselected spot on the runway (fig. 6). Our average miss distance on approximately 30 flights has been less than 250 feet, and we can stop the vehicles in a mile or less.

Another fact that many fail to recognize or remember, or that they ignore, is that high performance vehicles handle better at the higher speeds where stability is greater and the control surfaces are more effective. A 3° to 4° , dragged-in, high power, low speed approach is much more demanding upon a pilot, in addition to being tantamount to catastrophe if an engine fails. The aircraft is generally operated on the back side of the L/D curve where the pilot has throttling requirements to concern him because power is the only means of varying the flight path; the visibility over the nose may be reduced by the high angle of attack; the vehicle's stability and handling qualities are degraded; and more control power is required.

There also seems to be excessive concern about approach and landing speeds. I am sure you are aware that many of our current fighter and bomber aircraft are routinely and safely landing at speeds higher than the cruise speeds of the fastest commercial airliners in service 20 years ago. I believe the shuttle vehicle, or any vehicle for that matter, should be landed at a speed where the handling qualities are good, in other words, a safe speed, even if it is 160 knots to 190 knots. For example, if I were an F-104 wing commander and really desired a safe operation, I would have my pilots discontinue the normal landing pattern. This is a relatively slow, very high power, 360°

overhead pattern, flown from 1500 feet above ground level with a boundary layer control system blowing on the trailing edge surfaces. On a hot day, a go-around from final approach cannot be made without afterburner thrust augmentation. It is a pattern so critical that the only recourse if the engine fails is immediate ejection. One of the primary reasons for the pattern when it was first conceived was to afford the pilot the ability to land safely should the engine fail anywhere in the pattern. The standardization of the initial approach altitude and the penchant for slower approach and landing speeds have negated the advantages of this pattern. What I would have my F-104 pilots do is land using the "simulated flameout pattern," which is a circling approach from approximately 15,000 feet above the ground. It is flown at relatively high speed (240 knots to 260 knots), has no requirement for power, and yet the touchdown speeds are only 10 knots to 15 knots higher than the normal pattern.

Landing distances should not be a problem of major significance for the shuttle vehicle. The military services have found that para-brakes and arresting gear are effective in reducing the landing roll. It might be advisable to increase the length of the runways that will be used for the shuttle vehicle. Pouring a few extra cubic yards of concrete on the ground is likely to be far cheaper and pose fewer problems than having to design these vehicles to land at very slow airspeeds.

The criticality of our lifting body approach, flare, and landing is really much less than you might realize. The USAF Aerospace Research Pilot School at Edwards graduates approximately 30 students every year. Each of those pilots must demonstrate proficiency in accomplishing unpowered approaches and landings in the F-104 airplane that are much more critical than the lifting body task. Assuming that the shuttle vehicle will have reasonable stability and handling characteristics, I cannot foresee any significant problems with an unpowered approach and landing. In addition, although the shuttle vehicle is intended to operate somewhat like a commercial airliner, I seriously doubt that the first shuttle pilots are going to be ex-airline captains. Rather, I imagine they will be experienced test pilot/astronauts.

FIELD OF VIEW

DANA: The lifting bodies are all small aircraft in which the pilot is located on the centerline of the vehicle, very far forward. This should provide excellent outside vision; however, as shown in figure 7, for the HL-10 vehicle it does not. There is no bulge for the canopy; it is faired into the basic shape. The pilot's head is positioned just forward of the headrest, visible in the figure. The canopy rails are high, providing a sideward field of view depression angle of only 16° to the right and somewhat less than that to the left, because of a canopy defrost duct along the left canopy rail.

The HL-10 aircraft is fitted with a Plexiglas nose which provides excellent forward vision for navigation and for maneuvering to the touchdown point. Unfortunately, this nose window is lenticular and serves as a giant demagnifying lens close to the ground, giving the pilot the impression that he is higher than he really is at the landing gear deployment and "feel for the ground" phases of flight. On their initial flights, most HL-10 pilots have waited until they were critically low to extend the landing gear. This is a problem which tends to alleviate itself with increasing pilot experience. The pilot learns to use side vision for low altitude height perception and eventually discovers the

precise portion of the nose window which provides undistorted vision. The lenticular quality of the nose window is, I believe, the single most unattractive design feature of the HL-10 vehicle.

The high canopy rails also contribute to the difficulty which the HL-10 pilot experiences in "finding the ground" at touchdown. The very oblique angle of view of the runway to the sides noticeably deteriorates height and rate-of-sink perception. The rails also affect the roll rate requirements of the lifting bodies in the traffic pattern. Figure 8 shows roll rate and bank angle during a typical HL-10 traffic pattern. This particular time history is of the downwind leg and the turn onto the base leg. The maximum roll rate used is about 8 deg/sec except when the pilot rolls the vehicle up on its side to see where he is in the traffic pattern. At these times, roll rates of up to 18 deg/sec are used. If the HL-10 vehicle incorporated a more depressed sideward field of view, some of this lateral motion requirement would be eliminated. It is interesting to consider a two-man lifting body cockpit with side-by-side seating. If the pilot in the left seat were flying a right-hand approach, he would have similar traffic pattern roll-rate requirements if it were intended to provide him with visual pattern control capability.

The M2-F3 vehicle is equipped with a bulge type of canopy (fig. 9), which provides excellent forward visibility. The over-the-side visibility in the M2-F3 vehicle is superior to that in the HL-10 vehicle; the M2-F3 side view depression angle is 21° . Like the HL-10 vehicle, the M2-F3 vehicle is equipped with a nose window. Subsystems in the nose area, however, form a barrier to sight in the central vertical 9 inches, leaving only two side quarter windows to provide depressed view. My sentiments after one flight are that these windows do little for the pilot and could be removed without significantly affecting navigational capability or vehicle control.

GENTRY: I agree with the comments about the visibility from the HL-10 vehicle, and I never found the nose windows on the M2-F2 vehicle to be of any value. Of the three aircraft, I believe that the X-24A vehicle affords the best visibility by far. The bubble canopy (figs. 10 and 11) is similar to canopies on many fighter aircraft, except that it is quite wide which somewhat limits over-the-side visibility. Forward visibility is outstanding, and I have never lost sight of the runway even when landing at the slower speeds.

DANA: Although the X-15 airplane had very small view ports (fig. 12), it had one of the best fields of view of any airplane I have flown. The pilot's head was very close to the panes, and the panes were planar surfaces, providing minimum distortion. Future spacecraft would do well to emulate the field of view of the X-15 airplane.

STABILITY CONSIDERATIONS

DANA: Throughout the design of most lifting entry vehicle shapes, much attention has been focused on improving performance in the terminal phase of flight. There has often been a concurrent indifference toward basic vehicle stability, with the attitude that any stability irregularities can be rectified with stability augmentation.

The lifting body pilots are satisfied that there is adequate performance even in the poorest performer, the M-2 vehicle, to accomplish the terminal maneuvers and landing.

The problems we have encountered in making our traffic patterns have come from handling-qualities inadequacies and from constraints placed upon us to avoid areas of marginal control. Figure 13 shows the boundaries that had to be observed in the M2-F2 vehicle. This aircraft experienced considerable adverse yaw with aileron deflection, which coupled with a high positive dihedral effect to cause roll reversal. To maintain roll control, it was necessary to incorporate a rudder-to-aileron interconnect. The interconnect alleviated the roll reversal, but when the ratio of rudder to aileron was high enough to provide good roll control at the higher angles of attack, it intensified already existing tendencies for pilot-induced oscillations (PIO) at the lower angles of attack required for the approach. This PIO-prone area was entered on four M2-F2 flights; an inadvertent entry contributed to the M2-F2 crash in 1967.

The addition of the third fin to the vehicle (designated M2-F3) eliminated the adverse yaw due to aileron deflection and the requirement for rudder-to-aileron interconnect, and it has reduced the tendency for pilot overcontrol at low angles of attack. Figure 14 shows comparative time histories of the M2-F2 and the M2-F3 bank angles and pilots' lateral control inputs during final turn and approach. The M2-F2 vehicle was deficient in lateral stability. Although it was perhaps also deficient in performance, it was the stability deficiency that was corrected in the M2-F3 vehicle, and the pilots are in agreement that this was the area that required improvement. We believe that inherent stability should be designed into lifting entry shapes; it will contribute more than is often realized to their successful recovery.

VEHICLE RIDING QUALITIES, INCLUDING EFFECTS OF TURBULENCE

DANA: Every lifting body pilot has, on several occasions, experienced flight through turbulence which has caused anxiety out of proportion to the upsets involved. We have not yet isolated the particular sensations which trigger the anxieties; there is no common opinion among the pilots on this. There is also only very limited experience by any one pilot, in any one lifting body, in turbulence. The subject warrants mention, however, because turbulence response of the lifting bodies has been a matter of concern to the pilots. It has drawn out our test program while we have attempted to analyze the reasons for such pilot concern, and it will probably crop up in future lifting entry vehicle flight tests. Turbulence response prediction should be accorded its due importance, and the effect of turbulence upon passengers should be scrutinized.

GENTRY: It is a difficult assignment for a pilot to divorce riding qualities from handling qualities or stability and control characteristics when asked to rate the flight characteristics of a vehicle. They probably cannot be completely separated; however, qualitative comments do indicate some differences in the riding qualities of the three lifting body vehicles.

In general, the riding qualities have been satisfactory. The only real problems have been in the high speed portion of the landing pattern. In the M2-F2 vehicle at low angles of attack and high dynamic pressure conditions, we were in an area of very high lateral control sensitivity as well as reduced lateral-directional stability. This area could actually be sensed by the pilots, and we were reluctant to make any abrupt or large control inputs. Any light-to-moderate turbulence encountered in this area deteriorated both handling and riding qualities. On a few occasions, I reluctantly elected to

increase the angle of attack and fly a slightly slower final approach rather than fly in this uncomfortable area.

I believe the HL-10 vehicle has a slight edge in riding qualities. During my first few flights, though, I had some concern when I encountered turbulence on final approach (from 10,000 feet down). Turbulence affects these vehicles somewhat differently than more conventional aircraft. Although all three axes are disturbed, the pilot notes primarily the lateral-directional perturbations. This is, no doubt, a natural phenomenon in vehicles with low natural roll damping and high roll-to-yaw ratios. Once I was convinced that there was no real instability and that the perturbations were caused only by turbulence, it became natural to ride through the disturbances with little concern.

As I mentioned earlier, the initial flights of the X-24A vehicle were made with the upper flap biased or set at a fixed 21° rather than the 13° we are now using for landing. This meant, of course, that we were using a steeper approach to obtain our desired pre-flare speeds. In addition, all the wind-tunnel studies had indicated that we would have adverse yaw due to aileron deflection. The simulator "flew" nicely with a relatively high roll gain and a low yaw gain. As it worked out, though, the X-24A vehicle had proverse yaw, and at high dynamic pressure the high roll gain destabilized the Dutch roll mode and the yaw gain was too low to effectively damp it. Lateral control sensitivity was also greater than the simulator predictions.

This condition manifested itself to the pilot with much the same sensation and feeling as I had previously experienced in the M2-F2 vehicle. On the first three flights in the X-24A vehicle, I again had to decelerate, and I used the landing rockets to fly a shallower and higher angle of attack on final approach. This problem was alleviated by increasing the yaw gain, reducing the roll gain, and changing the lateral gearing ratio and breakout forces. The riding qualities were further improved by reducing the upper flap setting approximately 8° , which allowed us to approach at the same speeds while using a more shallow flight path angle.

Turbulence seems to affect the X-24A vehicle slightly more than the HL-10 vehicle; however, the pattern is comfortable now even with some turbulence. We have often noted and responded to lateral accelerations that did not appear in the flight data. On a recent X-24A flight, a lateral accelerometer was mounted at the pilot's station. Figure 15 is a comparison of the data from this accelerometer with those from the accelerometer mounted at the center of gravity. The differences, of course, can be attributed to the fact that one accelerometer is mounted well forward and above the vehicle center of gravity. However, this acceleration is what the pilot senses, and this is what he is going to respond to. This could pose a more serious problem in larger vehicles.

CIRCLING APPROACH PATTERNS

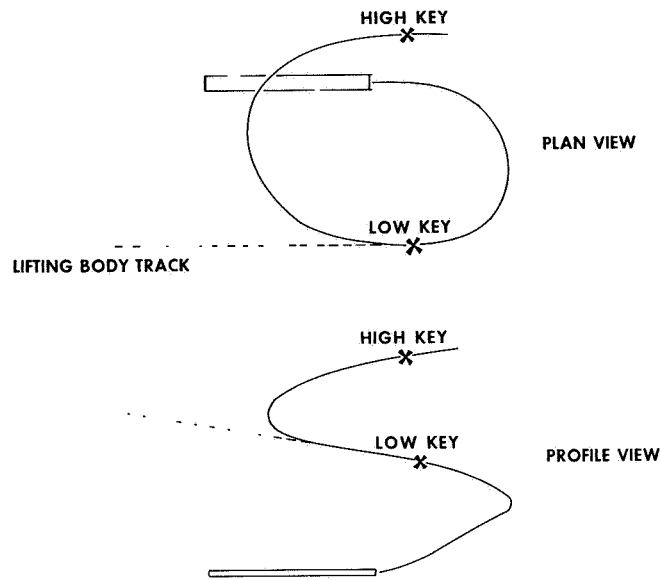


Figure 1

TYPICAL HL-10 POWERED FLIGHT TERMINAL APPROACH PATTERN

- POINT OF CLOSE UP FROM TRANSONIC TO SUBSONIC CONFIGURATION

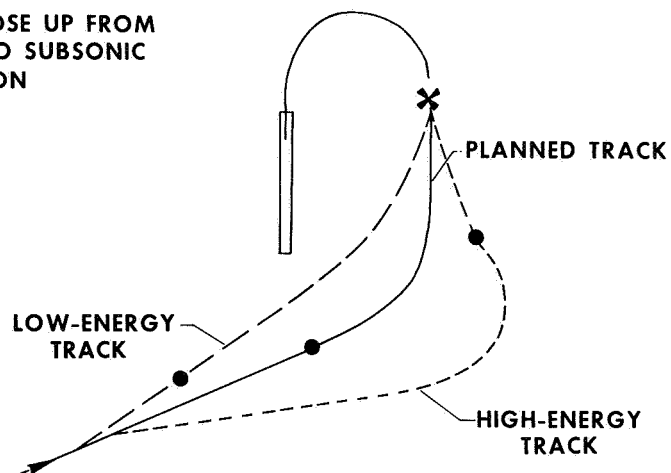


Figure 2

HL-10 PERFORMANCE

$M = 0.6$

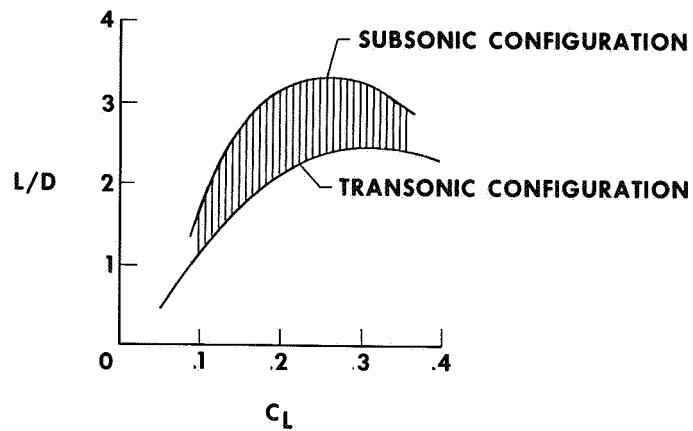


Figure 3

UNPOWERED FLARE AND LANDING TECHNIQUE

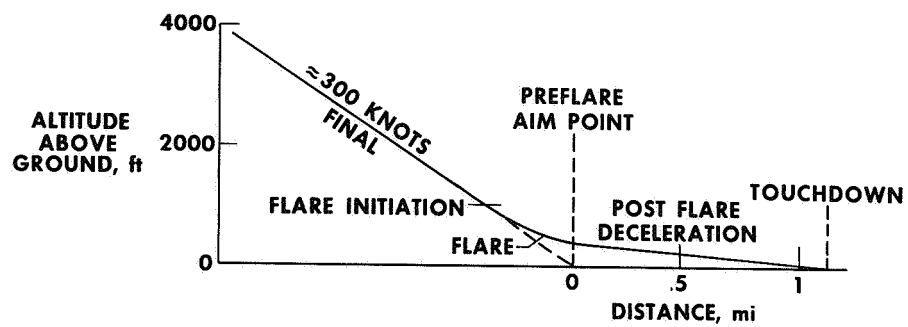


Figure 4

EFFECT OF SPEED BRAKE ON X-24A PERFORMANCE

$M = 0.5$

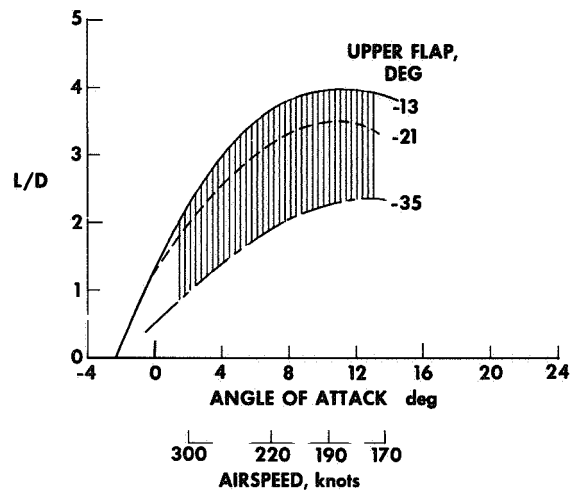


Figure 5

LIFTING BODY RUNWAY

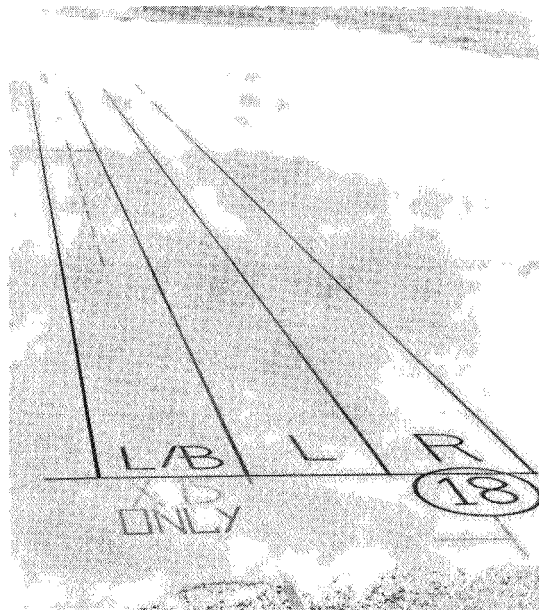


Figure 6

SIDE VIEW OF HL-10



Figure 7

TYPICAL ROLL RATE AND BANK ANGLE IN TRAFFIC PATTERN HL-10

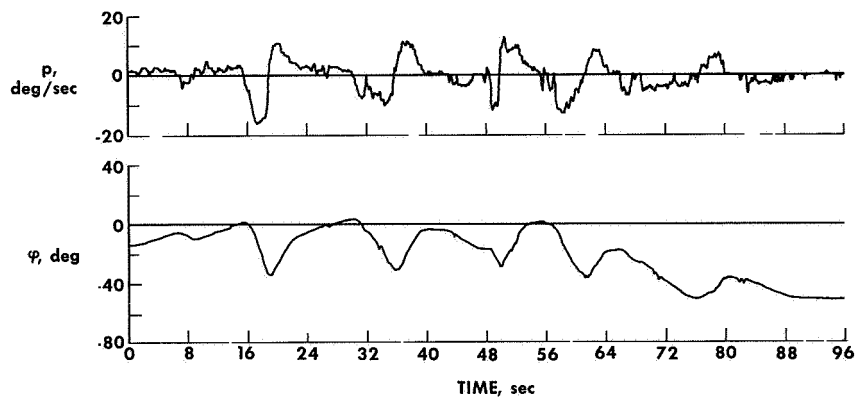


Figure 8

FRONT VIEW OF M2-F3

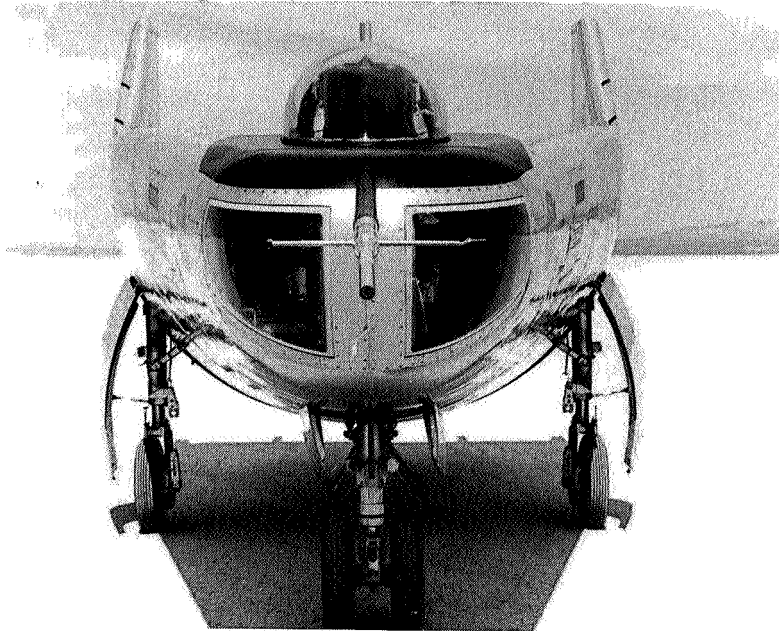


Figure 9

FRONT VIEW OF X-24A

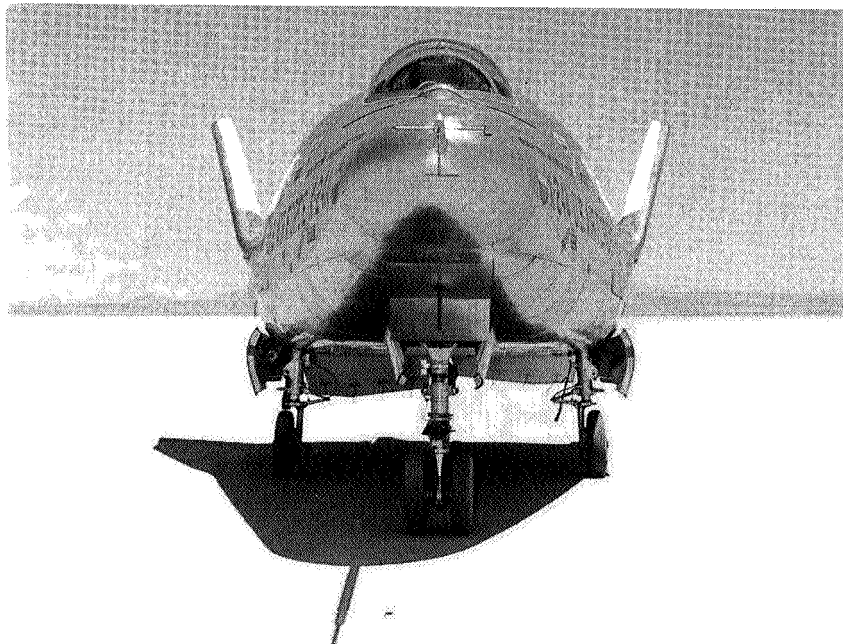


Figure 10

SIDE VIEW OF X-24A

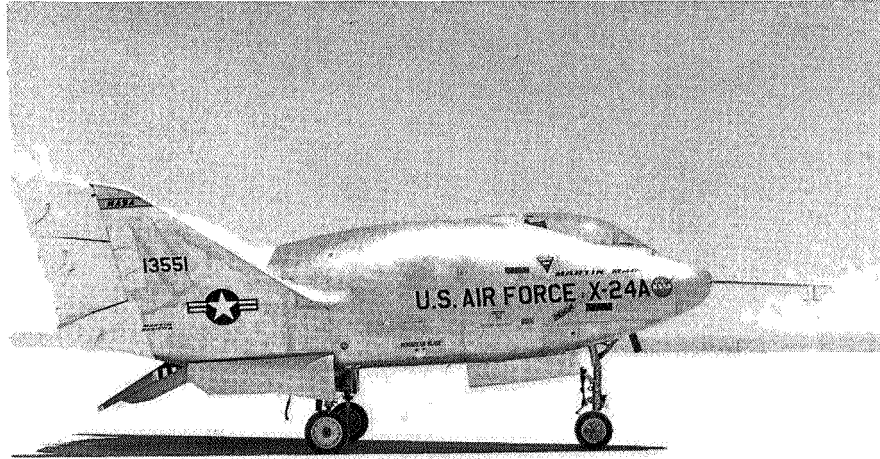


Figure 11

X-15 AIRPLANE



Figure 12

M2-F2 LATERAL CONTROL CHARACTERISTICS

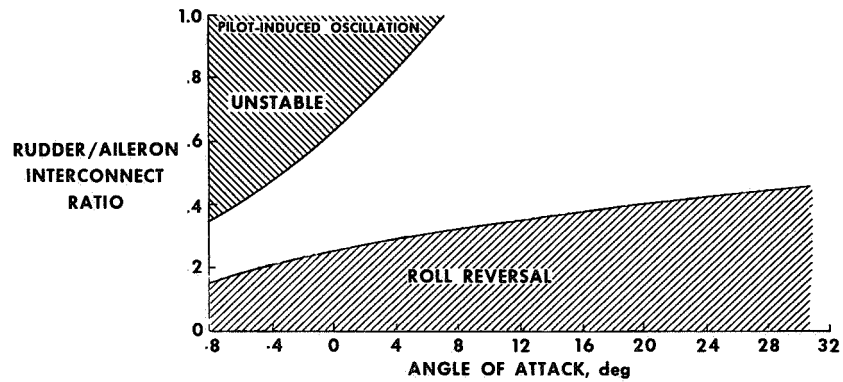


Figure 13

TIME HISTORY OF FINAL TURN AND APPROACH

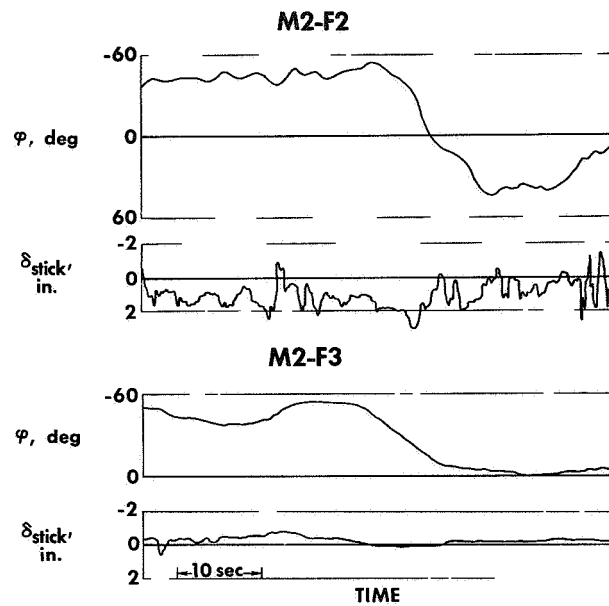


Figure 14

EFFECT OF LOCATION ON LATERAL ACCELERATION

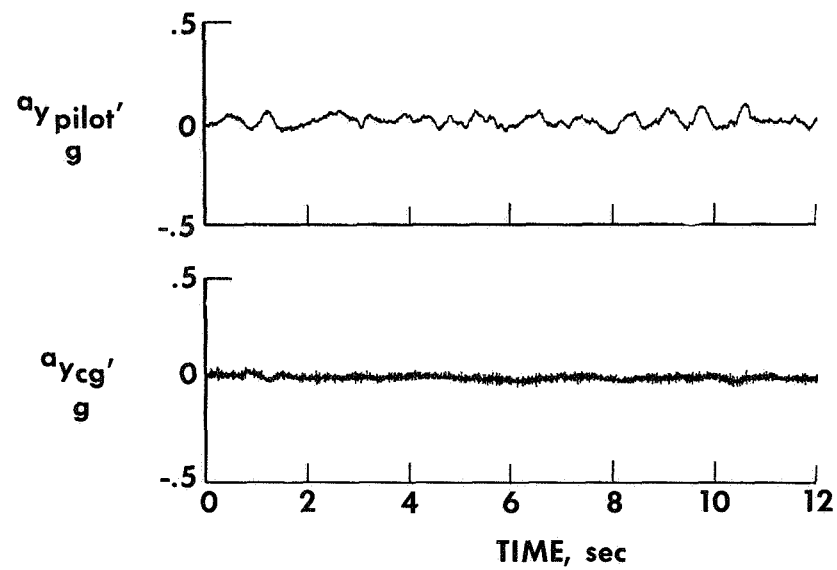


Figure 15

7. SUMMARY OF PRIMARY RESULTS OF THE LIFTING BODY PROGRAM

By Garrison P. Layton, Jr.
NASA Flight Research Center

INTRODUCTION

This summary paper will point out results of the lifting body program that have a bearing on the design of a large space shuttle vehicle. The initial program objectives, the primary program results, and the pertinence of these results to the shuttle will be outlined, as will the future direction of the program.

SYMBOLS

$C_{n\delta_a}$	aileron yawing-moment derivative, per deg
L/D	lift-to-drag ratio
M	Mach number
p	rolling angular velocity, deg/sec
q	dynamic pressure, lb/ft ²
α	angle of attack, deg
β	angle of sideslip, deg
δ_a	aileron deflection, deg
δ_{stick}	control-stick deflection, in.
φ	angle of bank, deg

ω_n undamped natural frequency, rad/sec

Subscript:

max maximum

PROGRAM OBJECTIVES

When the lifting body flight-test program was initiated in the early 1960's, it was geared to reentry vehicles 20 to 30 feet long, with wing loadings of 35 lb/ft² to 50 lb/ft², and carrying no more than 10 to 12 passengers. These vehicles were intended to be reasonably competitive with the ballistic spacecraft in terms of volumetric efficiency and weight and yet offer the advantages of substantially greater aerodynamic maneuverability and horizontal landing capability. For the vehicles to be at all competitive, unpowered landings had to be considered. Concentrating on this class of vehicle naturally, then, influenced the program objectives and, ultimately, the results presented in this symposium.

The objectives of the lifting body program were as follows:

- (1) To prove that this class of aircraft can be flown and landed
- (2) To determine the validity of wind-tunnel predictions through the transonic flight region
- (3) To determine and assess any unpredicted aerodynamic problems

Because of the unconventional shape and close-coupled controls, there were very real reservations about the flyability of this class of vehicle. There was concern also about whether vehicle performance would be sufficient to flare and land. Theoretical and simulator studies predicted that they would fly and land successfully; hence, the next step was to prove it in flight.

Most vehicles that had been flown in the transonic and low supersonic flight regions had been slim, pointed, and specifically designed for this purpose. Thus, a vast store of wind-tunnel and flight comparisons has been accumulated for these slender shapes. The lifting bodies, however, were designed as reentry vehicles which required blunt shapes. For these shapes there was no background of wind-tunnel and flight correlation. Thus, one of the prime program objectives was to assess the quality of small-scale wind-tunnel predictions.

The third objective is, in retrospect, probably the most important. Some problems that have arisen during the lifting body flight program could be expected in any development program, but others were unique to this vehicle class. The knowledge gained by solving these problems may help the designers of the next generation of vehicles avoid the same problems.

A fourth, generally unstated, objective of this program and of the Air Force's PRIME program was to bring lifting reentry out of the realm of the "paper airplane"

and into the real world. This had the effect of generating meaningful wind-tunnel data on a fixed configuration so that its problems could be studied in detail. In addition, establishing a definite flight program changed the primary emphasis of the wind-tunnel tests from optimization of performance to detailed studies of stability and control characteristics, which ultimately have the largest effect on vehicle configuration.

PRIMARY RESULTS

The primary results of the lifting body program have been that:

- (1) This class of vehicle is flyable and has sufficient performance for a safe power-off landing
- (2) Wind-tunnel predictions have been generally good, even through the transonic flight region
- (3) Some unpredicted or unappreciated problems have been uncovered

The prediction of stability and control derivatives has been such that simulation studies have been able to predict the airplane motions well enough that, after a flight, the pilots usually comment on the fidelity of the simulation. An example of this is shown in figure 1 in which the Dutch roll frequency for the HL-10 vehicle at $M = 1.2$ was computed from both flight and wind-tunnel data and the results compared. Throughout most of the angle-of-attack range, the agreement is good, which indicates reasonably accurate prediction of stability. The prediction was also good at most other Mach numbers. With the dynamics predicted well, the vehicle was accurately represented to the pilot on the simulator. The difference in frequency at high angles of attack was not noted in flight because of other problems that will be discussed later.

As discussed in paper 2, the flight values of the rotary derivatives have been consistently higher than predicted; however, this has not affected the program. With the size/inertia characteristics of the lifting bodies, most of the damping is provided by the augmentation system and very little by the aerodynamic damping. For a very large airplane, the basic damping term increases in direct proportion to the size of the vehicle; in fact, it approaches the magnitude of the augmentation damping. Thus errors in the rotary derivatives of the magnitude shown in paper 2 can cause large errors in the prediction of vehicle motions and, hence, handling, particularly in the approach and landing phase.

As discussed in paper 4, the prediction of lift and drag for the lifting bodies has occasionally not been good, at least in terms of transport standards. Errors in L/D up to 10 percent have been observed, which could lead to energy management problems. However, with approach techniques that use the high energy, front side of the L/D curve, these errors have had no significant effect. On a normal straight-in, power-off final approach, airspeed is used to make vernier adjustments to the glide angle and hence the aim point, as discussed in paper 6. A 10-percent error in drag is relatively insignificant when compared with the total L/D modulation available with this technique.

These types of errors are significant if the ferry mission or a powered, shallow, L/D_{\max} approach is considered. For this type of approach, a 10-percent error in L/D is directly a 10-percent error in installed thrust and fuel consumption, which are factors that would also directly affect payload in the shuttle vehicle.

In terms of requirements for shuttle vehicles, one of the more important lifting body program results is in performance. The flight program has shown that these vehicles have sufficient performance to execute a normal unpowered approach, flare, and landing. This result is backed up by the work at the Flight Research Center with the X-15 airplane, fighter aircraft, and low L/D approaches with transport aircraft. Pilot comments from the M2-F2 flights indicate that an L/D_{\max} of about 3.0 is near a minimum for normal unpowered operations with minimum desirable flare and float times. The HL-10 vehicle is considered good for normal operations, having an L/D_{\max} greater than 4.0 at approach Mach numbers (0.45 to 0.55). Pilots indicate that lift-drag ratios above 4.0 do not provide an obvious advantage, particularly in landing accuracy on a VFR approach. The shallower glide path makes the aim point harder to define, thus touchdown precision is degraded.

Acceptable handling-qualities results have been achieved with the existing lifting body vehicles, even with the damper systems not operating; however, these results do not apply directly to the shuttle, as will be shown in paper 10. The very large size and inertia of the shuttle vehicle result in order-of-magnitude differences in frequency and damping between the shuttle and the lifting bodies even when the same aerodynamics are used. Certain facts have emerged, however, that are applicable; namely, the job of making a flyable airplane is greatly simplified if the vehicle has directional stability, good roll power, and very small yaw due to aileron deflection. These characteristics have not been easy to achieve on the lifting bodies, as evidenced by the amount of wind-tunnel time used to develop the shapes.

UNEXPECTED PROBLEMS

Even though the prediction techniques have been generally good, there have been some unexpected aerodynamic and handling-qualities problems—the types that are always experienced in a normal aircraft development program. These problems and their solutions point out the requirement for small-scale (one-fourth to one-third) flight testing of the shuttle configuration, particularly if it is very unconventional in shape or in the way that it is used. In a sub-scale program, these problems can be solved with minimum cost and effort, as they were in this program; in a prototype effort, design and construction costs alone can become prohibitive if configuration changes are required at a late date.

The most serious unexpected problem was the tip-fin flow separation on the HL-10 vehicle. This problem had been observed in the wind-tunnel data, but its magnitude was not appreciated until after the first HL-10 flight. At that time, wind-tunnel tests which carefully matched flight conditions fairly well duplicated the problem seen in flight. As shown in figure 2, the vehicle was unstable and uncontrollable during the period of separated flow on this flight. The main lesson to be learned is that the boattailing of these shapes to achieve better subsonic performance can lead to

serious flow separation problems, and, as pointed out in paper 4, surface roughness can further aggravate the problem.

Another generally unappreciated factor that makes consideration of flow breakdown important is the relatively high Mach numbers experienced in the approach and landing. Mach numbers greater than 0.6 on final approach and greater than 0.55 at the start of flare are common. Thus tailoring the shape for very low subsonic conditions ($M < 0.3$) is futile.

Another major concern was the handling-qualities problem on the M2-F2 vehicle. This resulted from the very unconventional aileron characteristics of the vehicle and a pilot input that coupled with the long-term lateral mode to drive the vehicle unstable. A typical neutrally stable pilot-induced oscillation during the approach phase is evident in the M2-F2 plots of figure 3. Improved aileron characteristics resulting from the addition of a center fin, plus other modifications to the M2-F2 vehicle, thereby converting it to the M2-F3 vehicle, have permitted the augmentation system to operate effectively, providing enough damping in roll to solve the problem. The improvement is obvious in the M2-F3 time history. This type of problem may exist on the shuttle vehicle at hypersonic speeds at which basic roll damping ceases and the ailerons are relatively ineffective.

Prediction of yawing moment due to aileron deflection appears to be a general problem with vehicles of this shape, as does sensitivity to yaw due to aileron, the worst possible combination. A more positive $C_{n\delta_a}$ than predicted led to an unexpected unstable Dutch roll mode on the HL-10 vehicle, as shown in figure 4. Recovery was made as a result of increasing dynamic pressure and the pilot reducing angle of attack. On the X-24A vehicle, $C_{n\delta_a}$ was predicted to be slightly negative, but actually was slightly positive. Thus the carefully optimized control system features originally designed into the system were invalid in flight. Because of the sensitivity of these lifting body shapes to $C_{n\delta_a}$, resulting from low directional stability and high dihedral effect, large values of yaw due to aileron of either sign, are to be avoided.

CONTROL SYSTEMS IMPLICATIONS

The lifting body flight tests have demonstrated that, with reasonable aerodynamics, only a simple flight control system is required to achieve an aircraft with good flying qualities. In this context, "simple" means conventional hydraulic controls with rate-feedback dampers. Throughout nearly all of its flight envelope, the HL-10 vehicle has good handling qualities based on airplane standards. In addition, the HL-10 vehicle has been flown satisfactorily without any augmentation.

Conversely, the lifting body flight-test program has also shown that it is unlikely that a control system could compensate for basic vehicle aerodynamic deficiencies. A prime example of this was the original M2-F2 handling-qualities problem. A simulator study with complete freedom to change gains, interconnect, and even provide a complete rate command system showed only a marginal improvement in the low-angle-of-attack handling problems. By contrast, a relatively simple aerodynamic

change—the addition of a center-fin to reduce yaw due to aileron—has been shown in flight to have completely solved the problem.

Thus, the primary lesson learned in the program in regard to control systems has been that black-box control systems should not be relied on to correct fundamental vehicle aerodynamic deficiencies. Every effort should be made to achieve the best possible basic aerodynamic characteristics.

FUTURE PROGRAM

The status of the lifting body program and future plans are shown in figure 5. The HL-10 program as originally envisioned is essentially complete. The vehicle is being used in the powered landing program to be discussed in paper 8, and we are planning for other programs to directly support the shuttle activity. These possible programs include power-off, IFR, terminal-area energy management studies and the determination of the effects of thermal protection system roughness.

The other two vehicles will be flown through the transonic region to further assess the ability of the wind tunnels to predict the characteristics of these blunt shapes in this region and to investigate vehicle handling and unforeseen problems. Additionally, the M2-F3 vehicle will be flown with reaction controls in the normal aerodynamic flight region down to landing. If this effort is successful (and the simulator studies indicate it will be), it could mean potentially large savings in control system weight and complexity on the shuttle vehicle.

CONCLUDING REMARKS

The lifting body program has been successful in that it has provided insight into the usability of wind-tunnel results and pointed out some interesting problem areas. In addition to the planned follow-on work, a similar program on a sub-scale version of the final shuttle configurations is being considered. Such a program could result in considerable cost and time-saving for the final vehicle.

HL-10 DUTCH ROLL FREQUENCY

TRANSONIC CONFIGURATION; DAMPERS ON;
 $M = 1.2$; $q = 100 \text{ LB/FT}^2$

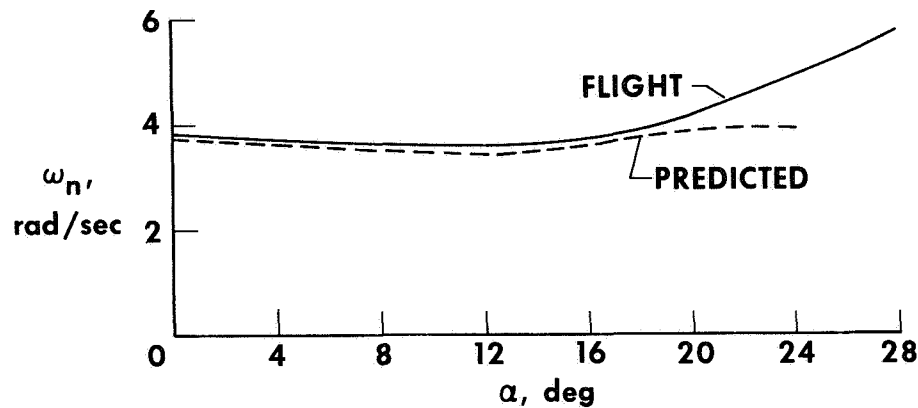


Figure 1

EXAMPLE OF HL-10 FLOW SEPARATION

SUBSONIC CONFIGURATION; $M \approx 0.65$

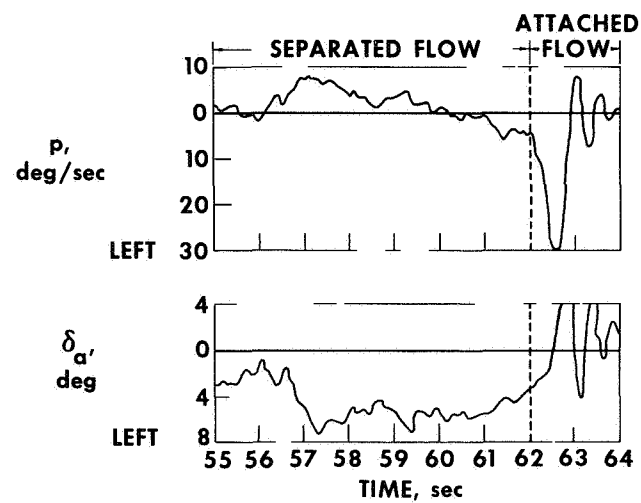


Figure 2

TIME HISTORY OF FINAL TURN AND APPROACH

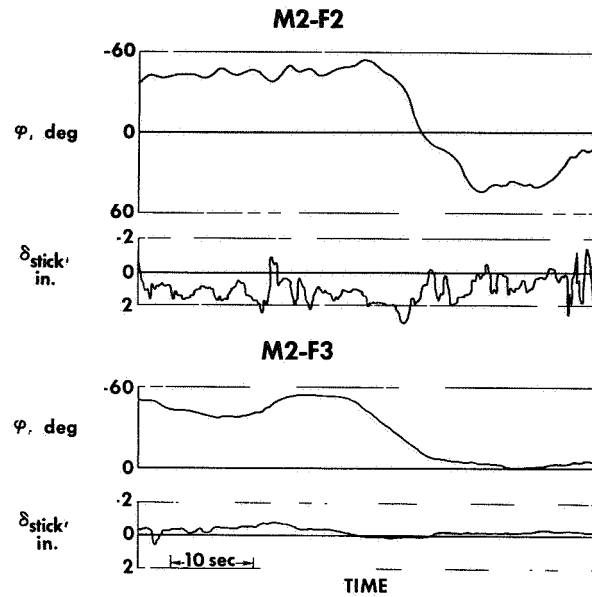


Figure 3

HL-10 DUTCH ROLL INSTABILITY

TRANSONIC CONFIGURATION; $M = 1.2$

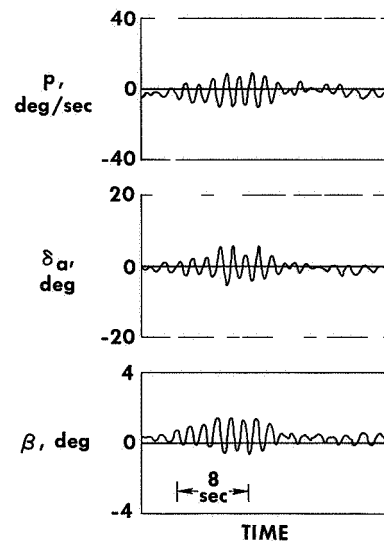


Figure 4

LIFTING BODY PROGRAM STATUS

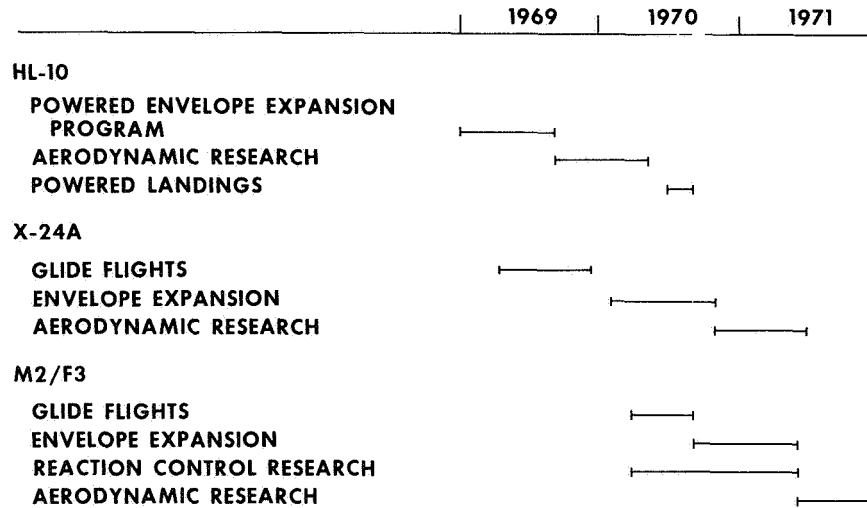


Figure 5

8. APPROACH AND LANDING STUDIES

By Berwin M. Kock and Fitzhugh L. Fulton, Jr.
NASA Flight Research Center

INTRODUCTION

This paper will discuss the application of recent approach and landing studies to the proposed space shuttle. These studies were conducted basically in two areas: powered approaches with the HL-10 lifting body, and unpowered types of approaches with shuttle-size vehicles, the B-52 and CV-990 airplanes.

SYMBOLS

a_n	normal acceleration, g units
C_L	lift coefficient, $\frac{\text{Lift}}{qS}$
L/D	lift-to-drag ratio
p	rolling angular velocity, deg/sec
q	dynamic pressure, lb/ft ²
S	reference planform area, ft ²
γ	flight-path angle, deg
φ	angle of bank, deg

HL-10 POWERED APPROACH

Several possibilities are being considered for the approach and landing phases of

a space shuttle vehicle mission, ranging from an unpowered approach to the use of airbreathing engines that would make it possible to fly a 3° glide slope with a go-around capability. Each of these extremes has advantages as shown in the following table:

Approach	Advantage
Unpowered	No weight penalty for fuel and engines Fewer subsystems/higher reliability Simple to fly – Positive speed stability/no power manipulation Good handling characteristics/simpler flight control system Large stall margins Good visibility
Powered	Go-around capability Experience Developed IFR guidance systems Better visual flare judgment

The HL-10 powered approach program evaluated the area between these two extremes.

After the HL-10 stability and control program was completed, the vehicle was modified to incorporate a propulsion system that could be used to reduce the approach angle from approximately 18° to 6°. The system included three H₂O₂ rockets, each capable of producing 500 pounds of thrust for 90 seconds of operation. All three rockets were required to provide the 6° glide slope at 300 knots airspeed. The operational technique developed to utilize the rocket engine capability is illustrated in figure 1. As shown, the approach was started at 15,000 feet altitude, and the aim point was at the end of the runway. At an altitude of 6500 feet mean sea level, the rockets were turned on and the thrust was used to shallow the glide slope while an air-speed of 300 knots was maintained on this glide slope to an altitude of about 200 feet, where the rockets were turned off and the landing gear extended. The landing was then made.

In a maneuver of this type it would be desirable to have two separate and independent systems, each capable of supplying the thrust required to maintain the desired glide slope. This was not practical with the HL-10 vehicle. A hydrogen-peroxide rocket system, installed when the vehicle was constructed, was retained as an emergency mode; however, this system provided 1000 pounds of thrust for 30 seconds and could not be considered a duplicate of the primary system. The required safety margin for the maneuver was obtained by designing the pattern so that a normal power-off landing could be performed if the rockets failed to operate. This required that an indicated airspeed of approximately 300 knots be maintained throughout the maneuver. Ground simulator and F-104 flight simulation tests indicated that if the rockets failed after the 6° glide slope angle was attained, a landing could be made from anywhere in the maneuver if the initial airspeed was maintained throughout the maneuver. However, the runway required for this technique was 7.5 miles long with a 3.5-mile emergency overrun. Thus, only Rogers Dry Lake met the requirement.

The first HL-10 flight made with this operational technique pointed out several negative features:

(1) It is more difficult to determine the aim point associated with the 6° glide slope than in a steeper approach, which tends to increase the touchdown dispersion.

(2) Airspeed is higher close to the ground than it is in an unpowered approach, thereby aggravating any control sensitivity problems.

(3) The pilot must be prepared for more contingency activities if the engine should fail, which would lead to a higher pilot workload in a critical part of the approach.

It can be concluded that the use of a limited duration propulsion system to shallow the final approach angle provides few of the benefits that can normally be obtained with power and introduces most of the disadvantages of weight, complexity, and reliability that the inclusion of power entails. Although the powered HL-10 experience showed that limited duration propulsion systems should not be used to shallow the glide slope, this conclusion may not be applicable to a space shuttle vehicle with air-breathing engines and perhaps 10 minutes of fuel together with a go-around capability. The inclusion of an airbreathing engine introduces some questions of reliability after a period in orbit, with attendant environmental considerations. In addition, the relatively low altitude airstart of multiple engines is questionable from an operational viewpoint, and, finally, unless some of the payload is sacrificed, the fuel available must be at a critically low level in relation to present military or airline requirements. Considering all these factors, it appears that the normal approach technique for the shuttle vehicle, even if airbreathing engines with go-around capability are installed, should be to operate the vehicle as if it were unpowered and rely on the engines only if the approach were greatly in error.

UNPOWERED TYPES OF APPROACHES WITH SHUTTLE-SIZE VEHICLE

Engineering Evaluation

Considerable experience has been obtained in making unpowered and simulated unpowered (using jet aircraft) landings; however, most of this experience has been with relatively small vehicles such as the X-15, HL-10, X-24, and F-104 aircraft. The NASA Flight Research Center has recently undertaken a program to investigate potential problems of operating a large, unpowered vehicle, such as the proposed space shuttle. A B-52 and a CV-990 airplane were used in this study. The B-52 work was conducted jointly with the Air Force Flight Test Center. The performance characteristics of these vehicles are shown in figure 2. The crosshatched areas show the range of lift-to-drag ratios (3.1 to 4.5) used during the approach, and the unshaded blocked areas are representative of the maximum lift-to-drag ratios used for flare. Deceleration to touchdown covered lift-to-drag ratios up to the maximum values shown.

The CV-990 airplane was operated with idle power, the landing gear extended, spoilers deployed, and 27° of flaps to obtain a configuration with a usable L/D as high as 5. The spoilers begin to blow back at an indicated airspeed of 200 knots, resulting in changes to the L/D as a function of gross weight. This feature is undesirable from

an analytical standpoint; however, it was not considered to be a problem in a visual approach. This configuration caused some horizontal stabilizer and airframe buffet. The buffet was within airframe limitations but was strong enough that operating time in this configuration was minimized to reduce wear on the airplane.

Another configuration of the CV-990 airplane resulted in lift-to-drag ratios as high as 8. In this configuration idle power was used, the landing gear were extended, and the flaps were deflected 36°. Most of the data were gathered in this configuration because no buffet problems were experienced.

The B-52 airplane was flown with the landing gear extended, airbrakes fully deployed, six engines at idle, and two engines at 75 percent rpm to supply power for the accessories. The maximum usable L/D was again about 8.

These configurations had some high-speed limitations. The B-52 approach speed was restricted to an indicated airspeed of 250 knots or less because of airbrake blow-down, and the CV-990 airplane was restricted to an indicated airspeed of 240 knots with 27° of flap and 220 knots with 36° of flap because of flap loads. These limits prevented operation in the very low L/D range where excess energy can be dissipated.

Most of the approaches were of the visual overhead type (fig. 3); however, several ground controlled types of approaches were made in the B-52 airplane to simulate instrument operation. These are discussed in paper 9. The CV-990 visual approaches were made in both the configurations previously described.

Simulated unpowered approaches were flown by pilots experienced in large airplanes and by lifting body pilots. The lifting body pilots commented that the pattern and approach performance characteristics were representative of those encountered in lifting body operation, but that the flare characteristics were not representative, probably because of the higher lift-curve slope and lower approach and touchdown speeds. However, they did not believe that this degraded the results of the approach studies with the large vehicles.

A brief touchdown pattern program was conducted with the CV-990 airplane in the high L/D configuration. Ten landings were made by two pilots (five each). Each pilot had previously performed approaches in the test configuration. The distance from the aim point to the touchdown point was computed to be approximately 2 statute miles with an approach speed of 220 knots and a touchdown speed of 135 knots. The end of the runway on the lakebed was used as the aim point, with the intended touchdown at the 2-mile marker. Because this was a visual task and the pilots did not vary the aim point from the end of the runway, the test was really an evaluation of the pilot's ability to establish the proper aim point and airspeed on final approach rather than a touchdown dispersion study. The results of this study are presented in figure 4 together with results obtained from a similar study in the X-15 airplane.

The CV-990 airplane was flown at the maximum allowable airspeed in the approach to simulate the low L/D range of shuttle vehicles, and touchdown was made at minimum speed to reduce tire wear. These airspeeds resulted in an excessive float time after flare (23 seconds), and no L/D modulation capability such as speed brakes was available to increase the deceleration. This contributed to the touchdown dispersion point at 2.7 miles shown in figure 4. The pilot was aware that he was going to be "long" at

a height of 3000 feet during this approach but had no means of dissipating the excess energy. An additional contributing factor was that the aim point was harder to determine at the higher approach lift-to-drag ratios. Conversely, the X-15 airplane had a lower approach L/D and very effective speed brakes for L/D modulation.

The CV-990 landing study points out that L/D modulation capability is necessary in unpowered landings and that approach and landing speeds must be compatible to avoid excessive float time after the flare. Some guidance in the approach would alleviate the problem of determining the aim point.

Pilot Comment

The technique used for this series of tests was to fly the airplane visually to the high key position and then set the proper configuration of flaps, landing gear, air brakes, and throttle to establish the desired L/D. As shown in figure 5, the high key position on these B-52 and CV-990 tests was from 20,000 feet to 26,000 feet above the ground (lower lift-to-drag ratios require higher altitudes). It was found best to offset the high key position approximately one-half mile to the right of the runway (for left-hand patterns). This prevented the higher true airspeed at that part of the pattern from causing the downwind leg to be displaced excessively from the runway. The bank angle from the high key position to the downwind leg was 40° to 45° and was essentially a mechanical turn, because judgment was not critical at that part of the pattern. It was not necessary to look at the runway until the downwind leg was reached, although it was comforting to see the landing point at all times. At the high key position, it was important to roll immediately into the bank without delay because there was a tendency in these larger airplanes to underbank when leaving the high key position, which would cause the pattern to be too wide. Bank angle modulations during the overhead patterns were similar to those used with the lifting body vehicles; that is, relatively small rates and accelerations were required. The time history of a CV-990 pattern shown in figure 6 is typical of the 360° overhead patterns flown. The bank angle averaged about 40°, with occasional excursions to 50°. The B-52 bank angles were slightly steeper and averaged around 45°, with up to 65° used on one occasion. In both the B-52 and the CV-990 airplanes the roll response was adequate but should be improved.

The test pilots who participated in this program included large airplane pilots, experienced lifting body pilots, and one instructor pilot from the USAF Aerospace Research Pilot School who was experienced in making F-104 low L/D approaches. None of the pilots had difficulty in flying this type of pattern with the B-52 or CV-990 airplanes; however, they all agreed that the lateral forces were too high and should be reduced. Experienced lifting body pilots have developed the technique of rapidly rolling into and out of a 40° to 45° bank to quickly view the ground to assure their position relative to the ground and make any necessary adjustments. They complained mildly about the inability to readily use this technique with the large airplanes. The slower lateral response and the higher aileron forces caused the maneuver to be physically demanding and too time consuming. The elevator forces were also too high during the turns but could be trimmed out. A more shallow force gradient is desirable.

Once the airplane was established on the downwind leg parallel to the landing area, approximately 3.5 to 4.5 nautical miles from the runway, it was important to be able to see the runway continuously until touchdown. Several left-hand patterns were flown from the right seat (copilot's seat), and the visibility was unsatisfactory on the

downwind leg and during approximately the first 30° of the turn from low key to final approach. In the last 150° of the turn, visibility was adequate because of the wing-down, nose-low aircraft attitude.

The low key altitude (fig. 5) was from 10,000 feet to 15,000 feet above the ground, again, depending on the L/D. At the low key position pilot judgment becomes an important factor. He has several options available in the B-52 and CV-990 airplanes for making pattern adjustments. He can steepen or shallow the bank; he can slow the airplane to increase the L/D. In these airplanes the most desirable options of diving off excess altitude and energy or opening speed brakes when above the desired glide slope were not available because of limitations on the airplanes. This resulted in a significant difference between the technique used in lifting body and F-104 L/D approaches and that used in the B-52 and CV-990 airplanes. In the smaller airplanes corrections to the desired approach angle were made by slowing the airplane when below the glide slope and by diving or using speed brakes to achieve a steeper angle when above the glide slope. The same technique would be desirable in the larger airplanes; however, because of flap limit speeds in the CV-990 airplane and speed brake blowdown speeds in the B-52 airplane, the technique of diving or extending speed brakes was not used when above the glide slope. In the smaller airplanes most pilots fly the pattern to arrive on the final approach with excess energy with the intention of diving off the excess or extending the speed brakes for a steeper approach. In the larger airplanes dissipation of excess energy was accomplished by S-turning the airplane, which was a less precise technique and could lead to greater touchdown dispersion.

The end of the runway was selected as the aim point. The approach angle was approximately 17° for the steeper approaches, but this did not appear to be excessively steep from the cockpit. All the pilots found that the aim point was easier to judge during the steeper approaches (low L/D) because the projected ground intercept point could be visualized more easily. The aim point was slightly easier to judge in the CV-990 than in the B-52 airplane because of the windshield configuration and the longer nose. Some type of sighting device, even a fixed gunsight, would probably assist in aiming the airplane at the projected ground intercept point. Additional practice approaches would also improve pilot judgment.

The flare altitude was 500 feet to 800 feet above the ground, depending upon L/D. The exact altitude was not critical, and the standard cockpit pressure altimeter in the B-52 airplane was adequate for beginning the flare. In both airplanes the longitudinal response during the flare was good, but the elevator forces were too high. The CV-990 airplane had a radar altimeter, and flare altitude was more precise and uniform. The altimeter was also helpful when the airplane was being held off the ground during the long float time between flare completion and touchdown. Some elevator trimming was needed as the airplane floated and slowed. The long B-52 float distance was undesirable, but the CV-990 float distance was even worse because the L/D increased significantly as the airplane slowed. It was difficult to judge the touchdown point because the airplane floated a mile or more after the flare was completed.

Many people are apprehensive about steep approaches in large airplanes, probably because it is not a normal procedure. Usually when a pilot in a large airplane dives at the ground, he does not know exactly how much altitude is required to pull out because he has not calculated or studied the problem. He has not practiced the maneuver, and he may not even know the exact terrain altitude. Therefore, it is not a

precision maneuver. In the power-off types of approaches that we advocate, we calculated the aim point and the flare altitude and practiced the maneuvers. In a relatively small number of approaches in large airplanes, we gained confidence that the approaches were safe and could produce acceptable repeatability without requiring undue pilot skill. Although we do not advocate using anyone other than experienced test pilots for the shuttle program, we are confident that almost any skilled pilot can be taught to perform VFR power-off approaches safely. Onboard or ground guidance systems can only improve this capability. IFR approaches appear to be completely feasible.

CONCLUDING REMARKS

It can be concluded from powered approach and landing studies with the HL-10 vehicle and unpowered studies with the B-52 and CV-990 airplanes that:

- (1) Limited duration propulsion systems used to shallow the approach angle produce few benefits and many disadvantages.
- (2) Unpowered types of approaches are feasible with large vehicles.

SCHEMATIC OF HL-10 APPROACH TECHNIQUES

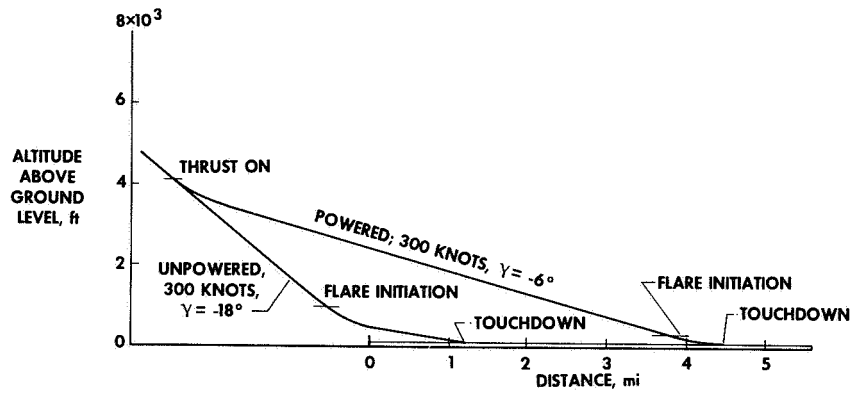


Figure 1

PERFORMANCE CHARACTERISTICS OF B-52 AND CV-990

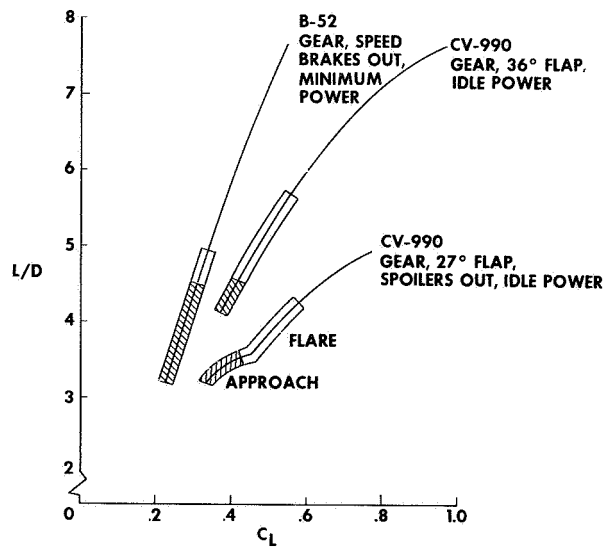


Figure 2

VISUAL OVERHEAD APPROACH TECHNIQUE

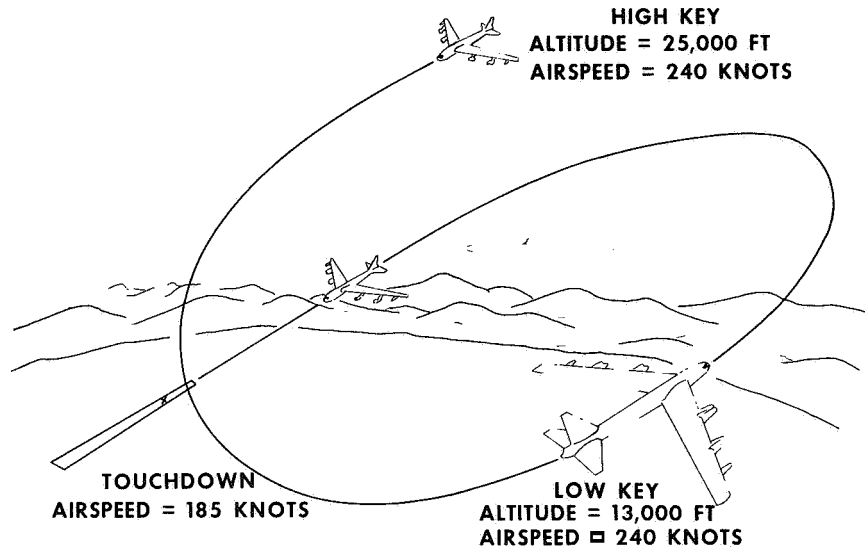


Figure 3

CV-990 TOUCHDOWN PATTERN

GEAR DOWN; 36° FLAP; 220-KNOT APPROACH SPEED

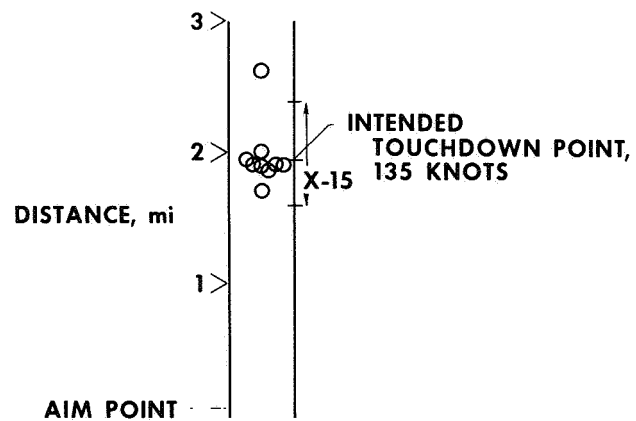


Figure 4

B-52 AND CV-990 LOW L/D APPROACH PATTERN

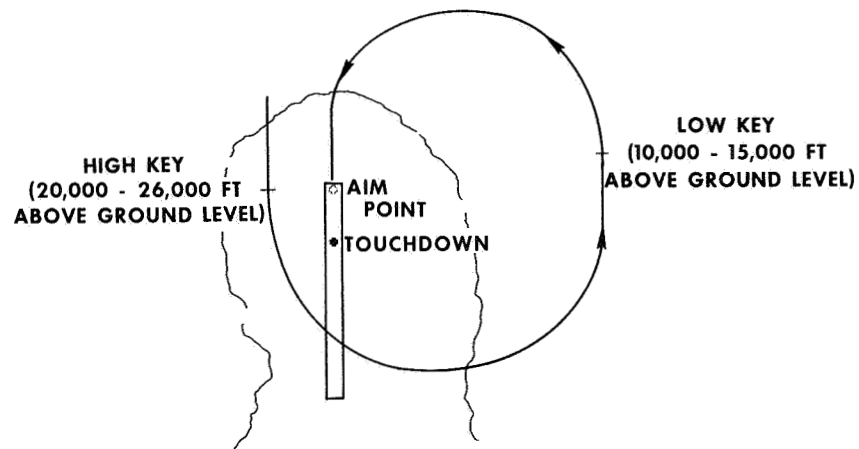


Figure 5

TIME HISTORY OF CV-990 360° OVERHEAD APPROACH

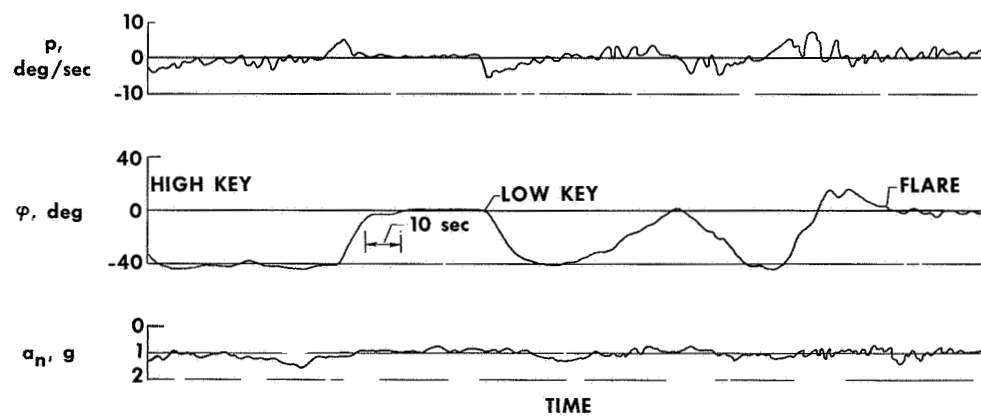


Figure 6

9. IFR EXPERIENCE WITH UNPOWERED, LOW-LIFT-DRAG- RATIO LANDING APPROACHES

By Peter C. Hoag and B. Lyle Schofield
Air Force Flight Test Center

INTRODUCTION

The space shuttle system, as now envisioned, is to have operational capability. In the words of the Phase B Statement of Work, this requirement is for "an airline-type operation for passengers and cargo transport." Additionally, the Statement of Work specifies the requirement for a remote-controlled landing capability and that "the automatic landing capability should permit landing under FAA Category II conditions." The first statement implies the requirement for instrument flight rules (IFR) operation and, although directed at an automatic landing system requirement, the second statement would imply the same capability for piloted operation.

Before publication of the Phase B Statement of Work and in view of the anticipated IFR requirement, three coordinated studies were initiated at Edwards Air Force Base in 1969 to investigate instrument landing approaches for low L/D, unpowered vehicles. These studies were: (1) an instrument landing system (ILS) study conducted by the Air Force Flight Test Center (AFFTC) with an F-111A airplane (ref. 1), (2) a ground controlled approach (GCA) study performed by the NASA Flight Research Center with an F-104 airplane (ref. 2), and (3) a joint AFFTC/NASA program conducted with an NB-52B airplane (ref. 1).

The most important question to be answered by these studies was whether an unpowered, low L/D vehicle could be operated safely under IFR. Other factors such as the effects of aircraft size, maximum L/D, L/D variations, planform loading, and ceiling minimums were investigated. A guidance technique was evolved as a result of flight planning for ILS approaches.

Some of the visual approach aspects of these studies were discussed in paper 8. This paper discusses the results of the IFR flight studies and briefly presents two terminal area guidance schemes specifically designed for terminal area energy management and guidance of unpowered, low L/D vehicles.

SYMBOLS

C_L lift coefficient, $\frac{\text{Lift}}{qS}$

L/D	lift-to-drag ratio
M	Mach number
q	dynamic pressure, lb/ft ²
S	wing area, ft ²
Δ	change or increment
Λ	wing sweep, deg

Subscripts:

max	maximum
min	minimum

F-111A LOW L/D ILS APPROACHES

The variable wing sweep and relatively large variation in gross weight of the F-111A airplane made it possible to investigate the flight characteristics for a range of low lift-drag ratios and planform loadings (fig. 1). The 72.5° wing-sweep configuration with the gear retracted (clean) was representative of a reentry vehicle with a high fineness ratio. The maximum L/D was relatively high (6.0), and the associated speeds were also high (288 knots at 45 lb/ft² planform loading and 349 knots at 66 lb/ft² planform loading, the highest loading tested in this configuration).

The 72.5° wing-sweep configuration with the gear extended provided a maximum L/D of 3.7, which is representative of the HL-10 and X-24A lifting bodies now being flight tested. The F-111A gear limit speed of 295 knots prevented operation on the steep front side of the L/D curve where the lifting bodies operate during their landing approach. As shown in figure 1, this restricted L/D variation and, consequently, vehicle ranging.

From the standpoint of maximum L/D, the 50° wing sweep, gear-down configuration was representative of many configurations proposed for the space shuttle except that the peak L/D occurred at a somewhat higher speed (lower lift coefficient) than for the space shuttle configurations. At a planform loading of 45 lb/ft², the F-111A L/D_{max} speed was 226 knots; the space shuttle speeds are approximately 175 knots.

The 26° wing sweep, gear-down configuration has an L/D range which covers the maximum performance anticipated for reentry configurations.

The "nominal approach L/D" which was used in defining ILS approach patterns is indicated on each curve. The nominal L/D was selected to provide a moderately high L/D for the particular configuration as well as to provide for variations in L/D and speed while staying within the constraints imposed by the gear limit speed. Operation on the front side of the L/D curves was found to be important in the control of ILS approaches. The cues to the pilot in correcting to glide slope were in the proper direction; i.e., if the airplane was below the glide slope, he pulled the nose up which increased the angle of attack (and lift coefficient) and provided a higher L/D and a shallower flight path angle. When the shallower flight path intersected the desired glide slope, he pushed the nose down to maintain the glide slope and the speed began increasing to the desired value.

MODEL OF ILS APPROACH TECHNIQUE

The onboard F-111A inertial navigation system provided the capability to generate any desired glide slope to any preselected site below 10,000 feet altitude. The pilot was presented with distance, bearing, and glide slope and glide path centerline information to the preselected site. Additionally, a sensitive radar altimeter provided the pilot with accurate height information for flare initiation.

By using this onboard equipment, a navigational and terminal area energy management scheme was developed to investigate an ILS type of approach for unpowered, low L/D configurations. A model of this scheme is shown in figure 2. The approach technique can be divided into the following four phases, with a transition maneuver between each phase:

Energy dissipation - deceleration and descent at a constant radius around point A down to the initial approach altitude (similar to traversing the surface of a cylinder)

Initial approach - constant airspeed, straight descent toward point B for the turn to final approach (similar to traversing the surface of a cone)

Final approach - constant airspeed descent on the runway heading toward point C down to flare altitude

Deceleration and landing - deceleration on a very shallow glide slope to touchdown

The only assumption made in the implementation of this scheme was that a reentry guidance scheme would be capable of guiding the pilot to intersect the energy dissipation cylinder at speeds greater than Mach 0.85 and less than Mach 2.0.

A number of these approach maneuvers were performed starting at Mach 2.0 and 50,000 feet altitude (fig. 3). A supersonic configuration of 72.5° wing sweep, gear retracted (clean) was used down to Mach 0.85 where the airplane was reconfigured to 50° wing sweep, gear down, which was the configuration most representative of space shuttle configurations. At the start of the maneuver, the center coordinates (A) of the

energy dissipation circle were selected so that the inertial distance measuring equipment (DME) presented the distance or radius to the center. As the airplane slowed and descended, the bank angle was reduced and modulated to maintain the 16.5-nautical-mile turn radius. When the predetermined turn-in altitude of 34,000 feet and an indicated airspeed of 285 knots were reached, the gear was lowered and the wings were swept to establish the 50° wing sweep, subsonic L/D configuration. An initial approach radial was determined at that time, and the coordinates and glide slope for the radial aim point (B) were inserted into the inertial system. During the initial approach phase (fig. 4), the pilot modulated airspeed and bank angle to center the glide slope and glide path centerline displays while monitoring the DME, which presented the distance to the glide slope aim point (B).

Little attention to speed and altitude was required. The altitude was determined by the glide slope, and when on the power glide slope the airspeed tended to stabilize at the proper speed. When the precomputed turn distance appeared in the DME display, the pilot started a 30° bank to final approach while maintaining airspeed. During the turn, the final approach glide slope aim point (C) coordinates were selected. The airplane was rolled out of the turn on the final runway heading, and the pilot returned his attention to the glide slope and glide path centerline displays. These displays were centered during the final approach while the pilot monitored the radar altimeter. As the radar altitude reached the proper flare height above the runway, the pilot reverted to visual flight by removing the hood and initiated the flare. Because of the ground clearance and tire speed limits of the F-111A airplane, the wings were moved to 26° sweep between the start of flare and touchdown.

Two other methods of intersecting the energy dissipation circle were also demonstrated (fig. 5). These methods were based on headings directly toward the center of the circle at the time power was cut (Mach 2.0 and 50,000 feet altitude). In one instance, the power was cut 30 nautical miles from the center, and the pilot banked the airplane to intersect the energy dissipation circle tangentially (approach 2). In the other instance (approach 3), the power was cut directly over the center of the circle, and the pilot banked the airplane to intersect the energy dissipation circle from the inside. The energy dissipation circle constitutes, in essence, a landing approach window 33 nautical miles in diameter, because the approach can be made from any direction to intercept the dissipation circle. A speed range from Mach 0.85 to Mach 2.0 for interception with the landing approach window above 34,000 feet altitude was demonstrated during this program. Approaches 2 and 3 were representative of the positioning that would be available from a simple reentry guidance system such as the guidance scheme used in the Precision Recovery Including Maneuvering Entry (PRIME - SV-5D configuration) program. It should be pointed out that these two approaches were also performed under the hood. All three of the ground tracks are actual test results.

Four pilots flew more than 50 approaches (mostly hooded) using the range of lift-drag ratios and the configurations shown in figure 1. Of these, nine were started at about Mach 2.0 and 50,000 feet altitude, and five of the nine were performed hooded down to flare initiation. Two of the pilots were experienced lifting body pilots, and two were Air Force test pilots assigned to the F-111A Test Force. All pilots performed the hooded ILS type of approach in the four configurations. The approach conditions are summarized in table 1. The lowest start flare/hood removal altitude (200 feet) was with the 26°, gear-down configuration which provided the highest L/D (6.6) at the start of flare, the lowest approach glide slope and airspeed, and the

largest L/D variation (6.6 to 8.0) for flare. The highest start flare/hood removal altitude (800 feet) was associated with the 72.5°, gear-down configuration which exhibited the highest approach glide slope (lowest approach L/D) and essentially no L/D variation availability during flare. Hood removal altitudes were selected from tests which showed that the pilot could descend while hooded to flare altitude, remove the hood, and perform a comfortable flare.

TABLE 1. – UNPOWERED, LOW L/D F-111A REPRESENTATIVE APPROACH CONDITIONS

L/D		Configuration	Approach		Start flare/hood removal altitude, ft above ground level	Average planform loading, lb/ft ²
Maximum	Nominal		Glide slope angle, deg	Airspeed, knots		
8.0	6.6	$\Lambda = 26^\circ$, gear down	8.1	250	200	58
5.5	5.0	$\Lambda = 50^\circ$, gear down	10.1	285	450	55
3.7	3.7	$\Lambda = 72.5^\circ$, gear down	13.6	270	800	48
6.1	5.3	$\Lambda = 72.5^\circ$, clean	8.6	410	450	66

The major conclusion from the low L/D, simulated IFR tests was that it was possible to make hooded approaches consistently from Mach 2.0 and 50,000 feet altitude to flare initiation. Further, these maneuvers were performed by four different pilots, two of whom attempted and performed the maneuver from Mach 2.0 only once. The pilots considered the flying task for this type of ILS approach to be less demanding than that associated with normal, low speed, powered ILS approaches for the following reasons:

- (1) The higher approach speeds associated with low L/D approaches provided significantly better handling qualities than experienced in the low speed, powered approaches.
- (2) Approaching at the higher speeds provided stall margins large enough that the pilot was not concerned with speed changes associated with flight path control.
- (3) Operation on the speed stable side of the L/D curve allowed the pilot to make corrections to glide slope with pitch changes only rather than with a combination of power and pitch change, which is required for the conventional, low speed ILS approach.

F-104 LOW L/D IFR APPROACHES

The lowest L/D configuration that could be investigated with the F-111A airplane provided lift-drag ratios down to about 3.5. The F-104 airplane, with idle power, takeoff flaps, gear down, and speed-brake modulation, made it possible to investigate an L/D range of 4.2 to 1.9 (fig. 6). The high speed end of the F-104 L/D curve, like that of the F-111A airplane, was limited by gear-down speed, but unlike the 72.5°, gear-down F-111A configuration, the F-104 gear limit speed did not prevent operation

on the front side of the L/D curve. Consequently, better range control was possible with the F-104 low L/D configurations. The general shape and operating range of the F-104 curve made it representative of lifting body types of space shuttle configurations.

The lack of sufficiently sophisticated onboard navigation equipment made it necessary to consider external guidance techniques for the IFR flight studies. A ground controlled approach (GCA) technique which used precision radar for glide slope control and an ILS localizer for glide path centerline control was found to be most satisfactory.

A model of the resulting guidance technique is shown in figure 7. The terminal area approach window was defined at a particular altitude (35,000 feet) by the maximum and minimum L/D performance down to the intercept point. The glide slope from the intercept point down to flare was defined by a glide slope which would have adequate energy (airspeed) for flare and still have enough time for small altitude adjustments during deceleration prior to touchdown. A preflare glide slope of 16° was selected (nominal approach L/D, fig. 6). For stabilized flight, with speed brakes retracted, this resulted in an approach speed of about 300 knots. The preflare glide slope entry altitude (intercept point) was selected to be 10,000 feet above ground level (AGL). When the pilot reached this altitude, he was directed to the preflare glide slope. Flare was started at about 1000 feet AGL. After the airplane passed through the approach window, the piloting technique for this guidance scheme was to fly toward the nominal glide slope. This was done by modulating pitch attitude (and speed brake if required) to vary the flight path and intersect the nominal glide slope at or prior to the intercept point.

A series of approaches were used to define the size of the 35,000-foot altitude approach window. Profiles of several of these approaches are shown in figure 8. To obtain these data, the ground controller vectored the airplane to a start-descent point at an altitude of 37,000 feet. Ten seconds before reaching this point the pilot configured the airplane to the required configuration. The airplane was then pushed over to attain the desired approach speed. Glide slope adjustments were made by using pitch changes in accordance with the ground controller's callouts on aircraft position above or below the planned glide slope. In addition to transmitting altitudes above and below the glide slope, the ground controller provided some trend information on convergence with the glide slope. (It should be pointed out that for conventional, powered GCA operations trend information is available to the pilot through rate of sink. The rates of sink for unpowered, low L/D approaches exceed the limits of normal rate-of-sink instruments.) The pilot had glide path centerline information from the ILS display.

The length of the approach window at 35,000 feet altitude was slightly greater than 7 nautical miles. The width of the approach window was roughly determined by the ILS localizer width (2 nautical miles) at approach window altitude. There was no attempt during this program to accurately define a minimum safe descent altitude for GCA operations. It was the opinion of the pilots, however, that a ceiling of at least as low as 1500 feet could be negotiated easily with the F-104 airplane.

Three pilots participated in this evaluation. The most interesting finding of the program was the ease with which the task could be performed. The airplane had excellent handling qualities as a result of the high approach speed, and adjustments to the flight path angle were made by simple pitch changes. Because there was no power

to adjust and monitor, the workload was less than that for a normal GCA.

Three flights were flown under actual IFR weather conditions; however, the lowest ceiling was 4000 feet AGL. Approaches under this ceiling were no challenge to the GCA procedure.

Another interesting occurrence on a weather flight was an encounter with icing. On three separate approaches, icing was encountered at about 20,000 feet altitude. The high descent rates associated with these low lift-drag ratios prevented any significant buildup of ice and consequently did not hinder the flight operations. Such may not be the situation with shuttle configurations which depend upon cruise for cross range or use slow speed, powered approaches. The most favorable cruise altitudes for these vehicles are likely to be around 20,000 feet. For engine-out operation this altitude will probably drop to approximately 13,000 feet. The probability of encountering ice in the 10,000- to 20,000-foot altitude band is 5 percent or better from fall through spring throughout most of the continental United States (ref. 3). Shuttle configurations and the cruise speed and altitude range they are likely to use are conducive to ice collection. Flow disturbances caused by icing could have severely detrimental effects on the performance of these marginally powered aircraft.

NB-52B LOW L/D GROUND CONTROLLED APPROACHES

Hooded ground controlled approaches were made in the NB-52B airplane (with idle power, gear down, and airbrakes fully deployed) at lift-drag ratios from 3.2 to 4.4. There was no attempt to define an approach window as was done with the F-104 airplane, but straight-in approaches were flown from about 18,000 feet mean sea level through flare to touchdown (fig. 9). The approach airspeeds for these maneuvers varied from 230 to 250 knots, and the flare initiation altitudes were from 500 to 800 feet AGL.

As in the F-104 tests, glide slope information from the NASA Flight Research Center's precision radar was used by a ground controller to provide glide slope corrections to the pilot. Glide path centerline steering information was provided to the hooded pilot by the non-hooded safety pilot through visual contact with the runway.

The three pilots who participated in this portion of the evaluation concluded that the piloting task associated with this maneuver was no more demanding than for normal, powered GCA operations. Here, again, as in the F-111A and F-104 instrument approaches, the piloting task was less demanding because the airplane was being flown in the speed stable region, which required no throttling, and the handling qualities were better at the higher approach speeds. However, because of the lack of vertical speed indications (the rate-of-climb meter was pegged throughout the approach), it was necessary to use pitch attitude alone to make corrections to the glide slope. This was a somewhat more difficult task than using pitch attitude and vertical speed for corrections to the glide slope in a normal GCA. As a result, the overall task was about as demanding as a normal, powered GCA. The addition of trend indicators such as vertical speed would undoubtedly improve the pilots' ratings of the unpowered ground controlled approach.

It should be noted that ILS approaches in the F-111A evaluation were easier than the GCA operations. Trend information was available to the F-111A pilot through

monitoring the glide slope and centerline displays, but only position information with some delayed trend information was available using the ground control procedures.

WIND EFFECTS ON INSTRUMENT APPROACHES

The results of all three (F-111A, F-104, and NB-52B) unpowered, low L/D flight studies showed that effects of wind on instrument approaches can be significant. Both the ILS and GCA types of approaches incorporate relatively long straight-in final approaches which are performed on a specific glide slope. The glide slope is an earth-fixed reference path, but vehicle glide performance (flight path) is related to the air mass in which it is operating. Therefore, the glide slope and flight path angles are the same only when there is no wind. Under wind conditions, the glide slope angle had to be slightly modified to permit an approach at a given L/D.

Two wind compensation techniques were used during these test programs. With the F-104 airplane, a descent was made on runway heading at a particular L/D before the start of testing and the resulting glide slope was measured. The measured glide slope was compared with a flight path computed from L/D and approach speed. The difference between the actual glide slope and the computed flight path was assumed to be wind effect, and all subsequent test glide slopes were modified by this angular difference.

An approximation based on a steady wind analysis of glide slope change with wind was used in the F-111A and NB-52B programs. Wind data from balloon soundings were used to determine head or tail winds which would be encountered on final approach. Engineering judgment was used to select an effective steady headwind, and the ratio of effective headwind to approach speed was used to obtain a change in glide slope due to wind (fig. 10 and ref. 4).

This technique for wind compensation worked moderately well, but program limitations prevented a full exploration of proper wind compensation. Additional study is required to determine how variable winds can be resolved into an effective steady wind component for glide slope correction, or other analytical techniques must be devised to provide proper wind compensation. It should be noted that the model technique used during F-104 testing was effective for wind compensation and could be used operationally if other techniques were not available. A powered airplane such as the F-104 could be sent up a short time before shuttle landing to determine the necessary wind compensation by descending at the approach speed and L/D of the space shuttle.

TERMINAL AREA GUIDANCE SCHEMES

Approach and landing of unpowered shuttle vehicles will require a terminal area energy management and guidance scheme for IFR flight conditions. It has been demonstrated in the F-104 and NB-52B approach studies that unpowered approaches and landings can be made using GCA techniques down to altitudes of at least as low as 1500 feet AGL. A simple, manually selected, onboard guidance scheme was demonstrated with the F-111A airplane down to altitudes as low as 200 feet AGL. Two other guidance schemes which can be fully automated have originated at the NASA Flight

Research Center and at the AFFTC. These schemes, which typify the guidance system that will be required for space shuttles, will be discussed in simplified form because of the limited time and scope of this paper. It appears that both schemes would require a system of about the same complexity as that available in the F-111A airplane except that it would be optimized from the inception around the scheme to be mechanized.

The final approach, flare, and deceleration to landing of any unpowered instrument approach now envisioned should be the same as in the F-111A low L/D approaches, i.e., a relatively long final approach at an airspeed high enough for a flare and a shallow deceleration of at least 8 seconds to touchdown. A system must be devised to provide the best method of placing the aircraft on this type of final approach with the proper airspeed.

Guidance Scheme 1

The first scheme considers L/D modulation capabilities but basically emphasizes bank angle modulation for energy management (ref. 2). Heading command would be provided to the pilot on the vertical bar of a flight director display. By turning the vehicle to satisfy this command, the vehicle would converge on a predetermined flight path. Elevation error would be provided on the horizontal bar to indicate a situation (not command) relative to the precomputed flight path.

Figure 11 shows the means of generating this approach technique. For a given vehicle and constant indicated airspeed, constant bank angle descents are determined for several bank angles. This results in a family of descending spirals. The cross section at any radial (azimuth angle A), as it intersects the flight path for each bank angle, generates a straight line with a particular elevation angle (E). These straight lines throughout the range of azimuths generate, loosely speaking, a conical surface. Obviously, a mirror image exists for right-hand turns. In application, if a vehicle enters the terminal area with high energy, it intersects the conical surface rather high and wide and flies a shallow bank angle approach. Conversely, low energy at the start of the approach results in low, close in acquisition of the surface and steep bank angle maneuver.

Some advantages of this scheme are:

1. The concept is simple.
2. Correction for winds down to the start of final approach appears to be inherent.
3. Large L/D variation capability is not required.
4. Arrival in the terminal area with substantial excess energy is possible.

Some disadvantages are:

1. The guidance accuracy begins to degrade if the heading change required to line up on the runway is greater than 180°.

2. The needle indications on the attitude director indicator (ADI) are coupled; that is, bank corrections change the pitch situation, and pitch corrections (if made) affect the bank error. This is abnormal and may be confusing. Additional research is being done to define an appropriate display and command system.

3. Wind compensation for final approach may be required.

Guidance Scheme 2

The second terminal area guidance scheme is modeled after the low L/D F-111A guidance scheme without the energy dissipation circle. The initial approach segment would extend outward possibly 100 miles. Energy management could be accomplished either by turning or by L/D variation, or both, and would provide a smooth continuation of the reentry guidance task.

Figure 12 depicts how this guidance scheme would operate. On the basis of the position, total energy, and nominal (mid range) performance of the shuttle, the on-board computer would compute a guidance trajectory to the runway which consists of a straight-line initial and final approach with a constant banked turn from initial to final approach. From any particular position and energy condition, only two such trajectories exist. One trajectory would have a left-hand turn to final approach (trajectory 2), and the other would have a right-hand turn to final approach (trajectory 3). Energy level at a particular position defines the path length which must be flown. Thus, with a low initial energy level, the vehicle might follow trajectory 1. With somewhat higher energy, the pilot would elect to follow either trajectory 2 or 3, and with very high energy a trajectory similar to 4 might be followed.

The key in this system is the altitude at which the vehicle rolls out on final approach. Before the turn to final approach is started, the system automatically compensates for winds by continuously updating the computed trajectory. Once on final approach, the glide slope can be adjusted to correct for the "effective" head/tail winds. Because winds normally decrease as the surface is approached, required wind compensations are smaller and can be made more precisely as the altitude decreases for the rollout on final approach. Of course, the final approach must have some length to permit the vehicle to be stabilized on final approach at the flare airspeed before the flare. Thus, if the shuttle had the energy to fly trajectory 2 but point A was the desired rollout point, the pilot would fly the shuttle at a lower L/D , which would then drive the rollout altitude to point A, or he would select a right-hand pattern (3). He would then return to and maintain the nominal L/D for the rest of the trajectory.

Some advantages of this scheme are:

1. This approach is easily visualized by the pilot, which allows him to stay well oriented throughout the approach (virtually the same type of pattern as a VFR approach).
2. Transition from reentry guidance is easy.
3. Pitch and bank commands are uncoupled.
4. Energy management by either bank angle or L/D variation can be used.

5. Wind compensation is inherent down to the base leg turn.

A disadvantage to this system is that the final approach and possibly the base leg turn may require wind compensation.

CONCLUDING REMARKS

Unpowered, low lift-drag-ratio, IFR landing approaches are practical and realistic for space shuttle recovery operations. When an ILS technique was used, these approaches were easier to perform than normal, powered, ILS approaches. A comparison of unpowered, low lift-drag-ratio approaches made with ILS and ground controlled approach techniques established that the ILS approaches were easier to perform than the ground controlled approaches under the same conditions. Unpowered IFR approaches made in the NB-52B airplane, which is similar in size to the space shuttle, were no more difficult to fly than similar approaches in small aircraft, such as the F-111A and F-104.

Wind compensation may be required for terminal area guidance schemes of unpowered space shuttle vehicles. Additional analysis and testing are necessary to determine optimum techniques for wind compensation.

Preliminary investigation into guidance schemes for terminal area energy management and IFR landing approach shows that a number of schemes are possible.

REFERENCES

1. Schofield, B. Lyle; Richardson, David F. ; and Hoag, Peter C. : Terminal Area Energy Management, Approach and Landing Investigation for Maneuvering Re-entry Vehicles Using F-111A and NB-52B Aircraft. Tech. Doc. No. 70-2, Air Force Flight Test Center, U.S. Air Force, June 1970.
2. Gee, Shu W. ; Kock, Berwin M. ; and Schofield, B. Lyle: Operational Experiences With Unpowered Terminal Area Instrument Approaches. Proceedings of the ION National Space Meeting on Space Navigation - Theory and Practice in the Post Apollo Era, NASA Ames Research Center, Feb. 17-19, 1970, pp. 211-223.
3. Jailer, Robert W. : Potential Aircraft Icing Probabilities in the Northern Hemisphere. Tech. Rep. 56-659, (ASTIA No. 110676), Wright Air Dev. Center, U.S. Air Force, Nov. 1956.
4. Schofield, B. Lyle: Gliding Flight Equations. FTC-TIM-70-1007, Air Force Flight Test Center, U.S. Air Force, Apr. 1970.

SUBSONIC F-111A LOW L/D PERFORMANCE

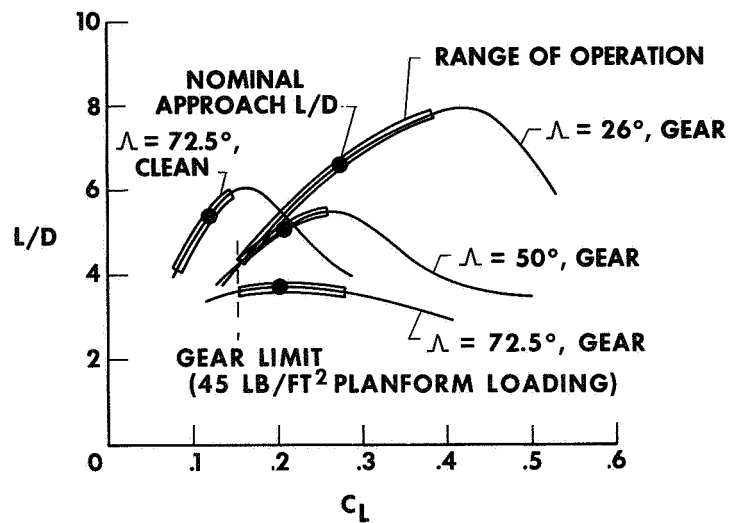


Figure 1

MODEL OF ILS APPROACH TECHNIQUE

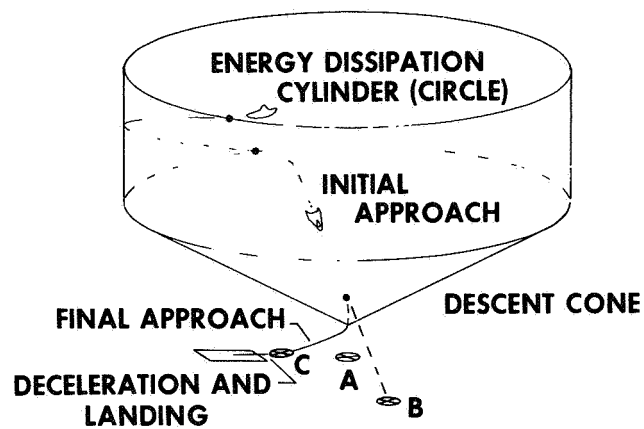


Figure 2

ILS APPROACH TECHNIQUE

PLAN VIEW

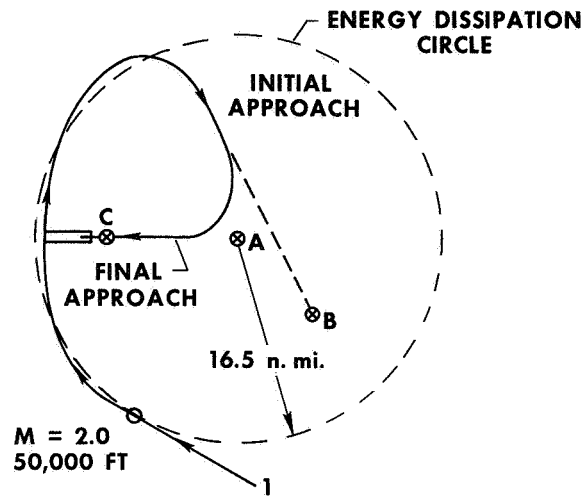


Figure 3

INITIAL AND FINAL APPROACH PHASES

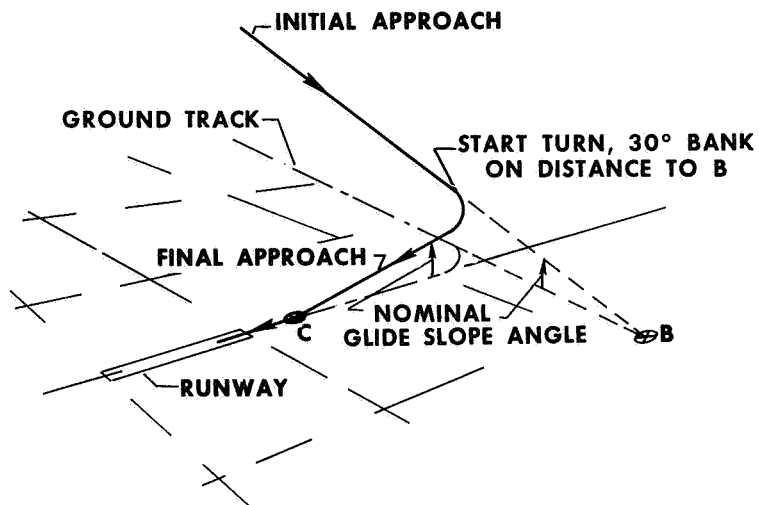


Figure 4

THREE TYPES OF HIGH-ENERGY APPROACHES

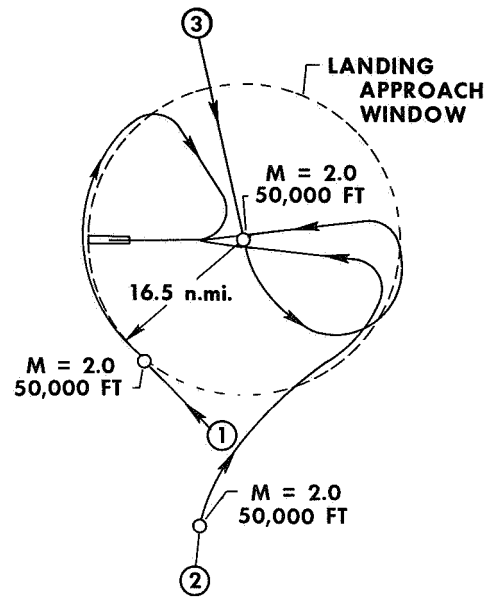


Figure 5

F-104 LOW L/D PERFORMANCE

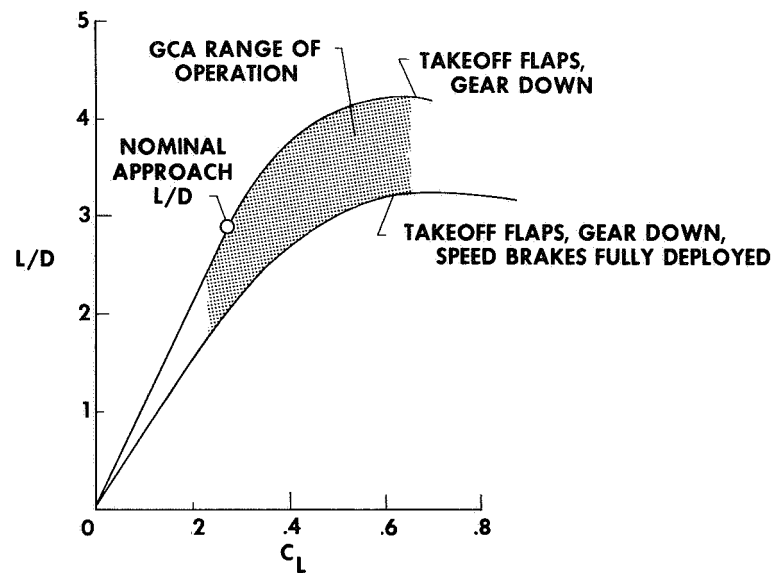


Figure 6

MODEL OF GROUND CONTROLLED APPROACH TECHNIQUE

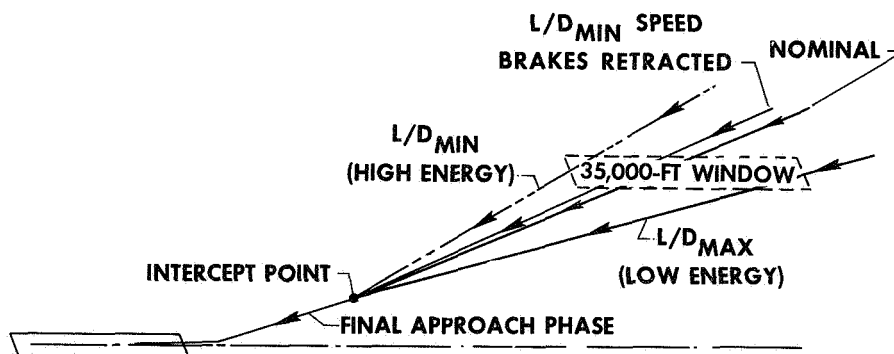


Figure 7

F-104 GCA PROFILES

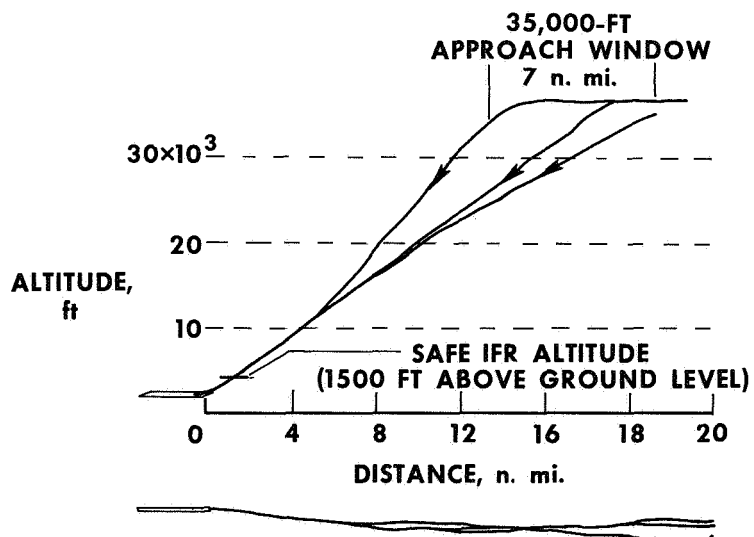


Figure 8

NB-52B GROUND CONTROLLED APPROACHES

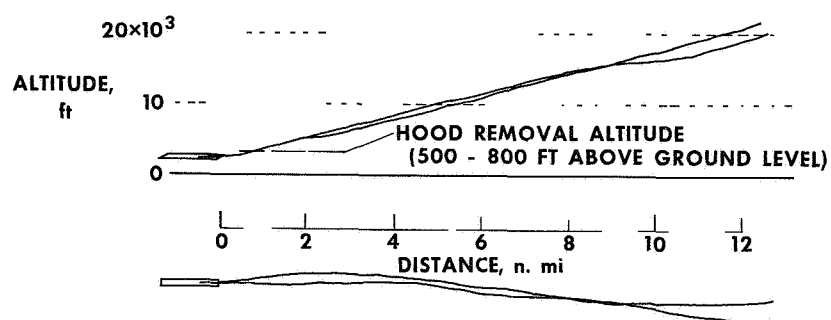


Figure 9

GLIDE SLOPE WIND COMPENSATION

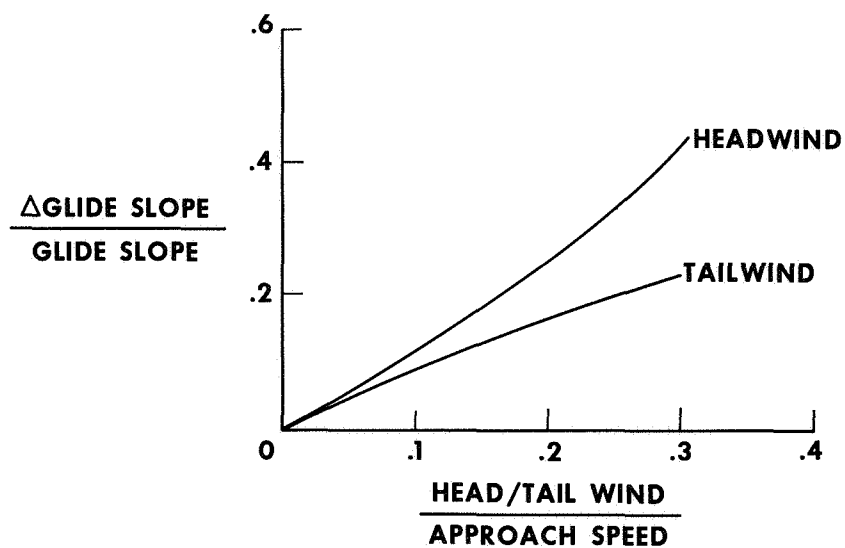


Figure 10

TERMINAL AREA GUIDANCE SCHEME 1

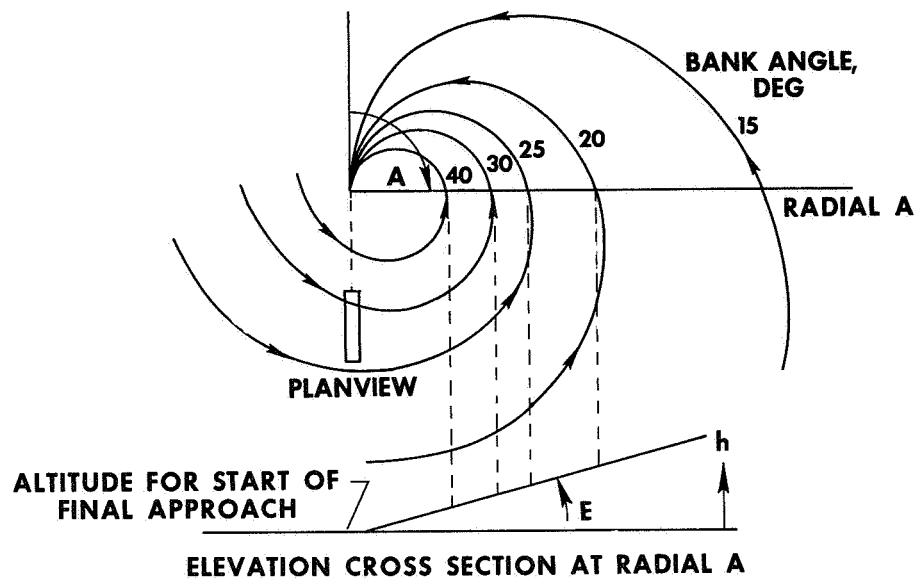


Figure 11

TERMINAL AREA GUIDANCE SCHEME 2

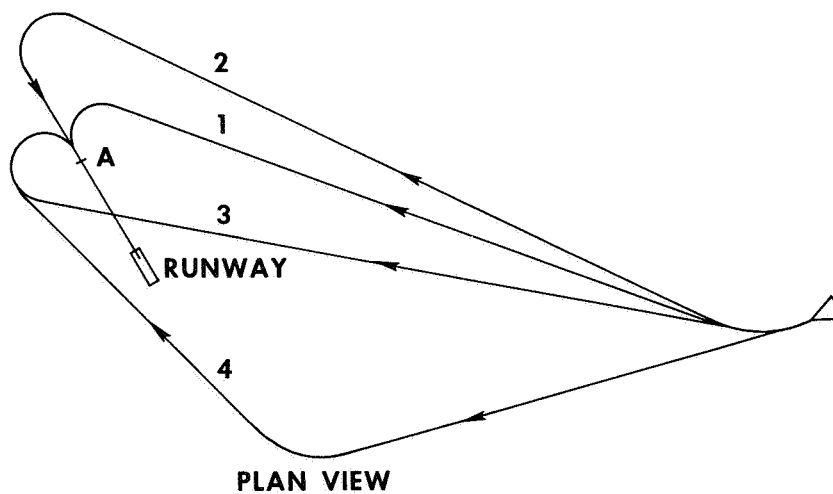


Figure 12

10. RATIONALE FOR PROPOSED FLYING-QUALITIES SPECIFICATIONS

By Euclid C. Holleman
NASA Flight Research Center

INTRODUCTION

Over the years flying-qualities specifications have been developed for airplanes in normal aerodynamic flight by summarizing flight and simulation experience and the results of analytical studies directed toward flying qualities. This experience provided guidance for future designs as long as the future design flight envelope or performance was not much greater than that of previous airplanes and the design was not too dissimilar. Each new vehicle with increased performance, however, has prompted a review of flying-qualities criteria. Typical mission trajectories for the booster and orbiter shuttle vehicles are shown in figure 1. A substantial increase in performance is indicated over the operational envelopes of transport airplanes with similar missions, or even the XB-70 Mach 3.0 bomber. In addition, the need to operate in a zero dynamic pressure environment results in requirements not necessary for normal airplanes; thus there are no specifications for that region.

The large increase in the envelope for the shuttle vehicle casts some doubt that normal airplane flying qualities will be applicable to a vehicle with much higher performance capability. At least, the applicability of the airplane flying-qualities specifications requires careful consideration.

The NASA Flight Research Center is reviewing the applicability of flying-qualities experience to the shuttle mission for the purpose of preparing a shuttle flying-qualities specification. This paper is a progress report on this review; the results presented are, of course, preliminary.

SYMBOLS

h	altitude, ft
Δh	change in altitude, ft
$L_{\delta_e} \delta_e$	lift acceleration produced by maximum elevon deflection from trim, g

$M_{\delta_e} \delta_e$	pitching angular acceleration produced by maximum elevon deflection from trim, deg/sec ²
n/α	normal acceleration change per unit angle of attack, g/rad
p_{ss}	steady-state roll rate, deg/sec
q	dynamic pressure, lb/ft ²
t	time, sec
V	velocity, ft/sec
γ_0	initial flight-path angle, deg
ζ	damping ratio
τ_R	roll-mode time constant, sec
ω_n	undamped natural frequency, rad/sec

APPLICABILITY OF FLIGHT EXPERIENCE AT LOW DYNAMIC PRESSURE

The shuttle is envisioned as a vehicle to carry cargo and passengers to and from orbit. For this study the missions (fig. 2) were considered to include four phases: low dynamic pressure, entry, glide, and approach to a landing. The zero dynamic pressure of space flight was not considered, because there has been extensive experience in space and other Centers are studying those control requirements. Flight experience (refs. 1 and 2) closest to the shuttle mission was obtained at the Flight Research Center with the X-15 airplane (fig. 3). The X-15 design altitude mission compared favorably in altitude with the shuttle booster mission, but the velocity was lower. However, all four phases of the shuttle mission were experienced during an X-15 flight to high altitude.

The X-15 airplane was the first airplane designed to be controlled in a very low, near zero, dynamic pressure flight environment (ref. 3). The reaction control maneuvering capability was approximately 11 deg/sec² in roll and 4 deg/sec² in pitch and yaw from two systems in each axis. This afforded much more control than was required for the X-15 altitude mission, but the pilots liked the rapid maneuver capability of the reaction controls. The pitch control was important for trimming to the desired entry attitude.

Three types of reaction controls (ref. 1) were evaluated during the X-15 program (fig. 4). Ten pilots evaluated all the controls to be satisfactory. The attitude command or hold controls were rated as most satisfactory. The angular rate command was rated next most satisfactory, and the angular acceleration command was rated to be just satisfactory. The pilots preferred to fly the pitch mode with the rate command controls and used the attitude command or hold in roll and yaw. A blending of reaction and aerodynamic controls on the same control stick was preferred. A deadband in reaction control was required to conserve reaction control fuel, but the X-15 design value of 15 percent of total control was considered to be excessive.

Because aerodynamic controls were effective at low dynamic pressure with the X-15 airplane, the controllability of a 500,000-pound HL-10 lifting body shuttle vehicle without augmentation was investigated at low dynamic pressure on a fixed-base piloted simulator. For a nominal angle of attack such as used for set up for entry, controllability (fig. 5), represented by pilot ratings, decayed with decreased dynamic pressure; however, the vehicle was controllable with unsatisfactory, but acceptable, pilot evaluations to dynamic pressures of 20 lb/ft² with aerodynamic controls only. Further decreases in dynamic pressure resulted in the control and response being significantly degraded by coupled responses that made control with only aerodynamic controls unacceptable. Reaction controls will certainly be required on the shuttle vehicles; however, it appears that the aerodynamic controls can be used effectively to as low a dynamic pressure as was possible with the X-15 airplane. Aerodynamic trim will again be effective in conserving reaction control fuel, as it was with the X-15 airplane. Closed-loop or rate command reaction controls will probably provide more precise control than basic acceleration command controls. Rate command controls were used more efficiently than acceleration command controls by the X-15 pilots.

AERODYNAMIC FLIGHT EXPERIENCE

The other three phases of the shuttle mission, entry, glide, and approach to land, will be considered briefly. These phases occur in aerodynamic flight, for which present flying-qualities specifications and flight experience should be most applicable.

Extrapolation of Flying-Qualities Data

Most flying-qualities specifications are based on experience with relatively small airplanes, and much of the Flight Research Center flight experience has been with small airplanes. Therefore, a brief simulation program was conducted to investigate the effect of vehicle size on flying qualities. The aerodynamic characteristics (discussed in paper 2) of the HL-10 lifting body vehicle, with which we have had the most flight experience, were used as a base, and the gross weight of 6400 pounds was scaled up to 500,000 pounds, a possible weight for a booster shuttle vehicle. Pilot evaluations were made of the basic HL-10 vehicle, a 250,000-pound and a 500,000-pound vehicle, and of each vehicle with simple damper augmentation in pitch, roll, and yaw. Aerodynamic flight at dynamic pressures of 300 lb/ft², 200 lb/ft², and 100 lb/ft², which might be representative of power-off approach, entry, and glide, respectively, and flight at a low dynamic pressure of 20 lb/ft², which might represent setup for entry, were evaluated by pilots for acceptability for the shuttle mission. Only aerodynamic controls were provided.

The pilot evaluation results are shown in figure 6 for the unaugmented HL-10 vehicle. The pilot ratings appear to be a function of mission phase as well as vehicle weight, with the large vehicles rated more satisfactory than the basic HL-10 vehicle. The HL-10 lifting body is known to be sensitive to controls at moderate-to-high dynamic pressures. The lower overall response of the heavier vehicle resulted in more acceptable control characteristics. Simple rate dampers (fig. 7) at relatively low gains improved all the vehicle flying qualities to satisfactory pilot ratings, or better than 3.5. There was very little effect of vehicle size on the pilot evaluations of the augmented vehicle.

These results were not unexpected, since examination of the shuttle transfer functions indicated that the response ratio was similar for large and small vehicles; however, the absolute response was, of course, reduced by the larger gross weight. Therefore, as might be expected, the mission must be considered in attempting to extrapolate small-vehicle flying qualities to much larger vehicles.

Maneuvering Requirements

The shuttle mission specifies that the vehicles be operated in a manner similar to that now used for transports. Large-airplane flying-qualities specifications were therefore a logical starting point in considering flying-qualities specifications. Fortunately, the most complete flying-qualities specification available for piloted airplanes was recently revised and updated by the Cornell Aeronautical Laboratory for the U. S. Air Force in a very comprehensive review and study. The Military Specification (ref. 4) includes flying qualities for all piloted airplanes intended for conventional aerodynamic flight. Flying qualities for large transports and bombers are designated as Class III--large, heavy, low-to-medium maneuverability airplanes--which closely describes the shuttle vehicle and mission.

A consideration of the maneuvering required during entry, glide, and approach to a landing indicated that, like the airplane flight phases, maneuvering requirements will vary somewhat with each shuttle mission phase. The maneuvering requirements for airplanes in various mission phases were reviewed, and the maneuvering requirements envisioned for the shuttle mission were defined. As shown in table 1, the Military Specification for nonterminal flight phases, Category A, requires rapid maneuvering, precision tracking, or precise flight-path control. Examples of this type of

TABLE 1. - AIRPLANE MANEUVERING REQUIREMENTS
[Mil Spec 8785B]

Flight phase	Category
Nonterminal	A - requires rapid maneuvering, precision tracking, or precise flight-path control Air-to-air combat, ground attack, weapon delivery/launch
	B - normally accomplished using gradual maneuvers and without precision tracking, although accurate flight-path control may be required Climb, cruise, loiter
Terminal	C - normally accomplished using gradual maneuvers and usually require accurate flight-path control Takeoff, catapult takeoff, approach, wave-off/go-around, landing

maneuvering are air-to-air combat and ground attack. In reviewing the shuttle maneuvering requirement, it appeared that there was perhaps less requirement for precise control during some phases of the shuttle mission; therefore, the Category A maneuvering requirements were defined as shown in table 2. It appeared that rapid

TABLE 2. - SHUTTLE MANEUVERING REQUIREMENTS

Flight phase	Category
Nonterminal	A - flight phases somewhat unique to a lifting entry spacecraft that do not require rapid maneuvering but do require precise flight-path control and good stability and damping characteristics
	Set up for entry, entry, glide and maneuvering following entry
	B - flight phases that do not require rapid maneuvering or precise flight-path control
Terminal	Ferry mission - climbout, cruise, letdown
	C - flight phases that require more maneuvering, precise flight-path control, and good stability and damping characteristics
	Terminal area maneuvering, approach, flare and landing, go-around

maneuvering was not always necessary, but precise flight-path control and good stability and damping were required in the entry and glide mission phases. The Military Specification for Category A should apply but perhaps can be relaxed slightly for the shuttle. As described in the Military Specification, Category B requires only gradual maneuvering. The shuttle ferry mission phase also has only gradual maneuvering requirements; therefore, it was designated Category B. The Military Specification terminal flight phase maneuvering requirements are given in Category C, which requires only gradual maneuvering but, usually, accurate flight-path control. Normal landing with a shuttle vehicle could be accomplished with a vehicle that satisfied the Military Specification Category C requirements; however, it was felt that more rapid and precise control would be required if the shuttle were landed without power. Therefore, the shuttle Category C requirement was tightened somewhat. A power-off approach will require precise flight-path control and more maneuvering than shuttle Categories A and B and good stability, control, and damping.

Shuttle Levels of Flying Qualities

Flying qualities may be defined as those qualities that govern the ease and precision with which the pilot-vehicle system performs the requirements of the mission. The Military Specification (ref. 4) levels of flying qualities are defined in table 3. In the Military Specification supporting study (ref. 5), these levels were related to the well-known Cooper-Harper pilot rating scale, as shown in the table.

The shuttle mission covers all normal flight regions and space flight, and thus should not be attempted unless adequate flying qualities can be provided. Because degradation in mission effectiveness could be more serious during a shuttle mission than during a normal airplane mission, it was reasoned that only two levels of flying qualities should be permitted for the shuttle mission. Therefore, we recommend that only some increase in pilot workload or some degradation in mission be allowed for shuttle flying qualities.

TABLE 3. - MILITARY SPECIFICATION DEFINITION OF
LEVELS OF FLYING QUALITIES

Level	Definition	Pilot rating
1	Clearly adequate for the mission flight phase	Satisfactory 1 - 3.5
2	Adequate to accomplish the mission flight phase, but some increase in pilot workload or degradation in mission effectiveness, or both	Unsatisfactory 3.5 - 6.5
3	The airplane can be controlled safely, but pilot workload is excessive or mission effectiveness is inadequate, or both	Unacceptable 6.5 - 9+

Applicability of Military Specifications

Although all facets of the pilot and vehicle dynamics influence the overall flying qualities, there are "key" parameters that exert strong influences on flying qualities. The Military Specification designates flying qualities in terms of these key parameters. The effects of a few of these parameters on the ability of a pilot to accomplish the shuttle mission will be discussed.

Longitudinal stability with respect to speed. - The Military Specification considers longitudinal stability with respect to velocity in five paragraphs. Each of these requirements was discussed with Flight Research Center pilots who had flight experience with operational and research vehicles such as the F-111, X-15, and HL-10 and with various controls, from conventional direct control of the aerodynamic control surfaces to adaptive gain changing rate, attitude, and normal acceleration command systems.

Longitudinal static stability: In response to the question, "Does the shuttle have to be longitudinally stable throughout the flight envelope to accomplish its mission?" the pilots with the most experience in airplanes with command systems said "No." They stated that a rate command system provided very positive, satisfactory control. Other pilots agreed that stability provided by a system was acceptable. One pilot thought the Military Specification was good as is but believed that less stability could be required for the shuttle mission.

The pilot who had experience with rate command systems at altitude flew attitude closely and did not notice lack of speed stability. In the approach condition in which some pilots found the rate command system to be objectionable, he flew airspeed very closely and had no trouble during the approach. One pilot commented that a pilot could be given an airplane with a rate command system and with no briefing would be able to complete an introductory flight without noticing the different response. He believed that the pilot would do what was required to obtain the desired attitude and airspeed.

One problem has been noted by most pilots who have landed an airplane with a rate command system. As the airplane enters ground effects, the rate command system holds attitude and the airplane balloons as a result of the ground effects. The statically stable airplane tends to push over with decreasing speed to hold airspeed. High gain systems, like very stable configurations, may produce high air loads in

turbulence. Command systems are usually designed to give superior response to stick displacement. The response damping is usually augmented to be superior to that of the basic airplane response. Divergences in speed can occur with a rate command system; however, Flight Research Center pilots used the commanded rate as a means of obtaining the attitude and airspeed desired. Close control of attitude and airspeed is the basic desire regardless of the control system. Such a system should prove satisfactory for the shuttle application.

Relaxation in transonic flight: The control requirements in any flight region depend on the mission. If it is required that precise control be maintained in the transonic region, then reasonably stable characteristics with gradual changes in parameters will be necessary. However, if it is just a matter of traversing the transonic region with no precise control task, larger stability changes can be tolerated.

The rate command systems with which we have had experience provided good control and an apparently stable vehicle operation throughout the transonic speed range. It is very desirable to have no control reversals in the transonic speed range; gradual force changes can be tolerated. The pilots believed that some stability requirement is needed in the transonic speed region; however, the requirement must be designed for the mission and/or piloting requirements in the region. A command system may control transonic trim changes or instability.

Longitudinal control force variations during rapid speed changes: The HL-10 deceleration through the transonic speed range has an "attention getter" pitchup. By now, the pilots are aware of it, and by fortunate design the trim rate is correct for trimming out the force change, so there has been little problem. Another airplane equipped with rate command controls also exhibits a nearly uncontrollable pitchup with control systems off, but, with the command system on, the pitching moment is trimmed by the system to provide a smooth deceleration in the region.

There is a need for the specification requiring available control beyond that needed for trim because the possibility of trimming to the limit of control deflection while traversing the flight envelope cannot be tolerated. There are at least two solutions to the problem: a command system with authority to control the rapidly changing moment, or a trim system with a rate capability to allow the pilot to control the moment satisfactorily and maintain the desired load factor.

Phugoid stability: The pilots believe that they should be able to control the phugoid response, but that the mode should be positively damped. If it has zero damping or is divergent, the pilot's workload can be increased. A divergent phugoid during approach can make the airplane appear to be constantly out of trim. If the pilot controls airspeed closely, the phugoid will not develop. However, the pilots believe that the phugoid should be damped to lessen the problem of holding airspeed and of trimming at a given airspeed.

Flight-path stability: In the Military Specification, flight-path stability is defined in terms of flight-path angle change where the airspeed is changed by the use of elevator only (constant thrust). At the Flight Research Center, power-off approaches have been made on the front side of the lift-drag-ratio curve to give the pilot the natural piloting task of pushing over to decrease the flight-path angle and pulling up to increase the flight-path angle. The pilots generally favor this type of approach, although it results in an approach at higher speed and generally a longer rollout on

landing. Pilots with experience in small airplanes and lifting bodies believe that operation on the back side of the lift-drag-ratio curve should be avoided. If powered approaches are to be made, the level of flight-path instability must be limited by specification to levels that can be controlled safely by the pilot. Because the Flight Research Center has had little experience applicable to the specification, as described in paragraph 3.2.1.3 (ref. 4), levels 1 and 2 of the Military Specification were accepted.

Shuttle stability and control. — Entry and approach to land, power off, were selected as the most demanding shuttle stability and control requirements. Scaled-up HL-10 shuttle characteristics were programed on a simulator, and lifting body pilots evaluated the suitability of the shuttle response for the shuttle mission phases specified.

Pilot ratings (PR) of the longitudinal responses were obtained (fig. 8) while vehicle design parameters such as lift-curve slope, static stability, and control power were varied over wide ranges and damping was held essentially constant. The results are presented in terms of the longitudinal correlating parameters ω_n and n/α , which are used also in the Military Specification. The use of these parameters resulted in acceptable correlation for many types of airplanes. The lower response ratios, n/α of 2 to 3, provided only marginally acceptable normal acceleration capability for entry and flare to land. An appreciable range of n/α provided satisfactory normal acceleration capability, but higher ratios of n/α resulted in somewhat sensitive controls. The low frequency, or static stability, with its long-period motion increased the pilot's workload and resulted in sluggish, less precise control. High static stability required too much control for maneuvering.

These results are compared with the Military Specification for Category C, Class III airplanes (fig. 9). The simulation results indicate a narrowed region of satisfactory maneuvering response for the shuttle missions, but the desired frequency was in agreement with the Military Specification. The unsatisfactory (PR = 6.5) region for the shuttle appeared to be expanded over the Military Specification requirements. Although it was hypothesized that the shuttle specification Category C would require more maneuver capability than specified by the Military Specification Category C, these results indicate that the Military Specification Category C may be adequate for the shuttle.

The shuttle simulation results were compared with the M2-F2 and HL-10 lifting body flight results (fig. 10). The lifting body longitudinal flying qualities were rated to be 3.5 or better for the flight research missions and in general substantiate the HL-10 shuttle simulation results and Military Specification for satisfactory stability and maneuvering. It appears that this Military Specification would be an aid in the design of the shuttle vehicles.

Longitudinal damping. — Damping is also fundamental to longitudinal controllability. Again, the entry and approach-to-land mission phases were evaluated on the simulator, and pilot rating results were obtained (fig. 11). From these data, 3.5 and 6.5 pilot rating boundaries were derived for comparison with other results and the Military Specification for longitudinal damping (fig. 12). During X-15 flights to high altitudes where aerodynamic damping was extremely low, the pilots accepted very low damping. Damping ratios of 0.01 to 0.05 were rated to be acceptable for the X-15 airplane

during the set-up phase of the entry mission at low dynamic pressure.

XB-70 cruising flight experience at Mach 2 to 3 at high altitude (ref. 6) indicated that a longitudinal damping ratio of 0.15 was satisfactory for cruising flight. These data, including the HL-10 shuttle results, are more permissive and allow less damping than the minimum required by the Military Specification for large airplanes.

Figure 13 compares the HL-10 shuttle longitudinal dynamics with the dampers-off flight experience in the HL-10 and M2-F2 lifting bodies. Lifting body longitudinal dynamics were evaluated by the pilots to be satisfactory ($PR < 3.5$). The results are in general agreement with the shuttle results. From these comparisons, it appears that the Military Specification for longitudinal damping may be conservative for the shuttle; however, additional study, perhaps with simulation motion cues, will be required before the requirements can be finalized.

A study is in progress with the Center's variable stability JetStar airplane to investigate longitudinal stability and damping requirements for transport airplanes. Preliminary results are in agreement with the shuttle simulation results presented. Controllability of unstable configurations is also being studied, and tests will be extended to the approach and landing phases.

Longitudinal control for landing. — Although most large transports and other large airplanes approach to land with partial power from shallow glide slopes of 3° or less, it has been proposed that the shuttle vehicles approach and land power-off as have high-performance research airplanes. One of the concerns of longitudinal control of delta wing, low-lift-curve-slope configurations is that the lift loss due to initial control input causes a response in the direction opposite to that desired (ref. 7). A so-called "standard" lifting body low-lift-drag-ratio approach at 300 knots and a flight-path angle of -15° was used to study the flare requirements for the HL-10 shuttle vehicle on the fixed-base simulator (fig. 14). The acceptable control boundary is shown in terms of lift loss due to pitch control and pitch control effectiveness. The pitch control used to flare may result in an initial loss in altitude, shown in the lower insert. At best, there may be an apparent lag in altitude change to the pilot. Since the power-off flare maneuver must be closely timed, a lag in response or a decrease in normal acceleration capability due to lift loss could result in inability to complete the flare. A specification of the type shown here is being considered; however, more study will be required to finalize it. Note that the XB-70 airplane was acceptable in the region shown for a constant-velocity, constant-flight-path approach of -1° to -2° . The HL-10 vehicle being flight tested has very effective pitch controls. Like the XB-70 airplane, the very effective rotational control of the HL-10 vehicle compensates for the loss in lift of the control surface by quick rotation in angle of attack.

Roll requirements. — Desirable roll flying qualities for airplanes are well defined. A rather comprehensive study (ref. 8) of transport airplane roll requirements was completed recently (fig. 15) using the Flight Research Center's variable-stability JetStar airplane (GPAS). Regions of satisfactory and acceptable steady-state roll rate and roll time constants were determined from pilot rating data for transport airplanes in cruise. Experience with large airplanes (XB-70 (ref. 6) and CV-990), the HL-10 lifting body, and the HL-10 shuttle simulation generally confirm the satisfactory region for roll response characteristics. These results are also in agreement with the Military Specification and other criteria. It appears that the specification for satisfactory airplane roll characteristics would be applicable for shuttle flying qualities;

however, it may be desirable to investigate the use of lower roll rates for some parts of the shuttle mission.

Desirable Response

Classically, desirable airplane response has been specified according to the basic response of airplanes with which we have had the most experience. Therefore, the longitudinal response has been considered to be a second-order response, and frequency and damping have become key parameters.

With higher performance vehicles, which should include the shuttle, control and augmentation systems have become vital elements in the design of the vehicles. The basic response of the vehicle is shaped less by the vehicle aerodynamics and dominated more by the control system design. For example, the X-15-3 airplane was flown through the MH-96 adaptive control system. The system was a high-gain adaptive system which attempted to provide invariant response to the pilot by suppressing the basic airplane aerodynamic response and providing a model response which was invariant with flight condition. The response of the airplane was commanded rate of change of vehicle attitude. The rate command controls were enthusiastically endorsed by the X-15 pilots. Initially, the airplane response model in pitch was a highly damped second-order model typical of contemporary airplanes, however, the model was changed to a first-order model with a one-half second time constant without drawing adverse comment from the research pilots. The model in roll was, of course, first order with a short time constant of one-third second. From this experience it appears that a design response to a step input in pitch or roll (fig. 16) would provide an acceptable design goal for both the aerodynamicists and the control system designers.

Conspicuous by its absence has been the effect that turbulence may have on lifting body handling qualities. These vehicles have very low damping in roll and usually high dihedral effect. Both parameters result in undesirable response to turbulence. This has severely limited flight operations even for a research program. One of the more difficult Military Specifications to fault indicates that the airplane will have acceptable response and controllability in atmospheric disturbances. Research work is needed and is being conducted to define acceptable response in turbulence for airplanes and lifting body vehicles.

CONCLUDING REMARKS

A brief review of Flight Research Center flight experience related to flying qualities indicated that much of the experience is applicable to the shuttle if the mission phase and control requirements are considered. The recently revised Military Specification provides an invaluable base for defining shuttle flying-qualities specifications. It is obvious that the definition of flying qualities for any class of flight vehicle is a large task, and the shuttle is certainly no exception. Particular specifications serve as good guides for flying-qualities design studies, but pilot evaluations of complete simulations of the vehicle are necessary throughout the program.

REFERENCES

1. Holleman, Euclid C.: Summary of High-Altitude and Entry Flight Control Experience With the X-15 Airplane. NASA TN D-3386, 1966.
2. Holleman, Euclid C.; and Adkins, Elmor J.: Contributions of the X-15 Program to Lifting Entry Technology. J. Aircraft, vol. 1, no. 6, Nov.-Dec. 1964, pp. 360-366.
3. Jarvis, Calvin R.; and Lock, Wilton P.: Operational Experience With the X-15 Reaction Control and Reaction Augmentation Systems. NASA TN D-2864, 1965.
4. Anon.: Flying Qualities of Piloted Airplanes. Military Specification MIL-F-8785B (ASG), Aug. 7, 1969.
5. Chalk, C. R.; Neal, T. P.; Harris, T. M.; Pritchard, F. E.; and Woodcock, R. J.: Background Information and User Guide for MIL-F-8785B(ASG), "Military Specification - Flying Qualities of Piloted Airplanes." Tech. Rep. AFFDL-TR-69-72, Air Force Flight Dynamics Lab., Wright-Patterson Air Force Base, Aug. 1969.
6. Powers, Bruce G.: A Review of Transport Handling-Qualities Criteria in Terms of Preliminary XB-70 Flight Experience. NASA TM X-1584, 1968.
7. Berry, Donald T.; and Powers, Bruce G.: Flying Qualities of a Large Supersonic Aircraft in Cruise and Landing Approach. Paper 70-566, AIAA, 1970.
8. Holleman, Euclid C.: Flight Investigation of the Roll Requirements for Transport Airplanes in Cruising Flight. NASA TN D-5957, 1970.

SHUTTLE MISSION TRAJECTORIES AND PRESENT FLIGHT EXPERIENCE

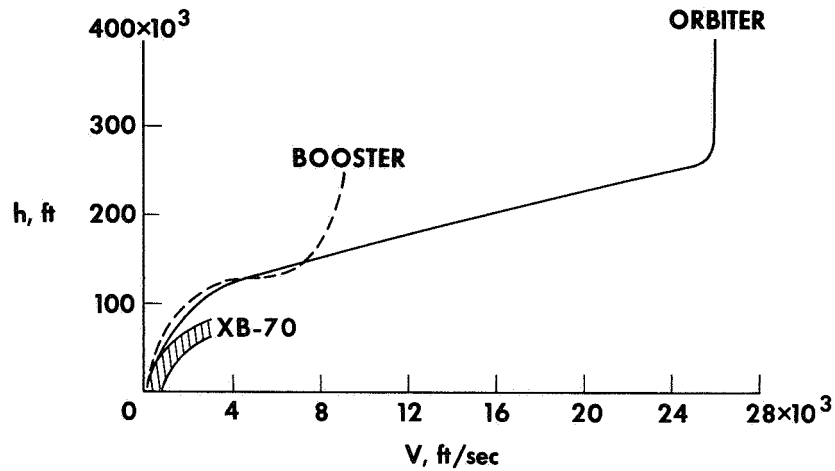


Figure 1

SHUTTLE MISSION PHASES

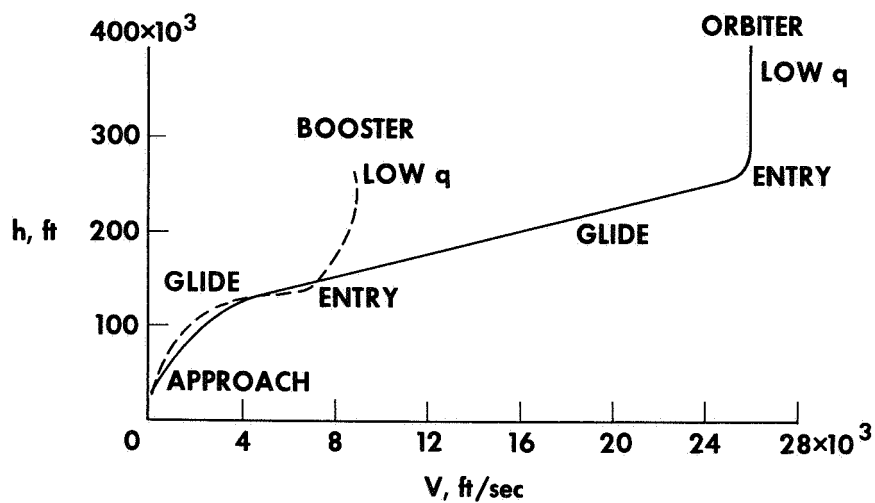


Figure 2

TIME HISTORIES OF X-15 AND BOOSTER MISSIONS

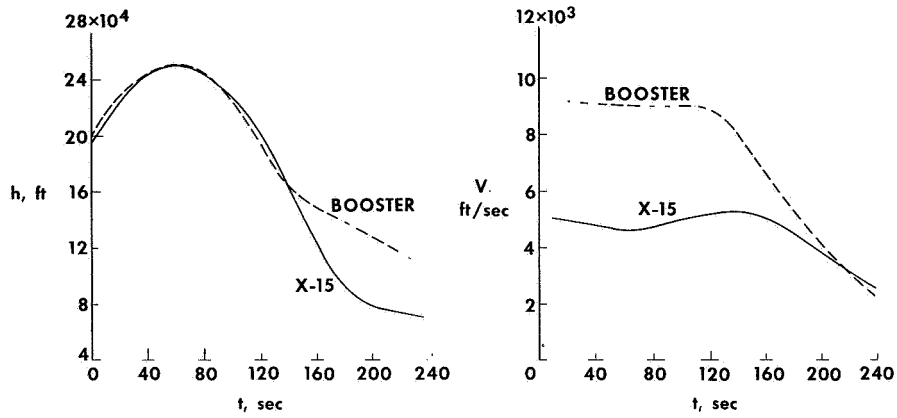


Figure 3

AVERAGE PILOT RATING OF X-15 REACTION CONTROLS

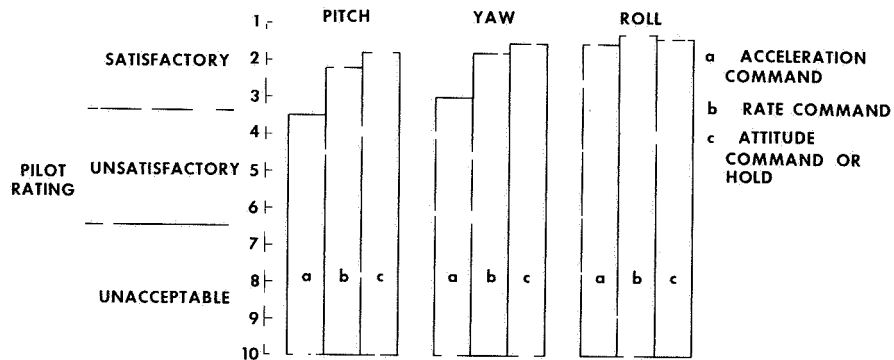


Figure 4

CONTROLLABILITY OF HL-10 BOOSTER VEHICLE AT LOW q AERODYNAMIC CONTROLS

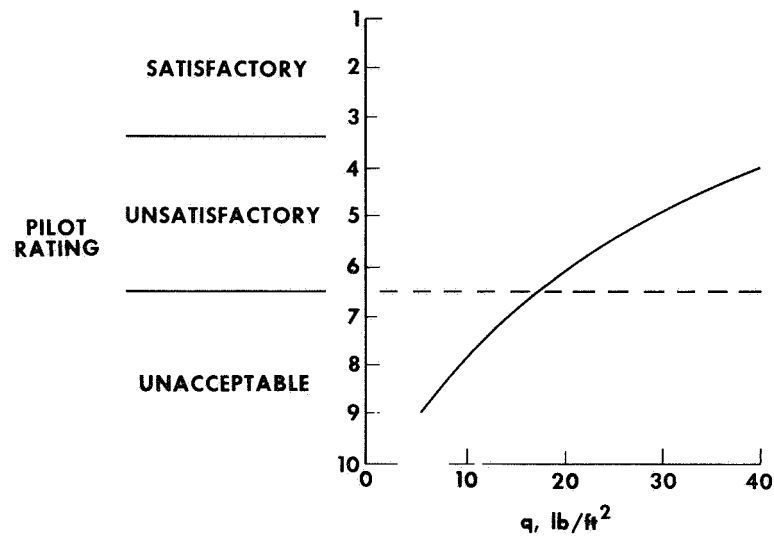


Figure 5

EFFECT OF WEIGHT OR VEHICLE SIZE ON FLYING QUALITIES HL-10; DAMPERS OFF

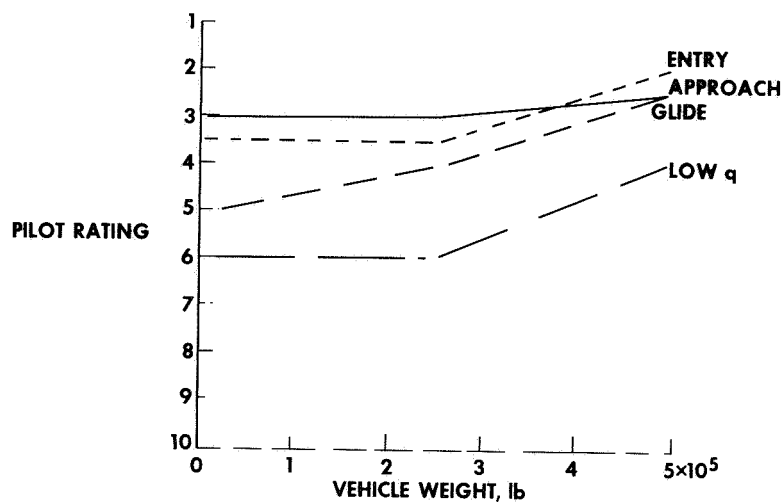


Figure 6

EFFECT OF WEIGHT OR VEHICLE SIZE ON FLYING QUALITIES

HL-10; DAMPERS ON

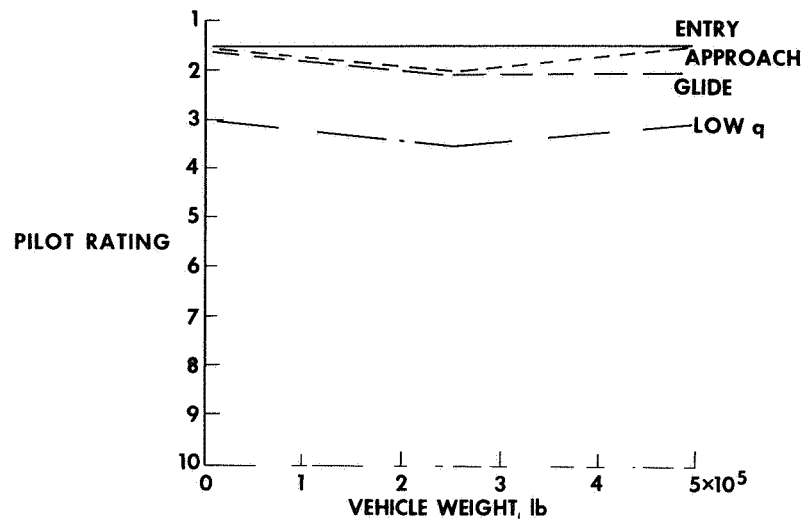


Figure 7

RESULTS OF HL-10 SHUTTLE SIMULATION

LONGITUDINAL MANEUVERING

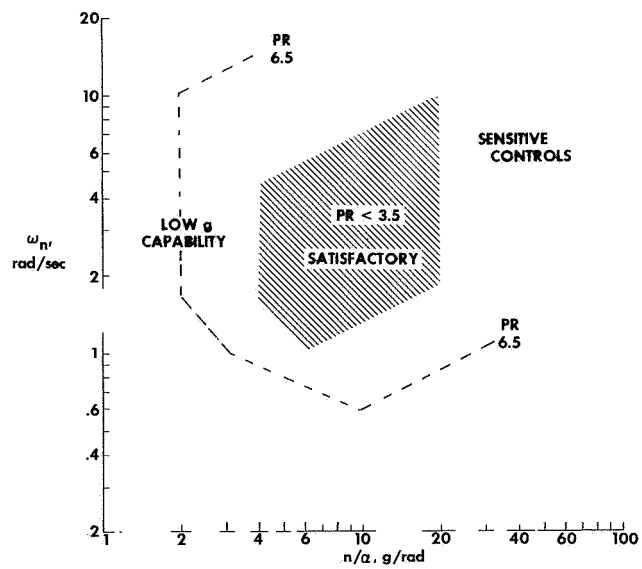


Figure 8

COMPARISON OF LONGITUDINAL MIL SPEC AND RESULTS OF HL-10 SHUTTLE LONGITUDINAL MANEUVERING

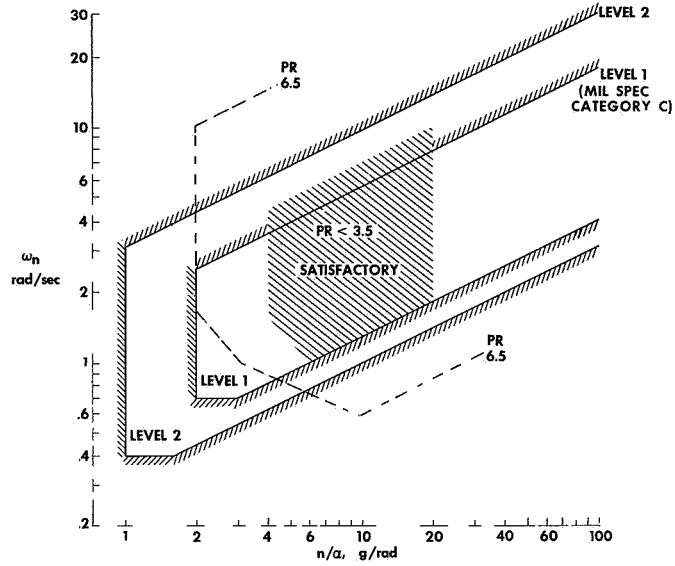


Figure 9

COMPARISON OF LIFTING BODY FLIGHT EXPERIENCE AND HL-10 SHUTTLE LONGITUDINAL MANEUVERING

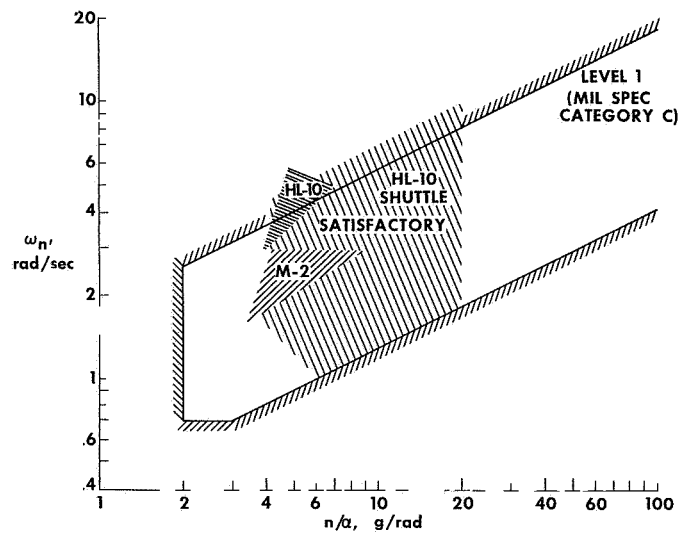


Figure 10

PILOT RATING OF HL-10 SHUTTLE LONGITUDINAL DYNAMICS ENTRY AND APPROACH MISSION PHASES

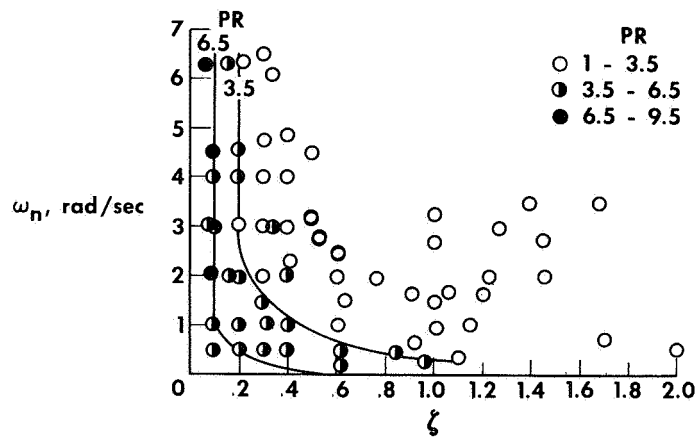


Figure 11

LONGITUDINAL DAMPING REQUIREMENTS

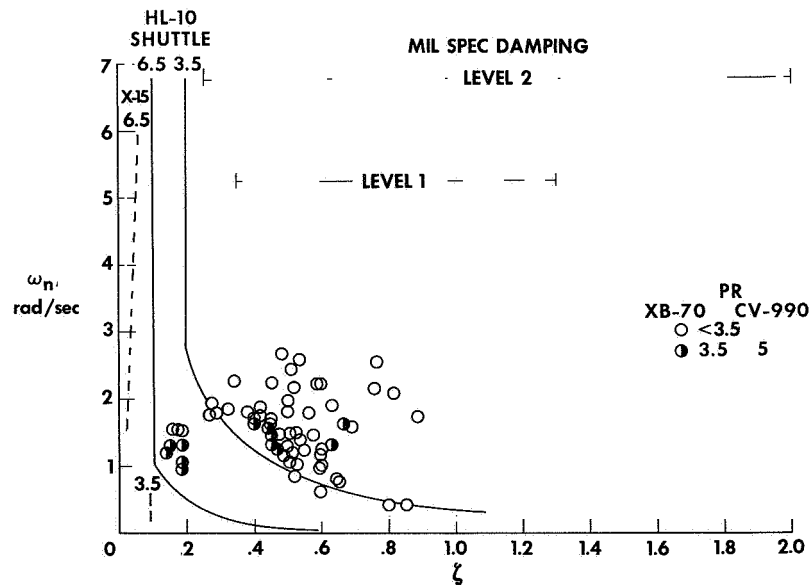


Figure 12

COMPARISON OF HL-10 SHUTTLE LONGITUDINAL DYNAMICS WITH DAMPERS-OFF LIFTING BODY FLIGHT EXPERIENCE

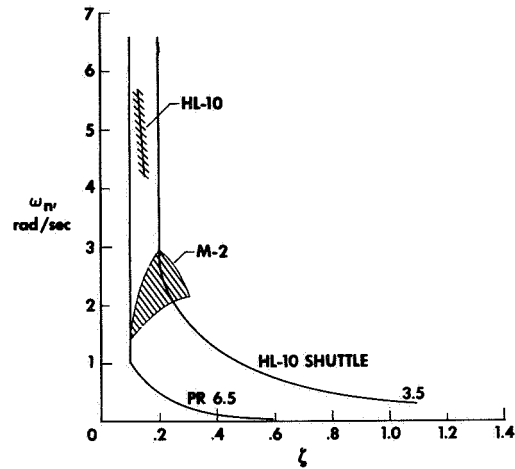


Figure 13

EFFECT OF LIFT LOSS ON LANDING CONTROL

$$\gamma_0 = -15^\circ$$

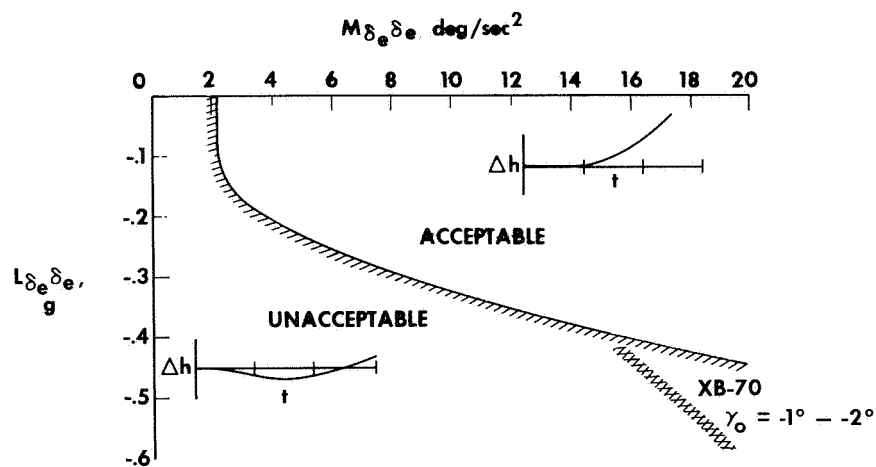


Figure 14

ROLL CHARACTERISTICS

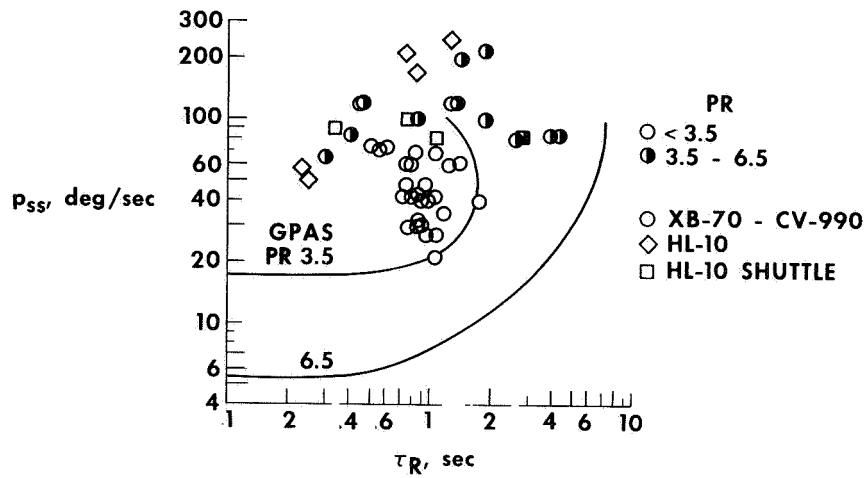


Figure 15

DESIRED LONGITUDINAL OR LATERAL RESPONSE

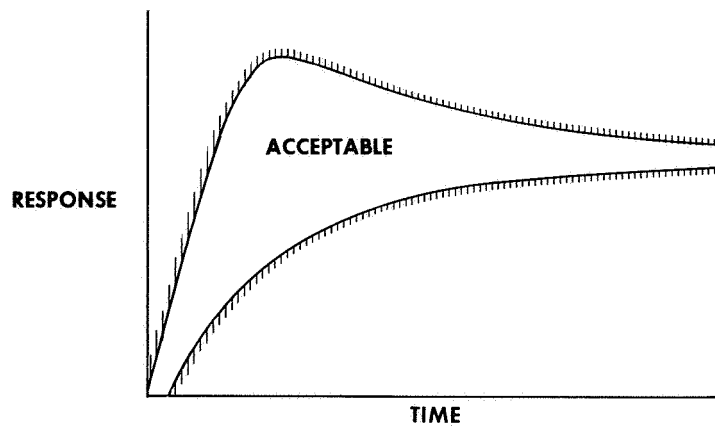


Figure 16

11. FINAL REMARKS AND FUTURE PLANS

By Milton O. Thompson
NASA Flight Research Center

INTRODUCTION

At a symposium such as this, it is not customary for the hosting organization to interpret the results or attempt to bias the audience opinion of information presented. However, the NASA Flight Research Center is far from NASA Headquarters and the influence of Eastern protocol, so I will tell you what you should have concluded as a result of these presentations.

DISCUSSION

From the papers presented in the first session, it should be obvious that the seemingly unconventional high-cross-range configurations proposed for the space shuttle are practical. Our lifting body experience demonstrates that vehicles designed to maneuver hypersonically, in order to achieve substantial aerodynamic cross range, can still have acceptable low-speed stability and control characteristics and adequate performance for unpowered horizontal landings. Satisfactory unaugmented handling qualities can also be designed into such vehicles, as illustrated by the SAS-off pilot ratings for the HL-10 lifting body. Where marginally acceptable unaugmented handling qualities have been observed (as in the lateral-directional axis of the M-2 and X-24A vehicles), simple rate dampers have proved to be effective in improving the vehicles' flight characteristics. Some of the more sophisticated state-of-the-art control systems can insure not only satisfactory, but excellent, handling qualities over the entire flight envelope. As stated in paper 7, these control systems should not be provided in lieu of, but, rather, in addition to, good basic vehicle characteristics. This type of control system should be used as a safety factor added to compensate for anticipated, but unpredictable, variations in stability and control characteristics such as might result from the limbering effects of aerodynamic heating on the shuttle structure.

The comparisons shown between wind-tunnel and flight data in the areas of stability, control, performance, and aerodynamic loads should provide confidence in the ability to predict the characteristics of the full-scale vehicle using existing facilities and current techniques. However, our flight experience indicates that more detailed wind-tunnel testing and analysis of the wind-tunnel results is essential to detect, before flight, such major problems as flow separation. Using the wind-tunnel data, extensive analytical and simulation evaluations of the vehicles' flight characteristics are still necessary to preclude potential handling-qualities problems. Some of the problems we have encountered in flight illustrate that the flight characteristics of these vehicles can be sensitive to small variations in certain aerodynamic derivatives Simulation

evaluations should, therefore, include detailed studies of the effects of variations of individual derivatives above and below the predicted values. If I have convinced you that you can forego flight testing by careful wind-tunnel testing, analysis, and simulation, I have led you astray. Flight testing is still essential. For the lifting bodies, we did all the things we have advised you to do. We had time in which to do this preliminary work, because we had no schedule to meet. Yet, as you have heard, we were caught short. We now feel we have three good flying vehicles, but we and those who performed the wind-tunnel tests had to spend much effort to achieve these results.

We believe so strongly in the need for early flight testing, or what might be called configuration verification, that we have recommended the early construction and flight testing of manned sub-scale versions of the selected orbiter and booster configurations to the OART Space Shuttle Technology Working Group. These vehicles would be designed to perform comparably with our existing lifting bodies and to have supersonic flight capability. These vehicles will certainly not provide the answer to all possible questions. Ideally, you would like to have a reentry research vehicle, but such a vehicle may not be practical. The low-speed vehicle would at least provide some confidence in the configuration if it could be successfully flown through the transonic speed region and landed. The low-supersonic and transonic flight characteristics of these vehicles are generally the most critical and the least well predicted. It is in both these and subsonic speed regions that maximum maneuvering occurs; thus, this is where the aerodynamic control system is mainly defined. We feel that a low-speed vehicle would be very worthwhile. However, this vehicle is to be built sometime in the future because a final configuration selection is at least a year away. It is also after the fact. Of course, it would be much more desirable to be able to evaluate a number of the more promising candidate configurations in flight before the final configuration decision is made. Certainly this is only practical if these flight-test articles can be constructed quickly and cheaply and tested within a reasonable time

One possible approach to configuration testing and selection would be to construct scaled models to be remotely controlled during free flight. In the past we have constructed and flown remotely a number of small models, and we recently flew an unmanned, 32-foot-long model of the Hyper III. The remote control technique used to fly the Hyper III worked extremely well in allowing the ground pilot to fly the vehicle in the same manner that he would have if he had been in the cockpit. We feel that this technique of using a ground cockpit has considerable future potential, not only for possible shuttle-model testing, but also for aeronautics programs such as model propulsion systems testing and structural testing. We are preparing a proposal to NASA Headquarters for the construction and testing of a one-fourth-scale vehicle of the NASA Manned Spacecraft Center configuration (fig. 1). This vehicle would be initially unpowered and launched from our B-52 airplane. The high-angle-of-attack flight phase and transition maneuver could be evaluated on such flights. With the addition of a propulsion system, the vehicle could be flown to much higher altitudes and to supersonic speeds if desired to duplicate the final descent phase of the operational vehicle. Our future plans would include testing this vehicle as well as the manned sub-scale vehicle discussed previously, if these vehicles are approved.

You have heard much today about unpowered landings from some enthusiastic pilots. I am not sure what you have concluded. After listening to the rehearsals, Mr E. O. Pearson, of NASA Headquarters, said that he understood clearly that we were advocating an unpowered shuttle. If that is your conclusion, too, we may have overdone

it. We are not proposing that you eliminate landing engines or a go-around capability. If you, as designers, program managers, and users, decide that you can afford landing engines or need them for any other purpose, you should certainly include them. Even our experienced pilots would not reject the engines if they were flying the shuttle; however, they would refuse to rely upon them to make a successful approach and landing. The shuttle, whether it has landing engines or not, must be maneuvered, unpowered, to a point near the destination because the engines cannot be started until the vehicle is subsonic and only limited fuel will be available. To us it seems ridiculous to maneuver to a position where power must be relied upon to reach the runway. Instead, we would maneuver to a high key position to begin an unpowered approach. Then, regardless of whether the engines could be deployed, started, and kept operating, a successful approach and landing could be made.

If you decide to include the landing engines and the go-around capability specified in the space shuttle Phase B Statement of Work, we would strongly recommend that you not plan to use that capability, even with ideal recovery conditions. Routine Category II operations are impossible considering the fuel reserves contemplated. On the other hand, if you decide you cannot afford the associated penalties, we feel that it is entirely practical to consider an unpowered operational shuttle.

The flying-qualities document discussed in paper 10 is not an official NASA specification. We took it upon ourselves to prepare this document, which is a rough, first-cut draft based primarily on our flight experience. It requires much substantiation and lacks sufficient depth in its treatment of advanced control systems. However, the document reflects some of our unique flight experience which we feel is pertinent to the shuttle mission and the shuttle itself. Our X-15 experience in areas such as lifting entry and hypersonic maneuvering is directly applicable to the shuttle mission, and our lifting body experience is meaningful if a high-cross-range configuration is decided upon. If the popular low-cross-range configuration is selected, we are not sure which experience is applicable. However, the flying qualities document contains a section entitled "Miscellaneous Flying Qualities," which includes discussions of such factors as stall characteristics and stall and spin recoveries. If this section were appropriately modified, it might cover even the low-cross-range configuration. Nevertheless, our flight experience must be scaled up in terms of Mach number and vehicle size. We are doing this both analytically and by means of simulation. Some of our results were presented in paper 10. We are working with each of the other NASA Centers to provide the data required for the preparation of an official NASA flying-qualities specification.

Our future plans include continued work on unpowered approach and landing, using both small and large aircraft. We are developing an up-link command system which will be used to evaluate a number of unpowered terminal energy management concepts. We also plan to use one of our F-104 aircraft, which is equipped with an inertial platform and digital computer, to evaluate other terminal guidance schemes. Continued work on handling qualities and control system requirements will support those in NASA who must write these specifications. Envelope expansion will be the major effort in tests on the X-24A vehicle. The M2-F3 lifting body will be used to investigate a variety of control schemes involving both aerodynamic and reaction controls. After a few more powered approach flights, the HL-10 vehicle may be set aside temporarily in order to concentrate on the M2-F3 and X-24A vehicles. (At this point, I would like to solicit inputs, from those present, for suggested meaningful studies to be performed on the HL-10. Such inputs will be considered for extending the HL-10 flight program)

As may be seen from these future plans, we hope to play an active role in the space shuttle development program.

CONCLUDING REMARKS

I would like to say that we at the NASA Flight Research Center believe that a space shuttle is feasible. However, we are concerned about some of the requirements specified for the shuttle. It is not that any one of the individual requirements are unreasonable, but it is the multiplicity of these requirements. It almost seems as though we are asking for an F-111 spacecraft. We think that if the shuttle is only capable of returning a modest payload while maneuvering during a lifting entry to a horizontal land landing and is then reusable, we should not complain too much because we have never accomplished any one of these objectives with previous manned spacecraft. We at the Flight Research Center are not making the decisions on the shuttle. Possibly all of the requirements specified in the Phase B Statement of Work can be met. Someone more capable than we decided to reach for the moon. That worked. We are not all that pessimistic either.

We have been convinced of the feasibility of a lifting entry, horizontal landing spacecraft since we flew the M2-F1 vehicle 7 years ago. We have been advocating the development and testing of a lifting entry research vehicle since 1965. In the meantime, we have flown the X-15 airplane into and back from space many times and demonstrated that it could be maneuvered hypersonically, supersonically, and subsonically to precise landings on a preselected runway without power. We are convinced that configurations optimized for lifting entry can be designed to have satisfactory handling qualities and can thus be successfully flown from supersonic speeds to precise horizontal landings. In our opinion, which is reflected in our handling-qualities document, there is no reason that the shuttle cannot have handling qualities equal to, or better than, current transport aircraft regardless of whether it is a high- or low-cross-range configuration. We know through our own experience that there are control systems available which will provide good handling characteristics in addition to the desired aerodynamic maneuvering capability throughout the entire entry. On the basis of our own experience, we cannot discuss the practicality of the proposed launch, boost, and orbit operations, nor can we assess the status of required technology in such critical areas as materials, structures, and thermal protection systems. Yet we have watched in amazement the unbelievable results produced by the Office of Manned Space Flight Centers and have been highly impressed by the work of the Office of Advanced Research and Technology Centers. We were enthusiastic about the Air Force's ASSET and PRIME programs. If all the other NASA Centers, in conjunction with the Department of Defense and industry, can get the shuttle off the ground, into orbit, and insure that it survives the entry, we at the Flight Research Center can guarantee that it can be flown to the destination and landed safely.

SCALE MODEL SHUTTLE TESTING

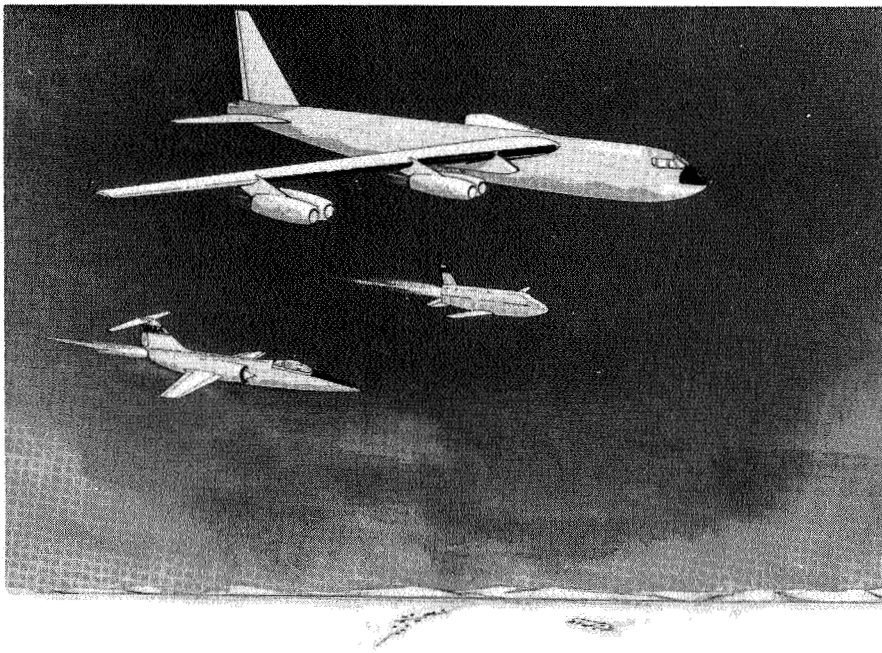


Figure 1

LIST OF ATTENDEES

ALEXANDER, Grover L.	Lockheed Missiles & Space Company
ALGRANTI, Joseph S.	NASA Manned Spacecraft Center
AMES, Milton B. , Jr.	NASA Headquarters
ANTONATOS, Philip P	Air Force Flight Dynamics Laboratory, Wright Patterson Air Force Base
ASH, Lt. Lawrence G.	Air Force Flight Test Center , Edwards Air Force Base
BANE, Don	Los Angeles Herald Examiner
BARTON, Richard L.	NASA Manned Spacecraft Center
BEARMAN, Lt. Col. Richard S.	Headquarters, SAMSO, USA F
BEELEER, De E.	NASA Flight Research Center
BEHM, William F.	McDonnell Douglas Astronautics Company
BEHUN, Michael	NASA Headquarters
BERENT, Maj. Mark E.	Headquarters, SAMSO, USA F
BIGHAM, James P. , Jr.	NASA Manned Spacecraft Center
BIKLE, Paul F.	NASA Flight Research Center
BLACKSTONE, John H.	NASA Marshall Space Flight Center
BORNEMANN, William E.	North American Rockwell, Space Div.
BRACKEEN, Richard E.	The Martin Marietta Corporation
BRENHOLDT, Maj. J.	Aerospace Research Pilot School, Edwards Air Force Base
BRENNAN, John J. L.	Northrop Corporation
BROOKS, Melvin	NASA Marshall Space Flight Center
BROWN, Lewis Edwin, Jr.	North American Rockwell Corporation
BROWNSON, Jack J.	NASA Ames Research Center
BUCHANAN, Robert S.	McDonnell Douglas Astronautics Company, Western Division
BURNER, Edward	McDonnell Douglas Astronautics Company, Western Division
BURNHAM, Frank	American Aviation
BUTCHART, Stanley P.	NASA Flight Research Center
BUTSKO, J E.	General Dynamics/Convair Division

CASSIDY, Daniel E	Bellcomm Inc
CHEATHAM, Donald C.	NASA Manned Spacecraft Center
CHIN, Jimmie	Grumman Aerospace Corporation
COBB, Stan M	Pan American
COCHRANE, John A.	The Martin Marietta Corporation
COULTER, John M. , Col. , USAF (Ret.)	NASA Headquarters
CREER, Brent Y	NASA Ames Research Center
CREWS, Lt. Col. Albert H.	NASA Manned Spacecraft Center
CROTTY, Maj. Patrick B.	Headquarters, SAMSO, USAF
DANA, William H.	NASA Flight Research Center
DECKER, John P.	NASA Langley Research Center
DE MERITTE, Frederick J.	NASA Headquarters
DOMOKOS, Stephen J.	North American Rockwell Corporation,
	Rocketdyne Div.
DONLAN, Charles J.	NASA Headquarters
DRINKWATER, Fred J. III	NASA Ames Research Center
EHLERS, Harold L.	North American Rockwell Corporation,
	Space Div.
ERB, Fred R.	Northrop Corporation, Aircraft Div.
FAGET, Dr. Maxime A.	NASA Manned Spacecraft Center
FELTZ, Charles F.	North American Rockwell Corporation,
	Space Div.
FERRYMAN, Peter R.	North American Rockwell Corporation,
	Space Div.
FEW, Albert G. , Jr.	NASA Marshall Space Flight Center
FIKES, Joe E.	NASA Marshall Space Flight Center
FINCH, Thomas W.	NASA Flight Research Center
FINKE, Dr. Rex	Institute for Defence Analysis
FISCHEL, Jack	NASA Flight Research Center
FRIEDMAN, George R.	General Dynamics/Convair Division
FULTON, Fitzhugh L. , Jr.	NASA Flight Research Center
GAFFNEY, Gerald P.	NASA Headquarters
GENTRY, Maj. Jerauld R.	Air Force Flight Test Center,
	Edwards Air Force Base

GERMERAAD, D. P.	Lockheed Missiles & Space Company
GODFREY, Roy E.	NASA Marshall Space Flight Center
GOERNER, Erich E.	NASA Marshall Space Flight Center
GRAHAME, W. E.	Northrop Corporation
GREGORY, Thomas J.	NASA Ames Research Center
HANSON, James R.	McDonnell Douglas Corporation
HARDY, Gordon H.	NASA Ames Research Center
HARDY, M. M.	Northrop Corporation
HARER, Richard J.	Air Force Flight Test Center, Edwards Air Force Base
HARPER, John A.	McDonnell Douglas Astronautics Company
HASTINGS, R. C.	Defence Research and Development Staff, British Embassy, Washington, D. C.
HELLO, Bastian	North American Rockwell Corporation
HENRY, Beverly Z., Jr.	NASA Langley Research Center
HOAG, Maj. Peter C.	Air Force Flight Test Center, Edwards Air Force Base
HOEY, Robert G.	Air Force Flight Test Center, Edwards Air Force Base
HOLLEMAN, Euclid C.	NASA Flight Research Center
HOLMES, Walter	North American Rockwell Corporation
HONDROS, James G.	NASA Manned Spacecraft Center
JENSEN, T. L.	McDonnell Douglas Astronautics Company, Western Division
JONES, Robert A	NASA Langley Research Center
KALVISTE, Juri	Northrop Corporation
KATZEN, Elliott D	NASA Ames Research Center
KEHLET, Alan B.	North American Rockwell Corporation, Space Div.
KELLY, J F.	North American Rockwell Corporation, Rocketdyne Div.
KEMPEL, Robert W.	NASA Flight Research Center
KIMBREL, Laddie	The Boeing Company

KING, Lauren W
KOCK, Berwin M
KUCHTA, Bernard J.

LAMAR, William E.

LARSON, V. R.

LASSEN, M. Morton, Jr.
LAYTON, Garrison P., Jr.
LESKO, James S.
LETHBRIDGE, Harrison B.

MAC DONALD, Ian A.
MACOUREK, Michael N.
MADDEN, John F.
MALVESTUTO, Frank S., Jr.

MANKE, John A.
MARKARIAN, H. P.
MC TIGUE, John G.
MEAD, Lawrence M., Jr
MELLEN, David L.
MIKKLESON, Daniel C
MILTON, J. R.
MINAR, Maj Gary H.
MORGAN, Gen. Thomas W.
MORGENSEN, Otto P.

MOSER, Robert E.
MOUL, Martin T
MOWERY, David K.
MOYLES, John A.

MRAZEK, Dr William A.

NASA Pasadena Office
NASA Flight Research Center
General Dynamics/Convair Division
Air Force Flight Dynamics Laboratory,
Wright Patterson Air Force Base
North American Rockwell Corporation,
Rocketdyne Div.
Pratt & Whitney Aircraft Corporation
NASA Flight Research Center
The Boeing Company
Hydraulic Research and Manufacturing
Company
Northrop Corporation
General Electric Co
NASA Headquarters
The Martin Marietta Corporation,
Denver Div.
NASA Flight Research Center
Northrop Corporation
NASA Flight Research Center
Grumman Aerospace Corporation
Honeywell, Inc
NASA Lewis Research Center
Lockheed Missiles & Space Company
SAMSO
NASA Kennedy Space Center
Aeronautical Systems Division,
Wright Patterson Air Force Base
NASA Kennedy Space Center
NASA Langley Research Center
NASA Marshall Space Flight Center
North American Rockwell Corporation
Space Div
NASA Marshall Space Flight Center

MURPHY, James T.	NASA Marshall Space Flight Center
NORRIS, John H. , Jr.	Grumman Aerospace Corp.
NORTH, Warren J.	NASA Manned Spacecraft Center
ODER, Frederic C. E.	Lockheed Missiles & Space Company
OSDER, Stephen S.	Sperry Rand
PATHA, John T.	The Boeing Company
PAUL, E. D.	Northrop Corporation
PAULSON, John W.	NASA Langley Research Center
PEARCE, R. B. , Jr.	North American Rockwell Corporation, Space Div.
PEARSON, Ernest O. , Jr.	NASA Headquarters
PEDERSEN, Odd	Bendix Corp. , Navigation and Control Div
PETERSON, Victor L.	NASA Ames Research Center
POWELL, Maj. Cecil W.	Air Force Flight Test Center, Edwards Air Force Base
PYLE, Jon S.	NASA Flight Research Center
RAINEY, Robert W.	NASA Langley Research Center
REED, Robert D.	NASA Flight Research Center
REED, Thomas G.	NASA Marshall Space Flight Center
RETELLE, Capt. John P.	Air Force Flight Test Center, Edwards Air Force Base
ROBERTS, Ray R.	NASA Kennedy Space Center
ROGERS, Alden L.	Grumman Aerospace Corporation
ROGERS, Francis	McDonnell Douglas Corporation
ROSAMOND, D. L.	McDonnell Douglas Corporation
ROSE, E. H.	Aerospace Corporation
ROSS, Russell H.	Chrysler Corporation, Space Division
ROTH, Henry J	Aerospace Corporation
ROWLEY, Frederick C.	Grumman Aerospace Corporation
RUPPERT, E. C. Edward	McDonnell Douglas Astronautics Company, Western Region Office
SALVADOR, Galdino	Chrysler Corporation, Space Division

SCHOFIELD, B. Lyle

SCOVILLE, Curtis L.

SHALL, Maj. Paul J., Jr.

SHAWLER, Lt. Col. Wendell H.

SHIPLEY, P.

SHUCK, Lowell M.

SHUTAK, Robert J.

SILVEIRA, Milton A.

SINGLETON, Capt. Ivan J.

SKLAREWITZ, Norm

SMITH, Donald R.

STALONY-DOBRZANSKI, Janusz A.

STANTON, Charles I.

STEVENS, Victor I., Jr.

STRUCK, Heinz

TANG, Ming H.

THARRATT, Charles E.

THEURER, Capt. Byron W.

THOMPSON, Milton O.

THOMPSON, Robert F.

TRAMMELL, Lt. Col. William H.

TUNTLAND, Richard

VERBLE, A. J., Jr.

VIDEAN, Edward N.

VITSKY, Larry

Air Force Flight Test Center,

Edwards Air Force Base

General Electric Space Division

Headquarters, SAMSO, USAF

Air Force Flight Test Center,

Edwards Air Force Base

North American Rockwell Corporation,

Space Division

Sperry Flight Systems Division

IBM, Federal Systems Division

NASA Manned Spacecraft Center

Aerospace Research Pilot School,

Edwards Air Force Base

U. S. News and World Report

Air Force Flight Test Center,

Edwards Air Force Base

Northrop Corporation

NASA Headquarters

NASA Ames Research Center

NASA Marshall Space Flight Center

NASA Flight Research Center

Chrysler Corporation, Space Division

Aerospace Research Pilot School,

Edwards Air Force Base

NASA Flight Research Center

NASA Manned Spacecraft Center

Air Force Liason Office, NASA Ames

Research Center

NASA Manned Spacecraft Center

NASA Marshall Space Flight Center

NASA Flight Research Center

McDonnell Douglas Astronautics Company,

Western Division

WALKER, Harold J.	NASA Flight Research Center
WALKER, Phillip E.	NASA Flight Research Center
WALL, Henry, Jr.,	McDonnell Douglas Corporation
WEIL, Joseph	NASA Flight Research Center
WENDT, Lt. Col. Warren W.	Headquarters AFSC, USAF,
	Andrews Air Force Base
WESESKY, John L.	Air Force Flight Test Center,
	Edwards Air Force Base
WIER, Bernard J.	General Dynamics/Convair Division
WILLIAMS, Dr. Walter C.	Aerospace Corporation
WINDLER, Milton L.	NASA Manned Spacecraft Center
WINTER, Dr. William R.	NASA Flight Research Center
WITTE, Norbert F.	North American Rockwell Corporation,
	Space Div.
WOLFE, Robert R.	Aerospace Corporation
WOOD, Frederick E.	Grumman Aerospace Corporation
WORTHINGTON, Roy H., Jr.	Headquarters AFSC, USAF,
	Andrews Air Force Base
ZIMA, William P.	Air Force Flight Dynamics Laboratory,
	Wright Patterson Air Force Base
ZIMMERMAN, R. A.	Northrop Corporation